



City Research Online

City, University of London Institutional Repository

Citation: Forster, J. (2018). Motion-induced position shifts in visual perception tasks and eye movement. (Unpublished Doctoral thesis, City, University of London)

This is the accepted version of the paper.

This version of the publication may differ from the final published version.

Permanent repository link: <https://openaccess.city.ac.uk/id/eprint/19926/>

Link to published version:

Copyright: City Research Online aims to make research outputs of City, University of London available to a wider audience. Copyright and Moral Rights remain with the author(s) and/or copyright holders. URLs from City Research Online may be freely distributed and linked to.

Reuse: Copies of full items can be used for personal research or study, educational, or not-for-profit purposes without prior permission or charge. Provided that the authors, title and full bibliographic details are credited, a hyperlink and/or URL is given for the original metadata page and the content is not changed in any way.

MOTION-INDUCED POSITION SHIFTS
IN VISUAL PERCEPTION TASKS
AND EYE MOVEMENTS

City, University of London
Applied Vision Research Centre
Department of Optometry and Visual Sciences
Psychophysics and Visual Neuroscience

This thesis is presented for the degree of
Doctor of Philosophy

by

Julia Förster

April 2018

Minimal im Haben,
maximal im Sein.

LIST OF FIGURES	1
LIST OF TABLES	5
LIST OF FORMULAS	6
DECLARATION	7
ABSTRACT	8
SYNOPSIS	9
1. INTRODUCTION	10
<i>1.1 Fundamental Concept</i>	<i>10</i>
1.1.1 Psychophysics	10
1.1.2 The Gabor stimulus	10
1.1.3 Motion-induced position shifts (MIPS)	11
1.1.4 Saccadic Eye Movements	11
1.1.4.1 Endogenously and exogenously driven Saccades	12
1.1.4.2 Saccadic Adaptation	13
1.1.4.3 Saccadic Suppression	14
<i>1.2 Literature Review</i>	<i>16</i>
1.2.1 Introduction MIPS	16
1.2.2 Fundamental physiological background	20
1.2.3 MIPS in different kinds of motion	25
1.2.3.1 Luminance defined motion and kinetic edges	25
1.2.3.2 Hard- and soft aperture	25
1.2.3.3 Contrast defined motion	26
1.2.3.4 Motion in depth	26
1.2.3.5 Cyclopean motion	27
1.2.3.6 Motion defined motion	27
1.2.3.7 Motion-after-effect induced motion	28
1.2.3.8 Pseudo plaid and plaid pattern motion	29
1.2.3.9 Component motion and global motion	33
1.2.3.10 Motion without spatially located motion cues	35
1.2.3.11 Remote and passive motion	36
1.2.3.11 Carrier motion, envelope motion and retinal motion	38
1.2.4 Why and how does MIPS arise?	41
1.2.4.1 Compensate delay in visual processing	41
1.2.4.2 Prediction of the likely future	44
1.2.4.3 Spatial summation process	45
1.2.4.4 Motion deblurring mechanism	47
1.2.4.5 Bayesian Theory	48
1.2.5 Magnitudes of MIPS depending on characteristics	51
1.2.6 Where do MIPS arise?	57
1.2.7 MIPS in action and perception	61
<i>1.3 Motivation</i>	<i>67</i>
1.3.1 Camouflage	68
1.3.2 Human-Machine Interactions	69

2. GENERAL METHODS	70
2.1 <i>Observers</i>	70
2.2 <i>Experimental Setup</i>	70
2.3 <i>Monitor Calibration</i>	71
3. MIPS IN PERCEPTION TASK AND VOLITIONAL SACCADDES	73
3.1 <i>Introduction</i>	73
3.2 <i>Methods</i>	73
3.2.1 <i>Stimuli</i>	73
3.2.2 <i>Procedure</i>	74
3.2.3 <i>Observers and Setup</i>	75
3.3 <i>Data Analysis and Results</i>	75
3.3.1 <i>Perception bias</i>	75
3.3.2 <i>Saccadic landing positions</i>	77
3.3.3 <i>Fixations</i>	83
3.3.4 <i>Saccade trajectories</i>	85
3.3.4.1 <i>Averaged saccade trajectories</i>	85
3.3.4.2 <i>Path length</i>	88
3.3.4.3 <i>Saccadic peak velocity</i>	92
3.4 <i>Summary</i>	95
3.5 <i>Discussion</i>	96
3.5.1 <i>Methodological comparison with previous studies</i>	97
3.5.2 <i>Perceptual effect</i>	101
3.5.3 <i>Saccadic eye movements</i>	104
3.6 <i>Conclusion</i>	107
4. COMPARISON OF MIPS IN PERCEPTION TASKS AND VOLITIONAL SACCADDES	108
4.1 <i>Introduction</i>	108
4.2 <i>Methods</i>	109
4.3 <i>Data Analysis and Results</i>	109
4.3.1 <i>Perceptual shifts</i>	109
4.4 <i>Summary</i>	109
4.5 <i>Discussion</i>	110
4.6 <i>Conclusion</i>	111
5. SACCADIC ADAPTATION IN MIPS	112
5.1 <i>Introduction</i>	112
5.1 <i>Methods</i>	113
5.1.1 <i>Stimuli and Procedure</i>	113
5.1.2 <i>Observer and Setup</i>	113
5.2 <i>Data Analysis and Results</i>	113
5.2.1 <i>Saccadic landing positions</i>	114
5.4 <i>Summary</i>	115
5.5 <i>Discussion</i>	115
5.6 <i>Conclusion</i>	115
6. MIPS IN REFLEXIVE SACCADDES: COMPARISON OF WITHIN-OBSERVER STATISTICS AND GROUP-LEVEL STATISTICS	116
6.1 <i>Introduction</i>	116
6.2 <i>Methods</i>	117

6.2.1 Stimuli	117
6.2.2 Procedure	117
6.2.3 Setup	118
6.2.4 Observers	118
6.3 <i>Data Analysis and Results</i>	119
6.3.1 Group-Level Statistics	120
6.3.2 Within-Observer Statistics	122
6.4 Summary	124
6.5 <i>Discussion</i>	125
6.5.1 Methodical comparison with previous studies	125
6.5.2 Comparison of effect sizes	126
6.6 <i>Conclusion</i>	127
7. MIPS IN REFLEXIVE SACCADDES TOWARDS PSEUDO-PLAIDS	128
7.1 <i>Introduction</i>	128
7.2 <i>Methods</i>	129
7.2.1 Setup	129
7.2.2 Observers	129
7.2.3 Stimuli	129
7.2.4 Procedure	129
7.3 <i>Data Analysis and Results</i>	131
7.3.1 Within-Observer Statistics	131
7.3.2 Group-Level Statistics	134
7.4 <i>Summary</i>	135
7.5 <i>Discussion</i>	136
7.5.1 Comparison of saccadic shift to Gabors and pseudo-plaids	136
7.5.2 Does the size of the saccadic shift depend on the motion processing stage?	136
7.6 <i>Conclusion</i>	138
7.7 <i>Further Investigations</i>	138
8. CIRCULAR DATA ANALYSIS	139
8.1 <i>Introduction</i>	139
8.2 <i>Methods</i>	140
8.3 <i>Data Analysis and Results</i>	140
8.4 <i>Summary</i>	148
8.5 <i>Discussion</i>	149
8.6 <i>Conclusion</i>	150
9. GENERAL DISCUSSION	151
9.1 <i>Summary</i>	151
9.2 <i>Reflection on previous studies</i>	153
9.2.1 Saccadic eye movements	153
9.2.2 Perception tasks	156
9.3 <i>Conclusion</i>	156
APPENDICES	158
Appendix A: <i>Cluster Algorithm</i>	158
Appendix B: <i>Psychometric Function</i>	160
REFERENCES	162

LIST OF FIGURES

Figure 1.1: Schematic showing of a motion-induced position shift of a stimulus with a static envelope but an internal moving sinusoidal waveform.	11
Figure 1.2: Experiment of Alfred Yarbus.	12
Figure 1.3: Saccadic adaptation.	13
Figure 1.4: Kinetic edges.	17
Figure 1.5: Visual illusion when a pitcher throwing a curveball.	19
Figure 1.6: Sketches of simple receptive fields.	20
Figure 1.7: Example of the organisation of a simple cell within the visual cortex.	20
Figure 1.8: Sketches of complex receptive fields.	21
Figure 1.9: The aperture problem.	22
Figure 1.10: Example of VS- and IOC-Method indicating true global motion direction.	22
Figure 1.11: Example of VS- and IOC-Method not indicating the same global motion direction.	22
Figure 1.12: An example illustrating two-stage motion processing mechanism introduced by Adelson and Movshon (1982).	23
Figure 1.13: First- order motion stimuli used by Kosovicheva, Wolfe & Whitney (2014).	25
Figure 1.14: Second- order contrast-defined Gabor.	26
Figure 1.15: Illustration of the stimulus used by Durant & Zanker (2009) when investigating whether motion defined motion stimuli induce illusory position shifts.	28
Figure 1.16: Rotating windmill causing motion-after-effects.	28
Figure 1.17: Plaid Type I and Plaid Type II.	30
Figure 1.18: Plaid used by Hisakata and Murakami (2009).	31
Figure 1.19: Example of a pseudo plaid.	31
Figure 1.20: Stimuli used to test whether component motion or global motion contribute to motion-induced position shifts.	34
Figure 1.21: Stimulus where motion signals cannot be separated by local spatial signals, or luminance profiles.	35
Figure 1.22: Stimulus inducing a position-after-effect ‘passively’.	36
Figure 1.23: Stimulus inducing a position-after-effect ‘remotely’.	37

Figure 1.24: Experiments conducted to test whether display-relative-velocity, envelope-relative-velocity or retina-relative velocity determines the motion-induced position shift in perception tasks.	39
Figure 1.25: Results of one observer obtained in a fMRI study by Whitney et al. (2003).	42
Figure 1.26: Motion-induced position shifts may be generated by a motion activated gain field.	43
Figure 1.27: Stimulus to measure detection threshold at trailing and leading edges of a Gabor.	434
Figure 1.28: Space-time plots of a Gabor.	45
Figure 1.29: A photo when the camera had a shutter speed of 125 ms.	47
Figure 1.30: Experiment to test whether trailing and leading edges of moving Gabors are perceived as being displaced.	51
Figure 1.31: Ebbinghaus Illusion.	61
Figure 1.32: Experiment by Caniard et al. (2011).	65
Figure 1.33: Experiment by Caniard, Bühlhoff & Thornton, 2015.	65
Figure 1.34: Camouflage.	68
Figure 1.35: Porsche Panamera 4S.	69
Figure 2.1: Angles define the distance between the two different target points A and B with viewing distance d .	70
Figure 2.2: The Eyetracker, camera, chair, head and chin-rest, and CRT Monitor.	71
Figure 2.3: Luminance values before monitor calibration of a CRT Monitor used in my experiments.	72
Figure 3.1: Procedure of experiment described in chapter 3.	74
Figure 3.2: Psychometric functions for data gathered with rightward drifting Gabors.	76
Figure 3.3: Perception effect.	76
Figure 3.4: Saccade velocity profile and saccade trajectories.	77
Figure 3.5: Cluster algorithm employed on saccadic start positions of observer AXS.	79
Figure 3.6: Saccade velocity profiles and saccade trajectories of one observer after applying filter.	80
Figure 3.7: Histogram of distances of saccadic landing positions (pixel)	

to the centre of the Gabor in one experiment conducted by observer BCD.	81
Figure 3.8: Saccadic effects of observer BCD.	82
Figure 3.9: Saccadic effect.	83
Figure 3.10: Last fixation before saccade onset.	84
Figure 3.11: Average saccade trajectories.	86
Figure 3.12: Averaged gradient of saccade trajectories.	88
Figure 3.13: Resulting mean saccadic path length.	89
Figure 3.14: Resulting mean saccadic path length.	90
Figure 3.15: Grouped path length.	91
Figure 3.16: Resulting mean peaks of the velocity profiles.	92
Figure 3.17: Resulting mean peaks of the velocity profiles.	93
Figure 3.18: Grouped saccadic peak velocity.	94
Figure 5.1: Procedure of experiment described in chapter 5.	113
Figure 5.2: Saccadic effect.	114
Figure 6.1: Experimental procedure to measure saccadic landing position to a single Gabor (chapter 6).	118
Figure 6.2: QQ-Plots.	119
Figure 6.3: Perception effect.	120
Figure 6.4: Saccadic effect group-level statistic.	121
Figure 6.5: Saccadic effect within-observer statistic.	123
Figure 7.1: Example of the stimulus I used in my experiment (described in chapter 7).	128
Figure 7.2: Experimental procedure to measure saccadic landing positions to a pseudo-plaid (chapter 7).	130
Figure 7.3: Perception effect.	131
Figure 7.4: Saccadic effect within-observer statistic.	133
Figure 7.5: Saccadic effect group-level statistic.	134
Figure 8.1: Example of two sets of saccadic landing positions that follow different distributions.	140
Figure 8.2: Paradigm of the experiment described in chapter 6.	140
Figure 8.3: Two rosedigrams presenting saccadic landing positions towards leftward (left diagram) and rightward (right diagram) drifting Gabors.	141
Figure 8.4: An example of a vector defined by direction and angle.	142
Figure 8.5: Resulting vectors of circular data analysis indicating direction and angle of saccade landing positions.	144

Figure 8.6: Length of vectors.	144
Figure 8.7: Results of circular data analysis – different latency bins.	146
Figure 8.8: Length of vectors – different latency bins.	147
Figure 9.1: Analysis of saccadic landing positions by De’Sperati and Baud-Bovy (2008).	154
Figure A1: Experiment of Alfred Yarbus (1967).	158
Figure A2: Example given by Santella & DeCarlo (2004): clustering of the region of interest of one observer.	159

LIST OF TABLES

Table 1.1: Key features affecting the magnitude of MIPS.	56
Table 3.1: Key features of the methods and measured perceptual effect.	104
Table 8.1: Circular standard deviation.	148

LIST OF FORMULAS

Eq. 2.1: Viewing distance in angles.	68
Eq. 2.2: Correction of luminance profile (CRT).	69
Eq. 2.3: Michelson Contrast.	69
Eq. 3.1: Averaged saccade trajectories (X).	85
Eq. 3.2: Averaged saccade trajectories (Y).	85
Eq. 3.3: Gradient of averaged saccade trajectories.	87
Eq. 8.1: Circular data analysis - Average vector length.	142
Eq. 8.2: Circular data analysis - Single angles.	142
Eq. 8.3: Circular data analysis - Sum of single angles (sin).	142
Eq. 8.4: Circular data analysis - Sum of single angles (cos).	142
Eq. 8.5: Circular data analysis - Average vector angle (direction).	142
Eq. A.1: Cluster algorithm - Kernel function.	158
Eq. A.2: Cluster algorithm - Shift function (x-axis).	159
Eq. A.3: Cluster algorithm - Shift function (y-axis).	159
Eq. B.1: Psychometric function - Probability of observer's decision in one trial.	160
Eq. B.2: Psychometric function - Relative frequency of each stimulus level.	160
Eq. B.3: Psychometric function - Probability of observer's decisions in row of trials.	160
Eq. B.4: Psychometric function - Maximum likelihood estimation.	161
Eq. B.5: Psychometric function - Log maximum likelihood estimation.	161

DECLARATION

I grant powers of discretion to the University Librarian to allow this thesis to be copied in whole or in part without further reference to myself. This permission covers only single copies made for study purposes, subject to normal conditions of acknowledgement.

ABSTRACT

Movement has an effect upon the perceived spatial position of moving objects, such that they are not perceived at their instantaneous spatial position. Vision scientists named this phenomenon motion-induced position shift (MIPS). The reason, neural loci, and the mechanisms causing the positional illusion have challenged scientists over the last century.

Nowadays, many vehicles, such as cars, planes and submarines are equipped with on-board computers containing touchscreens. Active controls of those on-board computers require visuomotor-actions, which could be affected by perceptual illusions, but also require time, and attention. Hence, it is becoming more crucial to fully understand how the visual system generates visuomotor-guided actions, and how it copes with visual illusions. Human-machine interactions could be designed such that perceptual illusions would be 1) avoided, or 2) predicted, and considered in human actions, or such that 3) the user interacted with visuomotor actions that resisted visual illusions.

One alternative to finger points towards on-board computers is saccadic eye movements. The saccadic system is very fast, and therefore, would not require as much time and attention as a finger point task towards the touch screen. Saccades are constantly facing the challenge of localising objects, which makes it interesting to study how they cope with visual illusions like the motion-induced position shift.

The purpose of this thesis was to establish if the saccadic system was affected by the motion-induced position shift in the same manner as the perceptual system was affected. I confirmed that movement had an effect upon the perceived spatial position of moving objects in perception-tasks and in volitional saccades. A previous study showed that reflexive saccades resisted the illusion, indicating that they were more accurate than other visually guided actions. I replicated these results, but claimed that the results are not representative. As a consequence, there is no evidence that reflexive saccades do escape the visual illusion while volitional saccades do not.

SYNOPSIS

Chapter 1 presents an overview of basic knowledge about the field of research. Chapter 1.1 will introduce the fundamental concepts, followed by a review of most popular and influential research that has been done on motion-induced position shifts.

Chapter 2 describes the general methods used in the behavioural experiments to provide a background for the different experimental sections.

Chapters 3, 4, 5 and 7 each comprise one experiment. Each chapter begins with an introduction of the main research question, and then I describe the methods, which include details about experimental paradigms, observer, setups and data analysis methods. Afterwards experimental results will be described and summarised, followed by a detailed comparison with previous studies and a discussion of the results. Finally, the main research questions will be answered in a conclusion.

Chapter 6 is constructed like chapters 3, 4, 5 and 7. Unlike those chapters, where I design a novel paradigm, the experiment attempts to replicate the data of a study by other vision scientists.

In chapter 8 I re-analyse the data of chapter 6 with a different statistical method. The structure is like the structure of the other experimental chapters.

In chapter 9 I summarise all results described in this thesis and finally, I discuss the result in relation to previous studies.

1. INTRODUCTION

1.1 Fundamental Concept

In this section fundamental concepts will be described to provide a common background for experimental sections. A literature review will introduce the motion-induced position shift (MIPS) extensively in a separate chapter.

1.1.1 Psychophysics

Psychophysics is a concept used to investigate the relationship between physical stimuli and experienced impression of them. In 1834 the physician Ernst Heinrich Weber had the idea of studying the relationship between the intensity of a stimulus (i.e. weight), and the just noticeable difference threshold (the difference in two weights that lead to someone's ability to discriminate between them). He found that it is easier to discriminate two light weights than to discriminate two heavy weights, a law that was later named the 'Weber fraction'. The physicist and philosopher, Gustav Theodor Fechner was inspired by Ernst Heinrich Weber's results, and established 'psychophysics' as a research field when he published 'Elemente der Psychophysik' in 1860.

1.1.2 The Gabor stimulus

Conventional Gabor patterns (or simply "Gabors") were named after the inventor Gábor Dénes. Each Gabor is the product of sinusoidal luminance defined waveforms (also called "gratings"), and a 2-dimensional Gaussian function to blur the edges of the gratings (see figure 1.1). The advantages of Gabors for psychophysical experiments over other stimuli, such as circles or diamonds, are that Gabors are identical in their surface extent, and therefore, uniformly stimulate the retinal region they cover. This circumvents the open question, of how the identification of spatially separate moving borders with a common object takes place (Movshon et al., 1985). I investigate motion-induced position shifts (defined below) within the striate cortex, which consists of orientation-selective neurons that respond strongly to the motion of

Gabors (e.g. Hubel & Wiesel, 1962). Detailed information will follow in section 1.2 Literature Review.

1.1.3 Motion-induced position shifts (MIPS)

A Gabor with a stationary envelope, but an internal drifting sinusoidal waveform causes misperception in its perceived position (DeValois & DeValois, 1991). Figure 1.1 shows schematically how the motion of a Gabor can influence spatial perception. The envelope of the Gabor is fixed in one position but the sinusoidal waveform is drifting to the right. On the right side (perceived image) you see how humans perceive the image on the left side (physical image). If the Gabor moves to the right side, the stimulus appears shifted to the right. Currently understanding of the motion-induced position shift (MIPS) is limited; however, there are some hypotheses that might explain MIPS (see section 1.2.4 Why and how do MIPS arise?).

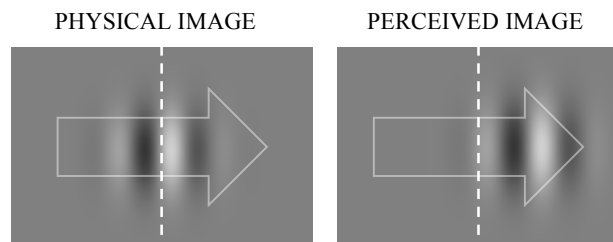


Figure 1.1: Schematic showing of a motion-induced position shift of a stimulus with a static envelope but an internal moving sinusoidal waveform. The figure on the left shows the physical position of a rightward drifting stimulus. The figure on the right shows the perceived position of the same stimulus. Arrows indicate the waveform inside the static envelope of the stimuli in both figures, dotted lines indicate the centres of the stimuli.

1.1.4 Saccadic Eye Movements

In everyday life, we have to process complex visual scenes. The highest visual acuity is reached by projecting the object of interest to the fovea. Figure 1.2 shows an experiment done by Alfred Yarbus (1967). Observers had to look at the woman for one minute. The resulting eye movements are shown as dark lines between different target-locations. The major kinds of eye movements are saccades, fixations, smooth pursuit movements, vergence movements, optokinetic movements and vestibular

ocular movements (Kandel et al., 2000). In the following experiments I investigate saccadic eye movements, rapid changes in the direction of gaze, having a maximum speed of $\sim 900^\circ/\text{s}$ (Kandel et al., 2000).

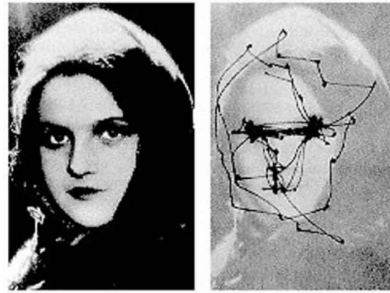


Figure 1.2: Experiment of Alfred Yarbus. Observers had to look at the woman for one minute. The resulting eye movements are shown as dark lines between different target-locations. From Kandel et al., 2000.

1.1.4.1 Endogenously and exogenously driven Saccades

A review of McDowell et al. (2009) states that previous research has led to the view of separation for exogenously and endogenously driven saccades: Exogenously driven saccades, such as pro-saccades (to a suddenly presented visual target) and express saccades (to a target that appears after saccade onset), are also called ‘visually guided saccades’ and ‘reflexive saccades’. Endogenously driven saccades, such as anti-saccades (in the direction opposite to a visual cue), memory guided saccades (to a remembered target that has been shown previously), and delayed saccades (to a permanently shown target after a go-signal) are also called ‘volitional saccades’ or ‘internally triggered saccades’. Both types of saccades require a similar basic processing circuitry (Leigh & Zee, 2006): Visual information enters in the form of light through the retina, is transferred to the optic chiasm by axons of the ganglion cells (the optic nerve) and then sent via the optic tract through the lateral geniculate nucleus (LGN) in the thalamus, and through pretectum and the colliculus superior within the brainstem. The pretectum uses these signals to control pupillary reflexes and the colliculus superior uses the signals to control eye movements (Kandel et al., 2000). The LGN uses the retinal signals to extract visual information and sends them to the higher visual areas such as the primary visual cortex. From there information is

sent to different areas along the dorsal stream to extrastriate areas, parietal cortices (parietal eye field) and the frontal cortex (frontal eye field, supplementary eye field) (McDowell et al., 2009). McDowell et al. (2009) reported that volitional saccades change the activity in this basic neural circuitry and recruit additional neural regions, for example within the anterior cingulate cortices. Latencies of exogenously driven saccades were found to be ~100 ms slower than endogenously driven saccades (e.g. Mort et al., 2003).

1.1.4.2 Saccadic Adaptation

McLaughlin (1967) performed one of the first experiments on saccadic eye movements. Observers were asked to make a saccade from a fixation point (A) to a new target (B) 10° away from the primary fixation point. While the observer started to shift the gaze to target B with a saccade, this target was replaced by a new target (B'), which was displaced 1° toward

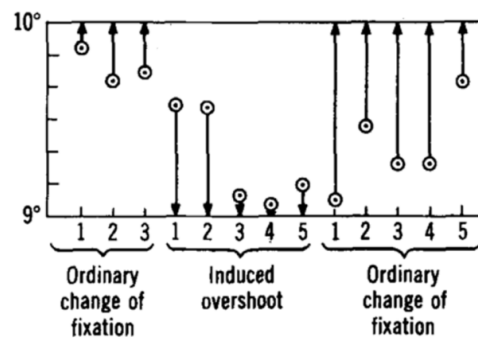


Figure 1.3: Saccadic adaptation. For more details see main text. From McLaughlin, 1967.

the original fixation point. This kind of experiment is called 'double step paradigm.' McLaughlin observed that the observer made an overshoot with respect to displacement of target B'. But after repeating the trial several times, the observers' eye movement system made an adjustment such that the overshoot gradually diminished. McLaughlin assumed that our eye movement uses an error signal after saccade landing for self-correction. Results of his experiments are shown in figure 1.3: The first three eye movements were ordinary changes of fixation (A to B movements). Humans tend to make an undershoot. In the next five trials, movements were A to B movements with B-B' switch. The first two of them show a clear overshoot, but the next three after them show the presence of a parametric adjustment. The visual target at 10° elicits an eye movement of only a little over 9° . During the last five eye movements (A to B movements without displacement), error feedback signals cause a new parametric adjustment. The second parametric adjustment is much slower than the first. McLaughlin (1967) assumed that it is because it works against the tendency to undershoot.

1.1.4.3 Saccadic Suppression

Our visual system generates a steady and clear perception of the visual world, while it is constantly executing saccadic eye movements to change the gaze. How is it that we perceive the world as clear and stable when we are moving our eyes? One answer lies in a mechanism called ‘saccadic suppression’ (Bridgeman, Hendry & Stark, 1975), which compensates for blurred and unsteady images in our perceptual system. Raymond Dodge (1900) first reported the apparent absence of visual information during the execution of saccades. He flashed small lights during the execution of rapid eye movements, and found that observers were not able to see the light. An informal demonstration of saccadic suppression is our inability to perceive our own eye movements in the mirror, while they are perfectly visibly when using the camera of a smartphone.

Is this vision impairment during saccades an achievement of an active suppression mechanism located in the cortex, or is the visual input limited because the eyes are simply moving too fast, and consequently, the brain cannot process the resulting retinal images? Thiele, Kubischik & Hoffmann (2002) investigated this research question by measuring neural signals in cortical areas MT and MST, which are assumed to process visual motion information. They compared two conditions: 1) in an active condition, rhesus monkeys were making saccades from a fixating-point towards a target, while the image that contained noise was static, 2) in a passive condition, rhesus monkeys were gazing at a fixation-point while an image containing noise was moving with the same speed as saccadic eye movements. The authors found that cortical cells did respond differently in both conditions; i.e. when the monkeys executed saccades (active condition), neurons were firing less than when the monkeys were fixating a point while the image was moving (passive condition). This finding indicates an active saccadic suppression mechanism in cortical areas MT and MST. Bremmer et al. (2009) also measured cortical response in area MT, MST, and even higher cortical areas VIP and LIP. Their data show that saccadic suppression starts well before the onset of eye movements, indicating that it is not a consequence of changes in visual input during eye movements, but rather involves a process that actively modulates neural activity.

So far, the studies briefly reviewed above indicate an active cortical saccadic suppression mechanism, but they do not deliver insight into the question of whether saccadic suppression might be implemented in a very early level of the visual system, such as the LGN in the thalamus, and inherited by later stages. To determine the locus

of saccadic suppression, Thilo et al. (2004) assessed the effect of saccades on visual sensations produced by direct stimulation of different stages within the visual pathway. More precisely, they generated small illusory visual perceptions (phosphenes) by transcranial magnetic stimulation (TMS) of the early visual cortex or by stimulation of the retina with a light emitting diode (LED). It was found that saccades suppress the visual perception, but only by stimulation of the retina. In contrast, stimulation of the cortex did not inhibit visual perception during saccades. Thilo et al. (2004) concluded that saccadic suppression arises very early in the visual processing pathway, before information feeds into early processing stages of the cortex. Other studies, however, showed that not all saccadic suppression is inherited from early visual processing stages. Chahine & Krekelberg (2008), for example, showed that the strength of saccadic suppression is determined by the combined properties of the visual input to both eyes, but binocular integration involves higher cortical areas.

1.2 Literature Review

The human visual system is excellent at determining the spatial locations of objects. For example, humans are able to determine the difference in spatial location of two objects that is smaller than the spatial resolution of the cone mosaic (Westheimer, 1975). However, as stated in section 1.1.3, motion information greatly influences the ability to determine the location of objects. Fröhlich (1923) discovered the phenomenon by showing that the starting position of a moving object appears to be shifted in the direction of motion. More than 40 years later, Thorson, Lange & Biederman-Thorson (1969) showed successively two nearby points in the periphery and parafoveally. Observers reported seeing apparent movement and that this movement extended much further than the distance between the stimulated points, but only when stimuli were shown parafoveally. Ramachandran & Anstis (1990) and De Valois & De Valois (1991) investigated these illusory motion-induced position shifts (MIPS). Hundreds of studies were introduced referencing these two publications, which shows how important they are. I will therefore begin by describing these studies in detail, before moving on to review influential and more recent publications on this field.

1.2.1 Introduction MIPS

Ramachandran and Anstis (1990) discovered MIPS when they studied the edges of moving objects that were not defined by luminance differences across their borders, but by kinetic edges. Transferring their research question into a real life scenario, a leopard standing still within fluttering foliage may be almost completely invisible (figure 1.4, right). However, as soon as the leopard is moving it becomes visible as a result of kinetic edges. Ramachandran and Anstis investigated these kinetic edges with four random dot patterns, which were continuously moving behind a static dot window (figure 1.4, left). The edges of the four small square windows were only defined by motion. Thus, if the motion of dots within these windows stopped, the windows vanished. The dots in the upper two windows drifted towards the midline, while the dots in the lower two windows drifted away from the midline and observers were fixating on a central point during a whole trial.



Figure 1.4: Kinetic edges. The figure on the left (from Ramachandran & Anstis, 1990) shows the stimulus used by Ramachandran & Anstis (1990). The four small squares were windows cut out of a stationary random-dot pattern. As indicated by the arrows, observers could see dots within the squares moving either towards the midline (upper two windows) or away from the midline (lower two windows). The picture on the right shows the research question of Ramachandran & Anstis (1990) transferred into a real life scenario: one can hardly find the leopard within the shown picture. (No photographer provided. Animal Leopard Camouflage [digital image] Retrieved from <http://imgarcade.com/leopard-camouflage.html>)

Within this stimulus arrangement Ramachandran and Anstis found that the static window positions appeared to move in the same direction as the moving dots even though their positions were stationary. Furthermore, the square array of the windows looked trapezoidal. So, the position of the kinetic edges defining the windows was displaced in its position along the direction of motion.

In a second experiment Ramachandran and Anstis studied the effect of colour information on kinetic edges on the position shift. As in the first experiment, the background was black, and the dots in the static windows were grey, but three different surround conditions were used: grey (no colour information), white (colour information), or black (invisible, no surround motion). The position shifts of the static windows were largest when the surround dots were grey, so that the kinetic edges were only defined by motion.

Furthermore, Ramachandran and Anstis tested whether the effect might be due to eye movements by using circles that contained centripetally and centrifugally drifting dots (eyeballs cannot contract or expand). Observers had to adjust the size of one circle until both were perceived to be of the same size. The same effect as in the first experiment was found: circles that contained centripetally drifting dots were perceived to be smaller than circles that contained centrifugally drifting dots. However, Ramachandran and Anstis also found a difference in position shift by using static and twinkling background dots. A twinkling background resulted in smaller position shifts, which might be due to static dots providing a frame reference.

The authors proposed that the illusory motion of the kinetic edge is caused by a sequence of events, in which strong motion signals derived from moving dots are

misapplied to the kinetic edge, so that it appears to move as well. The misperception in position was explained as a result of the anticipation of the visual system to the neural delay in visual processing (for more details see the next chapters).

Only one year later, De Valois and De Valois (1991) were wondering why the visual system performs well in vernier acuity tasks both with lines, and with large diffuse Gaussian blobs (Toet & Koendernick, 1988), and patches that differ from each other in orientation, spatial frequency or colour (Kooi, De Valois & Switkes, 1987; Burbeck, 1988) but not when there is a movement within the Gabor pattern. Neurons in the striate cortex (V1) carry information about spatial frequency, orientation, colour and direction of motion, but also about location, since they have spatially-localised receptive fields. More specifically, the data suggest that observers have precise information about which retinotopically related location on the striate cortex is activated by pattern, regardless of what particular cell types in this location may be most stimulated. However, an exception occurs when there is motion involved.

In the first experiment of De Valois & De Valois (1991), three Gabors were vertically aligned, but only the middle one contained a right or leftward sinusoidal pattern motion, while the two outer reference Gabors were flickering. De Valois & De Valois measured the perceived position of the Gabor placed in between the two static Gabors, and how the magnitude of the illusion changes with retinal eccentricity. Observers had to judge if the centred Gabor was misaligned in regard to the two reference Gabors. All observers had a positional bias in the direction motion that increases with eccentricity. Observers consistently judged the Gabors to be aligned when the centred Gabor was displaced in a direction opposite to its direction of movement.

In the second experiment, De Valois & De Valois performed an experiment to study how the bias varies as a function of spatial frequency (1, 2 and 4 cyc/°) and temporal frequency (1, 2, 4, 8 and 16 Hz). The greatest positional shift was found in the temporal frequency range of 4 Hz to 8 Hz and at low spatial frequencies (1 cyc/°). The large position shift seen at low spatial and high temporal frequency indicates that the effect is largest with high drift speed. However, the data do not indicate that the amount of positional bias is directly proportional to the speed. Using consistent spatial frequencies, the position shift decreases for temporal frequencies higher than 8 Hz.

The third experiment was conducted to test the effect of moving Gabors within four different stimulus configurations. Gabors were either placed along the horizontal

meridian (in a row) or along the vertical meridian (in a column). Each configuration consists of either radial motion (towards/away to the fovea) or tangential motion (perpendicular to the fovea). The motion-induced position shift was not confined to movement along the horizontal meridian, but radial movement gave larger biases than did the tangential movement. DeValois & DeValois also found that motion-induced position shift increases with retinal eccentricity.

De Valois & De Valois transferred their research questions into a real life scenario: Baseball players differ in regard to the perceived trajectory of a curveball. More specifically, batters report that they see the curveball suddenly dipping down before reaching the plate. De Valois & De Valois posited that the stitches in the spinning curveball are moving down diagonally on the side towards the batter as the ball approaches. When the ball gets close enough to the batter for him to perceive the movement of the stitches, the movement illusion would trigger the ball suddenly to appear to shift down.



Figure 1.5: Visual illusion when a pitcher throwing a curveball. Baseball batters report seeing a curveball dipping down just before reaching the plate. This would mean, the ball is not curving in an arc, but suddenly changing its direction, which is physically highly unlikely. For more details see main text. (Damon J. Moritz (Photographer). Baseball pitch release [digital image]. Retrieved from <https://en.wikipedia.org/wiki/Pitcher>)

1.2.2 Fundamental physiological background

The region of the retina over which visual information can influence the firing of a cell defines a receptive field of the visual system. Within the retina and the lateral geniculate nucleus we can distinguish between ‘On’- and ‘Off’-centre cells. Both cells are arranged into a central disc (the ‘centre’), and a concentric ring (the ‘surround’), with both having an inhibiting and excitatory area (see figure 1.6 A (on-cells) and B (off-cells)). ‘On’-centre cells are activated when the centre of the receptive field is illuminated, while the surrounding area is not. In contrast, ‘off’-centre cells are activated when the

surrounding area is illuminated, but the centre is not (Kuffler, 1953). Hubel (1959) measured single responses of cells within the striate visual cortex of cats when changing visual stimulation by for example lightening/darkening the room or doing hand movements along different eccentricities of the cats’ visual field. Hubel and Wiesel observed that cells have different kinds of structures, each corresponding to different stimuli and different movements. Four years later Hubel and Wiesel (1962) measured the activity of cells within the visual cortex of cats in order to investigate precisely what kinds of stimuli and

movements cause cells to start firing. They did not find circularly arranged receptive fields responding most strongly to spots of light such as described above, but cells that responded most strongly to slits, indicating that their receptive fields had a parallel arrangement of excitatory and inhibitory regions. Furthermore, they found large slits evoking a stronger signal than short slits, suggesting that

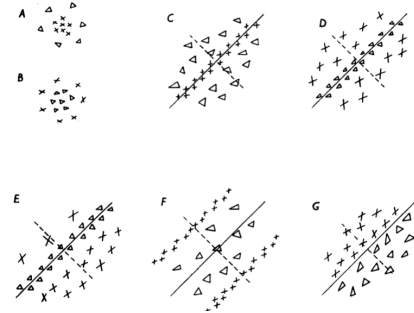


Figure 1.6: Sketches of simple receptive fields. Figure A (on) and B (off) show classical organizations of circular ‘on’ and ‘off’ receptive fields within the retina and LGN, while figures C-D show elongated receptive fields within the early visual cortex. For more details see main-text. From Hubel and Wiesel, 1962.

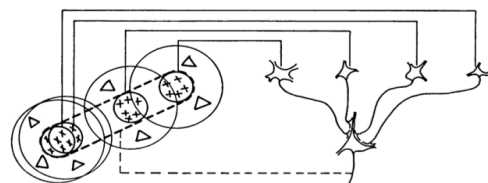


Figure 1.7: Example of the organisation of a simple cell within the visual cortex. Four ganglion cells illustrated on the left with ‘on’ centres arranged along a straight line on the retina are activated by a slit of light projected on the retina. All four ganglion-cells are activated, and send signals through the lateral geniculate body to a single receptive field within the visual cortex. The receptive field in the visual cortex has an elongated ‘on’ centre. From Hubel and Wiesel, 1962.

the cells summate signals within their receptive field. In contrast to circularly arranged 'on'- and 'off'-cells, receptive fields in the cortex are orientation selective. When the slit had a different orientation from the receptive field, the signal decreased dramatically or was even abolished. Moving stimuli were even more effective than stationary stimuli. Hubel and Wiesel suggested that this might be due to synergetic



Figure 1.8: Sketches of complex receptive fields. Crosses on the left indicate position of complex receptive fields, and the bar the position of a stimulus presented, responses of the receptive field over time are shown on the right, respectively. Bars indicate when the stimuli were presented. Upper row and lower row show responses to a stimulus presented on the upper part and the lower part of the receptive field, respectively. From Hubel & Wiesel, 1962.

effects of leaving an inhibitory area while at the same time entering an excitatory area (Hubel, 1959). Some cells responded equally to both motion directions orthogonal to the orientation of the receptive field (e.g. Figure 1.6 C-E), while others only responded to one motion direction (e.g. Figure 1.6 G). Also, the speed of the moving stimulus to which highest signals were evoked varied. Either cells responded best to speed up to 1 deg/sec, or to speed of at least 10 deg/sec. Example cells depicted in figure 1.6 F responded to slow speed.

Beside simple cells as described above, Hubel and Wiesel also found different cells with more complex structure. Cells' firing rate could only be influenced by thin, but long slits, that were arranged horizontally. When the slit was positioned on the upper half or the lower half of the receptive field, an inhibitory or excitatory response was evoked, respectively (see figure 1.8). For more details read legend of figure 1.8. Widening the slits when presented on the upper or lower receptive field did not result in a larger firing rate, indicating that there is no such summation mechanism involved as in simple receptive fields. Like simple cells, complex cells were orientation selective, and responded best to stimuli which were moving orthogonally to the direction of the receptive field in both directions. A second type of complex cell described by Hubel and Wiesel responded extremely well to slits moving orthogonally to the orientation of the receptive field. If movement stopped, the cells stopped firing. In summary, Hubel and Wiesel showed the existence of simple and complex cells within the first visual cortex of cats, and showed that orientation and motion direction plays an important role in visual processing. Because of this, and other studies Hubel and Wiesel were awarded the Nobel Prize in Physiology or Medicine in 1981.

When an object is in motion, local motion detection mechanisms do not necessarily indicate an unambiguous signal (as mentioned in section 1.1.2 The Gabor Stimulus). Figure 1.9 depicts a classical example of the aperture problem (Movshon et al., 1985); both figures have different motion directions, the diamond on the left moves downwards, while the diamond on the right moves to the right. However, local motion signals of regions as indicated by the circles, do indicate the same

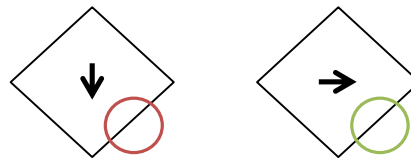


Figure 1.9: The aperture problem. The diamonds on the have different physical motion directions, the diamond on the left moves downward, while the diamond on the right moves to the left. However, motion processing mechanisms that process local motion signals, such as indicated by the circles, do indicate the same local motion direction. For more details read main text. Adapted from Movshon et al., 1985.

local motion direction. In other words, one-dimensional motion signals (such as a single edge of a diamond in figure 1.9) cannot indicate a unique motion direction, however, two-dimensional motion signals (such as a combination of at least two non-parallel edges of a diamond) can. Mathematical approaches to the aperture problem are given by ‘intersection-of-constraints’-method (Adelson & Movshon, 1982) and ‘vector-sum’-method (Wilson, Ferrera & Yo, 1992). Figures 1.10 and 1.11 shows an illustration of both the IOC-method and the VS-method by Movshon et al. (1985).

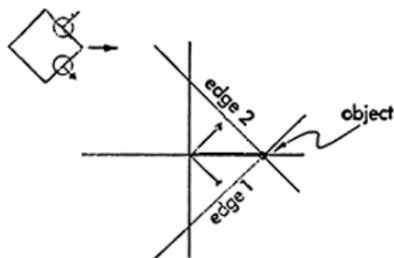


Figure 1.10: Example of VS- and IOC-Method indicating true global motion direction. The quadrant on the upper left side is moving straight to the right, while the four single borders indicate upward and downward motion. The VS-method sums up all local motion directions to the true global motion direction, and the IOC-method indicates the true global motion direction. From Movshon et al., 1985

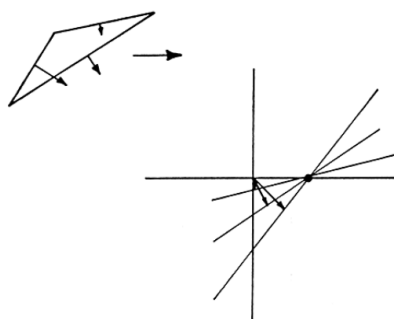


Figure 1.11: Example of VS- and IOC-Method not indicating the same global motion direction. The triangle on the upper left side is moving to the right. All three single triangle borders contain a downward component. The IOC method applied to all three borders indicates its true global motion direction, but the VS-method would fail in this stimulus, indicating a global motion direction downwards. From Movshon et al., 1985.

Adelson and Movshon (1982) investigated the neural background of global motion processing mechanisms. They asked when two superimposed gratings combine into a single coherent percept, and when they appear as moving across one another. They used one high-spatial frequency grating (target) with varying contrast, and a low-spatial frequency grating with fixed contrast. The absolute orientation and direction of both gratings were varied randomly from trial to trial. In the first experiment observers were asked to judge whether they saw a second grating. Adelson and Movshon (1982) found that the detection threshold increased monotonically with increasing contrast of the target grating. In a second experiment they asked observers whether they saw the two gratings moving coherently or sliding across one another. Data show that as the contrast increased, the likelihood of the coherence judgement also increased. In a third experiment they used this contrast dependence to measure the relative tendency of different pairs of gratings to cohere. Again, the contrast of one grating was fixed, while a staircase procedure changed the contrast of the second grating until observers saw coherent motion in half of the trials. Adelson and Movshon (1982) found that the coherence decreased as the relative and absolute speed of the component gratings increased, as the difference between their spatial frequencies increased, and as the angle between gratings increased. As described above, visual analysing mechanisms that are selective for orientation and spatial frequency exist in early stages of visual processing, and these mechanisms are sensitive to the direction of motion of one-dimensional contours (Hubel & Wiesel, 1962). The dependency of the coherence threshold on different attributes, such as spatial frequency, let Adelson and Movshon (1982) suggest that more stages within our visual system must be responsible for motion perception. More precisely, there must be a second stage of visual motion processing that computes outputs of one-dimensional motion analysers into a single coherent motion signal. For example, as shown in figure 1.12, a receptive field within higher stages processes signals arising from early stages that have different velocity preferences but similar spatial frequency preferences.



Figure 1.12: An example illustrating two-stage motion processing mechanism introduced by Adelson and Movshon (1982). The circle represents the receptive field in second-stage motion processing stage, while texture inside the circle contains random motion in all directions, but the whole texture is moving horizontally to the right (indicated by the arrow). Speed of each local motion stimulus inside the circle is proportional to the cosine of the angle between its direction and the horizontal (the global motion direction). As mentioned in the main text, such a receptive field would process signals arising from early stages that have different velocity preferences but similar spatial frequency preferences. Adapted from Adelson and Movshon, 1982.

Physiological studies revealed potential correlates of first and second order motion-processing stages in V1 and MT, respectively (e.g. Movshon & Newsome, 1984; Rodman & Albright, 1989; Movshon & Newsome, 1996). Movshon & Newsome (1996) discussed this area: MT inherits directional information from area V1, and performs more complex computations based on directional motion information originating from V1, rather than computing motion information de novo in area MT. Rodman, Gross & Albright (1989) and Girard, Salin & Bullier (1992) found, however, that selective visual responses can be elicited from MT neurons after surgical lesions or reversible cooling of area V1. Therefore, Movshon & Newsome (1996) also concluded that motion information in area MT is not completely dependent on information input from V1, but might receive visual information from other visual areas such as pulvinar (Bender, 1982) located in the thalamus.

1.2.3 MIPS in different kinds of motion

In this section I will review most recent studies that have been conducted in order to investigate what kinds of motions induce an illusory position shift. More details of these studies will be reviewed in following chapters.

1.2.3.1 Luminance defined motion and kinetic edges

As stated in chapter 1.2.1, Ramachandran & Anstis (1990) found that illusory position shifts occur in objects defined by kinetic edges, and De Valois and De Valois (1991) showed that MIPS occur in luminance-defined motion (also called first-order motion) Gabors.

1.2.3.2 Hard- and soft aperture

Kosovicheva, Wolfe & Whitney (2014) used Gabors like De Valois & De Valois (1991), but the envelopes had either a soft-aperture or a hard-aperture (see figure 1.13). They were asking whether an illusory position shift occurs when a hard-aperture indicates that the stimulus is - physically and perceptually - static, but the sinusoidal pattern contains motion energy. The MIPS was measured by (1) saccadic eye movements towards the centre of a single

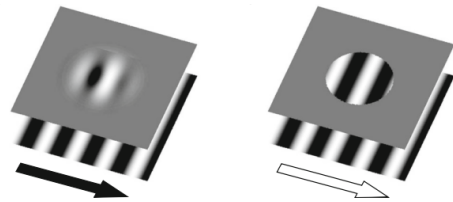


Figure 1.13: First order motion stimuli used by Kosovicheva, Wolfe & Whitney (2014). On the left: A soft-aperture stimulus as used by De Valois & De Valois (1991). The grating moves to the right, while the envelope is static on one position. On the right: A stimulus as shown on the left, but the envelope is replaced by a hard-aperture. From Kosovicheva, Wolfe & Whitney, 2014.

stimulus and (2) a key-press to indicate the relative position. In the saccade task, one Gabor with carrier moving randomly interleaved to the right or the left was presented in each trial. In the key press task two additional flickering Gabors were presented above and below the Gabor that contained carrier motion. The shift was smaller in the hard-aperture condition than in the soft-aperture condition, suggesting that the bias is not due to motion-energy on its own. Kosovicheva, Wolfe & Whitney (2014) claimed

that the visual system uses multiple information to localise objects, rather than motion information only.

1.2.3.3 Contrast defined motion

Bressler & Whitney (2006) measured and compared illusory position shifts induced by first- and second-order motion. First order motion is the movement of a luminance-defined grating, as previously described in the De Valois & De Valois (1991) stimulus. The second-order motion stimulus



Figure 1.14: Second-order contrast-defined Gabor. Dots are randomly flickering over time, while the contrast within the sine waves differs. From Bressler & Whitney, 2006.

was a dynamic random-dot pattern (see figure 1.14), modulated by a sinusoidal contrast-defined carrier that drifts in one direction, and a Gaussian contrast-modulated envelope to blur the edges of the stimulus. Luminance-defined motion and contrast-defined motion are thought to be processed by different mechanisms (e.g. Derrington & Badcock, 1985; Nishida & Sato 1995). In each trial, two Gabors (both either luminance-defined or contrast-defined) were presented above and below a fixation point, both moving in opposite directions. First- and second-order motion defined Gabors induced an illusory position shift in the direction of motion. However, the effect on perceived position was much smaller when induced by second-order motion than when induced by first-order motion.

1.2.3.4 Motion in depth

Tsui, Khuu & Hayes (2007) state that in all studies that were done before 2007, only two-dimensional stimuli were used. However, objects in natural scenes are usually in three dimensions, and thus, the visual system must generate a spatial location in depth. In order to address the question of whether illusory position shifts also exist in depth for three-dimensional stereo defined objects, Tsui, Khuu & Hayes created a three-dimensional cylinder stimulus defined by lifetime-limited dots, which were moving in depth by changes in their binocular disparities. The dots moved towards or away from the observer, or they were static, while two sets of reference lines were presented at

the bottom-left and top-right corner. Observers were asked to align the depth of the two reference corners with the near and far-end planes of the cylinder. First, they found an illusory position shift in the direction of motion. More precisely, when dots moved towards the observer, the perceived location of the two ends of the cylinder appeared to be closer in depth, and when the dots moved away from the observer, the perceived ends were further away in depth. Secondly, they found that the magnitude of the shift depended on speed, with fast moving dots inducing a larger position bias than slow moving dots.

1.2.3.5 Cyclopean motion

Murakami & Kashiwabara (2009) reviewed the study by Tsui, Khuu & Hayes (2007), and stated that the study did not distinguish whether monocular position shift was processed first, and followed by a stereo matching process, or whether a stereo matching process was followed by position shift in depth representation. Thus, in order to distinguish whether position shifts were mediated by the monocular stage or by higher visual areas in the binocular stage, Murakami & Kashiwabara (2009) presented cyclopean motion stimuli, which were only perceived as Gabors when goggle shutters presented one image to each eye. When viewed without goggles, no structure was visible. If the illusion was caused by the monocular stage exclusively, no shift would occur when showing cyclopean motion stimuli. Two vertically arranged stimuli were shown in each trial, moving in opposite directions, and observers were asked to judge whether the top stimulus was displaced to the left or to the right relative to the bottom stimulus. Cyclopean motion was found to induce position shifts, indicating that the existence of a binocular mechanisms that might cause illusory position shifts. However, they also compared the magnitudes of shifts induced by cyclopean motion to first-order motion, and found that position shifts of cyclopean motion were much smaller.

1.2.3.6 Motion defined motion

Durant & Zanker (2009) asked whether perceived position can also be shifted by

motion, which itself is defined by motion. They investigated a motion-defined motion stimulus, which is illustrated in figure 1.15: the small black and white arrows indicate opposite motion directions of black and white dots, the large arrow indicates the motion direction of the motion-defined boundaries. The dots were moving either horizontally to the right/left (parallel to the motion-defined contours) or vertically up/down (orthogonal to motion-defined contours), the envelope was moving up or downwards. Two stimuli were presented horizontally on either side of a central fixation target, and observers were asked to indicate, using mouse clicks, which stimulus was

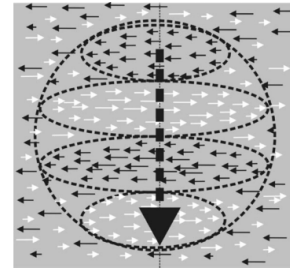


Figure 1.15: Illustration of the stimulus used by Durant & Zanker (2009) when investigating whether motion defined motion stimuli induce illusory position shifts. For more details see main text. From Durant & Zanker, 2009.

located higher. To measure the motion detection threshold, observers had to indicate, which stimulus contained upward motion of the motion-defined contours. They found that motion-defined motion induces an illusory position shift, that the shift was larger for orthogonal motion than for parallel motion, and that the size of the shift correlated with how detectable the motion-defined motion direction was. However, positional shifts still occurred when observers were not aware of the direction of the motion-defined motion.

1.2.3.7 Motion-after-effect induced motion

After adaptation to motion, a static stimulus that appears in the same position is perceived to move in the opposite direction. This effect is called ‘motion-after-effect’. In order to investigate whether there is a dissociation of visual motion and position processing, Nishida & Johnston (1999) studied the motion-after-effect on illusory position shifts.

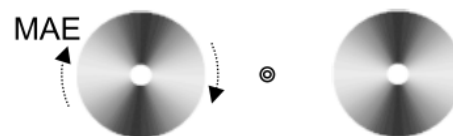


Figure 1.16: Rotating windmill causing motion-after-effects. After motion adaptation a static test windmill (left), and a static comparison windmill (right) were shown. Arrow around the test-windmill indicates the direction of the orientation shift after motion adaptation. From Nishida & Johnston, 1999.

Observers were fixating on a central fixation-dot, while a rotating adaptation-windmill was presented parafoveally (depicted in figure 1.16). After adaptation, a static test-windmill replaced the stimulus,

and on the other side of the fixation dot a static comparison-windmill appeared briefly. The dark area of the comparison-windmill as shown in figure 1.16 (right) was always vertical. Observers were asked to judge whether the dark region of the test-windmill (left) was rotated in a clockwise or anti-clockwise direction relative to the comparison-windmill. The authors found that the test-windmill was perceived as being rotated in the direction of the motion-after-effect, suggesting that this was a result of changes in apparent position. Furthermore, they found that the position-after-shift decreased more slowly and persisted longer than the motion-after-effect.

McGraw et al. (2002) investigated position-after-effects (motion-induced position shift after adaptation to motion) with relative differences in orientation, spatial frequency and contrast between adaptation and test Gabors. In addition, they asked if spatial position can be distorted in the absence of visual motion. They presented two Gabors moving in opposite directions, placed above and below a fixation-point, and observers were asked to do an alignment task. The position-after-effect remained constant over relative differences in orientation, spatial frequency and contrast, indicating that the effect was immune to changes of adaptation- and test-stimuli. However, due to previous studies it is commonly accepted that early levels of the visual cortex contain independent neural mechanisms that are selective to stimulus spatial characteristics (Blakemore & Campbell, 1969; Campbell, Cooper & Enroth-Cugell, 1969; Blakemore, Nachmias & Sutton, 1970). Therefore, McGraw et al. (2002) refer to a study of Favreau (1976), who distinguished two different kinds of motion-after-effects. Among other characteristics, one motion-after-effect can be transferred between two eyes, and another motion-after-effect showed only little interocular transfer. To investigate the role of binocularly driven neurons, McGraw et al. (2002) presented the adaptation stimulus to one eye, and the test stimulus to the other eye. They found a high degree of interocular transfer, suggesting that the interaction between position and motion processing occurs after binocular integration.

1.2.3.8 Pseudo plaid and plaid pattern motion

Two years later, McGraw et al. (2004) found additional evidence that positional after-effects might arise in area MT. When using transcranial magnetic stimulation (TMS) to disrupt cortical activity in area V1 after motion adaptation, positional after-effects were not affected, but when TMS was applied to area MT the positional after-effect

was reduced. Mather & Pavan (2009) addressed the question of whether illusory position shifts occur in the ‘first stage’ of motion processing (V1), or whether they occur in the ‘second stage’ of processing (MT). They studied different plaid pattern stimuli, which consisted of two one-dimensional motion vectors (Gabor with different motion directions) as shown in



Figure 1.17: Plaid Type I and Plaid Type II. On the left: Two one-dimensional motion vectors that form a two-dimensional motion stimulus (Plaid I). On the right: Plaid Type II motion stimuli. From Mather & Pavan, 2009.

figure 1.17. As described in section 1.2.2 Fundamental physiological background, it is assumed that the motion of plaid patterns is processed in area MT, which pools local signals to encode surface motion, while area V1 contains motion sensors, which respond to local luminance-defined motion. Thus, the logic behind the experiment of Mather & Pavan (2009) was as follows: if local motion signals at V1 influence the position assignment, position shifts of plaids should reflect the position shift induced by each component when presented separately. More precisely, either the magnitude of the plaid’s position shift is equal to the largest shift of its components, or the magnitude of the plaid’s position shift is equal to the average shift of its components. If position shifts are generated in area MT, the shift induced by plaids should be larger than the illusory shifts of single components, in accord with a motion integration computation on the components, such as intersection-of-constraints (IOC) or the vector-sum-computation (VS) (described in section 1.2.2 Fundamental Physiological Background). The use of both Type I and Type II patterns (see figure 1.17) allowed Mather & Pavan (2009) to investigate which of the two integration mechanisms (IOC or VS) were relevant to motion-induced position shifts. First, the horizontal position shifts of a Gabor (one-dimensional motion) with different orientations and velocities were measured. In a second experiment, the horizontal illusory position shifts from plaid were measured. In both experiments, two Gabors were presented above and below a central fixation point. Observers judged the relative horizontal position of two stimuli by indicating via key-press, whether the upper stimulus was displaced to the right or the left relative to the lower stimulus. After conducting both experiments, the expected motion-induced position shifts by IOC and VC method were predicted by the position shifts obtained for each component of the Gabors, using a method described by Bowns (1996). Mather & Pavan (2009) found that both pseudo plaids, Type I and Type II, appeared to be shifted much further in the direction of global motion than a

one-dimensional motion stimulus, and that the shift was consistent with an integration-mechanism that combines a vector-sum-computation and an intersection-of-constraints mechanism. Therefore, Mather & Pavan (2009) claimed that this was due to an integration process of higher visual areas.

In the same year, Hisakata & Murakami (2009) also investigated illusory position shifts of pseudo plaids (type I). In each trial two vertical gratings, oblique gratings, or pseudo plaids (as shown in figure 1.18) were presented above and below a central fixation point, moving in opposite directions. Since McGraw et al. (2002) suggested that illusory shift might be modified by perceived speed, perceived speed was equated to a vertically moving grating before comparing the illusion strength of oblique gratings to plaid patterns. Observers were asked to judge whether

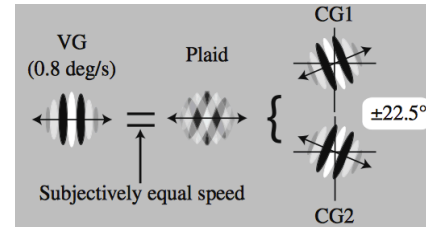


Figure 1.18: Plaid used by Hisakata and Murakami (2009). Four types of stimuli were used in the first experiment: vertical gratings (VG), plaid stimuli, and single component gratings (CG1, CG2). Plaids consisted of superimposed component gratings (CG1 and CG2), which had orientations of $\pm 22.5^\circ$, $\pm 45^\circ$, and $\pm 67.5^\circ$. From Hisakata & Murakami, 2009.

an upper stimulus was displaced horizontally to the left or to the right of a lower stimulus. Hisakata & Murakami (2009) assumed that, if illusory shifts of plaids are modified by global motion, not by components' motion, the magnitudes of shifts would stay constant regardless of angles. On the other hand, if component gratings induce illusory shifts, the magnitude of horizontal shifts in plaids should decrease as the angles decrease. Shifts obtained in plaid stimuli appeared to be constant across different plaid angles, and could not be explained by the mean of position shifts induced by oblique gratings. However, Hisakata & Murakami (2009) next considered the possibility that the luminance of two components was additive, and therefore, the intersections of two superimposed gratings could be transferred into feature-tracking motion (Bowns, 1996) that is consistent with the direction of global motion (Burke, Alais & Wenderoth, 1994). In order to distinguish whether the measured shift might be due to these motion cues, they investigated illusory position shifts of pseudo plaids. As shown in figure 1.19, pseudo plaids consisted of multiple Gabors with different orientations, and without spatial overlap of local motion components. Gabors were

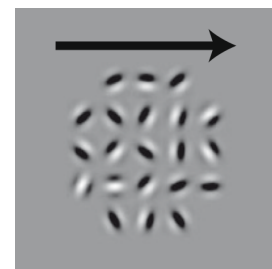


Figure 1.19: Example of a pseudo plaid. Pseudo plaids consist of multiple Gabors with different orientations, but different single speed, so that the global speed is consistent with one global motion direction. From Hisakata & Murakami, 2009.

moving with different single speeds, but the global speed was consistent with the global motion direction. The speed of each Gabor depended on its orientation. The procedure was the same as described in the first experiment, perceived speed was manipulated by changing the signal to noise ratio. Measured illusory shifts induced by pseudo plaids were compared to a prediction of averaged motion-induced position shifts of single Gabor patches. Hisakata & Murakami (2009) found that pseudo plaids (Type I) induced much larger position shifts than the single component motion of obliquely oriented gratings, and could not be predicted by average component motion. Furthermore, they found that magnitudes of illusory position shifts induced by pseudo plaids increased with perceived speed, and were not predictable by shifts of single Gabors, suggesting that illusory position shifts take place after global motion integration.

In summary, the conclusions of Mather & Pavan (2009) and Hisakata & Mukarami (2009) are consistent. Mather & Pavan (2009) attempted to establish whether position shifts were in accord with the VS-method or the IOC-method, but did not find a consistent pattern in data. My suggestion is to study the motion-induced position shifts of pseudo plaids with perceived speeds being consistent across different stimuli (one dimensional gratings and pseudo plaids).

Rider, McOwan & Johnston (2009) also found illusory position shifts in pseudo plaids. In order to test whether the perceived position shift was determined by the global motion of the whole pattern, or by a low-level mechanism that aggregates shifts of the elements, Rider, McOwan & Johnston compared pseudo plaid patterns with randomly oriented Gabors (as shown in figure 1.19) to pseudo plaid patterns with vertically oriented Gabors, both containing the same global velocity. The speed of the single Gabors in the parallel condition was set to the global speed times the cosine of the angle between the global motion and the direction normal to the contours of the Gabors. If the shift were determined by low-level mechanisms and aggregated, only those elements with carriers that moved in the global motion direction would be maximally shifted in the global motion direction, and the other elements would be shifted to a lesser degree in the global motion direction. The aggregate shift of randomly oriented pseudo plaid patterns should be smaller than the shift induced by pseudo plaid patterns containing Gabor elements oriented orthogonally to the global motion direction. On the other hand, if the illusory position shift occurs after motion integration, no difference in magnitudes of shifts was expected. In each trial, pseudo

plaid patterns were shown above and below a central fixation dot, both either drifting to the right left or to the right, but always in opposite directions. Observers had to indicate by button press whether the upper stimulus was shifted to the right or to the left relative to the lower stimulus. All observers had a position bias in the direction of global motion in both stimuli, but there was no difference between shifts in the parallel condition and the random condition. Rider, McOwan & Johnston took into account that the measured position shift might be a result of some mechanism that captures the illusory position shift of vertically oriented Gabors that have the highest drift speed, and therefore, will be shifted the most. Thus, Rider, McOwan & Johnston presented pseudo plaids consisting of only vertically oriented Gabors, which had the same distribution of horizontal velocity as in the random condition of the first experiment. The illusory shifts of those patterns were much smaller than the position shift in both conditions (parallel and randomly orientated Gabors) of the first experiment, suggesting that localisation of object position must indeed be generated after global motion computation.

1.2.3.9 Component motion and global motion

As described within this section, motion-induced position shifts may also arise in high-level processing stages that process global motion information (e.g. Mather & Pavan, 2009; Hisakata & Murakami, 2009; Rider, McOwan & Johnston, 2009). Kohler, Cavanagh & Tse (2015) investigated to what extent component motion or global motion contribute to motion-induced position shifts, when both signals compete against one another in the same stimulus. They evoked motion-induced position shifts using the flash grab effect, which induces biases up to several deg of visual angle (Cavanagh & Anstis, 2013). The flash-grab effect occurs when a static stimulus is briefly presented beside a moving stimulus that reverses its direction just at that moment. The static stimulus is perceived displaced in the direction of motion after reversal. Bistable diamond stimuli moving horizontally to the right and the left were shown, and were either without any occlusion (figure 1.20 upper panel), with occlusion (figure 1.20 mid panel) so that line segments of the diamonds appeared to be independent (Lorenceanu & Shiffar, 1992), or they were occluded and a thin outline indicated the edges of the occluders (figure 1.20 lower panel). In the latter case diamonds were perceived as a whole, since the colour indicated that occluders did not

belong to the background (Lorenceanu & Shiffar, 1992). Kohler, Cavanagh & Tse assumed that diamonds were perceived to move horizontally when no occluders were presented, and when occluder outlines were coloured. When occluders were indistinguishable from background, however, the diamond lines appeared to move vertically. In other words, the physical motion direction was the same in all three conditions, but the perceived motion directions were different ('aperture problem' as described in chapter 1.2.2 Fundamental physiological background). To confirm this, observers had to indicate the perceived motion direction of the three stimuli described above. Therefore, two diamonds

- either full diamonds, diamonds with outlined occluder, or only line segments - were presented at the same time, one on the right side, and the other one on the left side relative to a central fixation cross. Each diamond moved horizontally towards the central fixation, remained briefly, and then reversed its direction away from

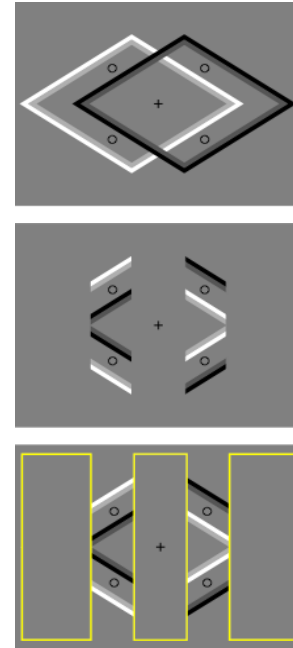


Figure 1.20: Stimuli used to test whether component motion or global motion contribute to motion-induced position shifts. For more details read main text. From Kohler, Cavanagh & Tse, 2015.

fixation where they remained while the other diamond made the same movement. Whilst presenting the moving stimuli, a dumbbell was shown on a second screen, and observers used keys to adjust its angle such that it matched the perceived motion direction. As expected, Kohler, Cavanagh & Tse found that full diamond stimuli were perceived to move horizontally, while in the line segment condition, the stimuli were perceived to move vertically. Against expectation, the perceived motion direction of diamonds with outlined occluders was closer to vertical than horizontal. In the main experiment, the direction and magnitude of the position shift were measured by presenting dots superimposed on one of the four diamond line segments just briefly when diamonds changed motion direction. When observers indicated by key press that they were aware of the dots' position, diamonds disappeared from the screen and were replaced by a dumbbell at the dot location. Observers next adjusted the dumbbell's angle and width such that it matched the perceived angle and distance between the previously presented dots. The complete diamond condition induced a significantly larger (more horizontal) angle in position shift than line segment and also outlined occluder conditions. Outlined occluders led to more horizontal shifts than line

segments. Regarding the magnitude of shifts, Kohler, Cavanagh & Tse found the line segment condition led to larger shifts than either the complete diamond or the outlined occluders conditions, but the magnitude did not differ significantly. Local component motion can only be read by motion detectors when they are almost orthogonal (up to 15 deg) to the angle of the moving edge (Nakayama & Silverman, 1988). Therefore, the expected angle of the shift induced by global motion of the diamond was predictable, and served to measure how much global motion affects the position shifts. The authors found that global motion had an influence on the direction of motion-induced position, but the perceived position of flashed dots was dominated by local motion. This finding may be consistent with a suggestion by Rider, McOwan & Johnson (2009), that the motion-induced position shift in pseudo plaids might be – to some extent – caused by a local motion processing mechanism.

1.2.3.10 Motion without spatially located motion cues

Mussap & Prins (2002) addressed the question of whether illusory position shifts still arise when motion signals cannot be separated by local spatial signals, or luminance profiles. Three vertically aligned horizontal rectangular apertures with 200 dots in each aperture were shown in each trial. ‘Background-dots’ were moving coherently to the right or to the left, superimposed on ‘envelope dots’, which were either static, or moving in randomised directions. The percentage of coherently moving ‘background-dots’ varied over trials between 5%, 10%, 20%, and 40 %. In experiment 1, the luminance of all dots was determined on the basis of the dots’ horizontal position according to a Gaussian function (see 1.21, upper panel). Observers were asked to indicate by key-press the

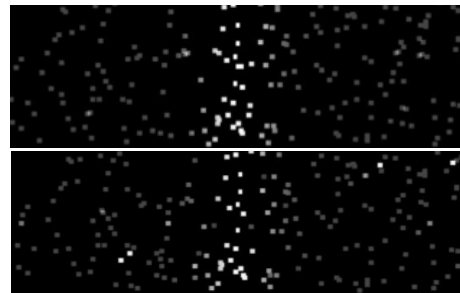


Figure 1.21: Stimulus where motion signals cannot be separated by local spatial signals, or luminance profiles. In both panels: ‘Background-dots’ coherently moving to the right or left were superimposed on ‘envelope dots’, which were either static, or moving in randomised directions. Upper panel: Experiment 1. The luminance of all dots - ‘envelope dots’ (which were either static or moving in randomised directions) and coherently moving ‘background dots’ - was determined on the basis of their horizontal position according to a Gaussian function. Lower panel: Experiment 2. The luminance of coherently moving ‘background dots’ is randomised, and therefore, it is uncorrelated with the luminance of ‘envelope dots’. For more details see main text. From Mussap and Prins, 2002.

perceived location (left versus right) of the global, luminance-defined envelope of the central region. The authors found illusory position shifts in the direction of coherently moving background-dots in both conditions (static and randomised envelope-dots), increasing as the percentage of coherently moving background-dots increased. However, the effect was smaller in the static condition when more than 5% of dots were moving coherently. Because the coherently moving background-dots had the same luminance profile as envelope-dots, Mussap & Prins suggested that the measured illusory shifts might be attributed to motion of some proportion of the dots forming the envelope. This would also explain why the condition with static envelope-dots, induced much smaller position shifts than the condition with randomly moving envelope-dots. In order to distinguish whether the effect in position might be due to the motion of parts of the luminance envelopes, the luminance of coherently moving background-dots in the second experiment was randomised at the onset of stimulus presentation, i.e. dots did not carry a luminance envelope (see figure 1.21, lower panel). Also in this experiment Mussap & Prins found illusory position shifts when at least 20 % of dots were coherently moving in one direction. The results indicate, that position shifts are not limited to coherently moving motion signals, still occurring with random motion directions that are integrated in higher visual areas to form global motion perception.

1.2.3.11 Remote and passive motion

As mentioned before, motion-after-effects of luminance-defined stimuli induce position-after-effects (McGraw et al., 2002; Nishida & Johnston, 1999). Position-after-effects even occur when the target is not at the site of adaptation ('remotely') (Whitney & Cavanagh, 2003), and when the direction of the motion cannot be detected ('passively') (Whitney, 2005; Whitney 2006). Since we know that contrast-defined motion induces illusory position shifts (Bressler & Whitney, 2006), and motion-after-effects (Ledgeway & Smith, 1994), Harp, Bressler & Whitney (2007) wondered, whether

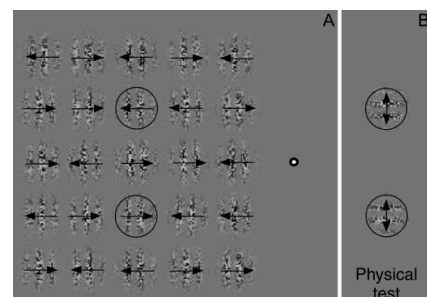


Figure 1.22: Stimulus inducing a position-after-effect passively. A: Motion adaptation to an array of Gabors. The circled Gabors had the same motion direction within all trials, while the motion direction of other Gabors was randomised. Dots on the right of the array indicate fixations dot. B: Drift balanced stimuli overlaid on the test Gabors after motion adaptation. For more details see main text. From Harp, Bressler & Whitney, 2007.

contrast-defined motion induced position-after-effects, and if so, whether they occurred passively and remotely. First, they investigated whether position-after-effects of second order motion stimuli (as shown in figure 1.11) arise passively. Therefore, an array of Gabors as shown in figure 1.22 (A) was presented parafoveally. The motion directions of adaptation Gabors were randomly determined, but motion directions of two target Gabors (circled in figure 1.22 (A)) were the same throughout all trials. After an adaptation period, test Gabors (shown in figure 1.22 (B)) were shown in the position of previously presented target stimuli. Test stimuli were identical to

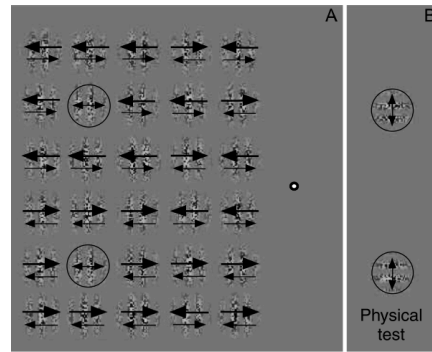


Figure 1.23: Stimulus inducing a position-after-effect ‘remotely’. A: Motion adaptation to an array of Gabors that contain motion information in two directions. The circled Gabors have drift balanced motion. Dots on the right of the array indicate fixations dot. B: Drift-balanced test stimuli overlaid on the test Gabors after motion adaption. For more details see main text. From Harp, Bressler & Whitney 2007.

target stimuli, but rotated by 90 deg and drift-balanced, which means that two contrast-modulated sine waves were moving upwards and downwards at the same time. Thus, stimuli contained no net directional motion. Within each trial all observers were asked to do two tasks. During the adaptation phase they indicated whether the upper target Gabor was moving to the right or to the left, measuring the effectiveness of crowding. After adaptation, they were asked to report whether the top test Gabor was displaced to the right or to the left relative to the lower test Gabor (figure 1.22 B). Observers reported seeing the test Gabors as being misaligned in the opposite direction of motion, while performing only at chance when judging the motion direction during the adaptation phase. These results indicate that position-after-effects occur after local motion adaptation to contrast-defined stimuli, although crowding prevents the observer from being aware of the motion direction of the adapting stimulus. In order to compare the results to position-after-effects of second order stimuli without crowding, the same procedure was used, but only two Gabors were shown during adaption and test periods. Harp, Bressler & Whitney found that the position-after-effect was smaller, but not significantly smaller than in the crowded condition, and observers were able to reliably detect the direction of motion. In the third experiment Harp, Bressler & Whitney (2007) tested whether position-after-effects also occurred remotely. In other words, whether a positional after-effect also occurred when Gabors were presented in an unadapted region of the crowded array.

The stimuli were similar to those used in the first experiment, but the two test adaptation Gabors (circled) were drift balanced, moving to the right and the left. As shown in figure 1.23 (A), surrounding Gabors were separated into a top half and a bottom half. Each half contained Gabors with oppositely drifting sine waves. As indicated by the size of the arrows, the Gabors were not drift-balanced. The modulation depth of one of the contrast-defined sine waves was increased up to 79% Michelson contrast, while the contrast depth of the oppositely drifting sine waves was reduced to 37%. Thus, top and bottom Gabor arrays contained net motion in opposite directions. The two columns closest to the fixation point differed to ensure that crowding was still effective. Test Gabors were the same as in the first experiment. First, observers were asked to judge the net motion direction of the top half Gabor arrays. Second, they judged the relative position of the two test Gabors. Harp, Bressler & Whitney state that central adaptation-Gabors contain no directional motion, and therefore, there should have been no motion adaptation, and thus, no positional after-effect. However, again they found shifts in the opposite direction of motion, when at the same time, observers were not aware of net directional motion in the crowded Gabor arrays. In summary, the authors showed that position-after-effects in second order stimuli occur 1) although crowding prevents the observer from being aware of the motion direction of the adapting stimulus ('passively'), and 2) when the target is not at the position of adaptation ('remotely'). These findings indicate that 1) feature or attentive tracking mechanisms - as described by Cavanagh (1992) - are not required to mediate motion perception, and 2) the mechanisms that are involved do not rely on location based attentional processes.

1.2.3.11 Carrier motion, envelope motion and retinal motion

In contrast to conventional studies, Hisakata, Terao & Murakami (2013) did not study the motion-induced position shift by using static envelopes and static eye positions (fixation), but motion-induced position shifts of Gabors when envelopes and eyes were either moving or static (see figure 1.24). They addressed the question of which kind of motion determines the illusory shift: 1) envelope-relative velocity, 2) retina-relative motion, or 3) display-relative motion. First, they asked whether the position shift still exists when the envelope of a Gabor-stimulus is moving and the eyes are fixating. Therefore, leftward and rightward moving envelopes were each combined with a range of right and leftward moving carrier motion velocities. By fixating on a

static target, the velocity of the envelope on the display (display-relative velocity), and the velocity of the envelope on the retina (retina-relative velocity) were the same, but with varying velocities of the carrier, different envelope-relative velocities were obtained. An envelope of a vertically oriented Gabor patch was moving rightwards

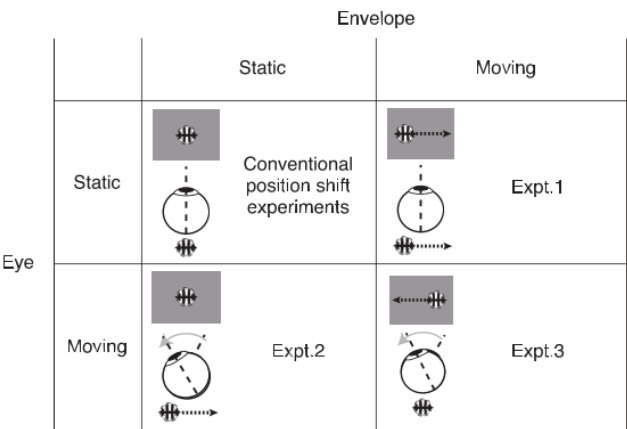


Figure 1.24: Experiments conducted to test whether display-relative-velocity, envelope-relative-velocity or retina-relative velocity determines the motion-induced position shift in perception tasks. For more details read main-text. From Hisakata, Terao & Murakami, 2013.

underneath a central fixation dot, while its carrier was moving. After 750 ms, a second horizontally oriented Gabor appeared above the vertically oriented Gabor. Its envelope moved rightwards with the same speed, but its carrier was static. 250 ms later, the observers were asked to judge the vertical alignment of the two Gabors. The results show that the position shifts occurred when the envelope of the stimulus was moving. Furthermore, they found that illusory shifts increased with the carrier-velocity; the higher the carrier-velocity, the higher the shift. No shifts were observed when envelope-relative-velocity was zero. Even when the carrier-velocity was zero and the carrier-envelope-relative-velocity was not, the motion-induced position shift was not zero. In a second experiment, the envelope or the Gabor was static, but the eyes were moving, following a moving target. By fixating on a moving target, the velocity of the envelope on the display (display-relative velocity), and the velocity of the carrier relative to the movement of the envelope (envelope-relative velocity) were the same, but with varying velocities of the carrier, different retina-relative velocities were obtained. Hisaka et al. found that the position shift increased when the envelope-relative-velocity was in the same direction as the retinally moving envelope, but it disappeared when the carrier relative velocity moved in the opposite direction. This asymmetry was not found in the third experiment, where a stimulus moving parallel to the eyes, cancelled out only the retinal motion. By fixating on a moving target, while the envelope of the Gabor was moving with the same speed, the velocity of the envelope on the retina (retina-relative velocity), and the velocity of the carrier on the envelope (envelope-relative velocity) were the same, but with varying velocities of the

carrier, different display-relative velocities were obtained. They found position shifts of equal size when envelope-relative-velocity and with that the retina-relative velocity were non-zero, and no position shift when those velocities were zero. In summary, they found that perceptual motion-induced position shifts are primarily induced by envelope-relative velocity. The authors suggested that MIPS are less reliable when they are towards the future direction of the retinal motion. This means that when eye movements are involved, the system interprets the position of the envelope as being more likely somewhere along the previous trajectory than being somewhere along the extrapolated trajectory. Therefore, Hisakata, Terao & Murakami assume that the visual system is presumably tracking objects by integrating incoming position and motion signals over time with predictive information from the recent past to continuously update perceptual estimates of an object's position and motion.

1.2.4 Why and how does MIPS arise?

Do we benefit from motion-induced position shifts (MIPS), or are they simply caused by an imperfect visual mechanism, and therefore, may even be misleading us in everyday life? In this section I will describe ideas of why MIPS occur and what neural mechanisms are underlying MIPS.

1.2.4.1 Compensate delay in visual processing

Motion perception is a basic skill of our visual system to cope with everyday-life situations, such as planning visually guided actions to avoid having a collision with static and moving objects. One explanation of why illusory position shifts occur is based on the hypothesis that retinal processing and transfer to the brainstem can take 30-100 ms (Maunsell & Gibson, 1992). In order to conduct visually guided actions, we have to compensate for this temporal asynchrony between physical changes within our environment and visual perception (e. g. Ramachandran & Anstis, 1990; De Valois & De Valois, 1991; Yamagishi, Anderson & Ashida 2001). In other words, the motion-induced position shift is a product of a mechanism compensating for the fact that we are living in the past.

How does the visual system compensate for that delay?

One possible mechanism for compensating for this temporal asynchrony between the environment and our perception might be a shift in the receptive field position within the first visual cortex (V1). Normally, a stimulus that is presented eccentrically to the fovea should be represented in a more anterior location in the visual cortex than a stimulus that is presented closer to the fovea (Serenio et al, 1995; Daniel et al. 1961). However, Whitney et al. (2003) investigated drifting Gabors through an fMRI study where they found that the perceived position of the Gabor pattern was shifted in the direction of motion, but the peak activity in the visual cortex was always shifted in the opposite direction of the motion direction. In other words, Gabor patterns with an internal motion direction away from the fovea were represented closer to the occipital pole (see figure 1.25). The result of a single cell recording study by Fu et al. (2004) is consistent with the results of Whitney et al (2003), who showed that motion induces cortical shifts in receptive fields in the primary visual cortex of a cat. But the

hypothesis is inconsistent with psychophysical studies described in the previous chapter (Mather & Pavan, 2009; Hisakata & Murakami, 2009; Rider, McOwan & Johnston, 2009) which found that MIPS are produced by plaid and pseudo plaid motion. Their idea is based on the assumption that low-level motion processing in the visual system involves two stages (described in chapter 1.2.2 Fundamental physiological background). The first stage of visual processing within the striate cortex V1 responds to local motion. The second stage of visual

motion processing within higher visual areas combines local signals into a global coherent motion percept. Another property of motion-induced position shifts is that they occur when edges are blurry, but not when edges are hard (Kosovicheva, Wolfe & Whitney, 2014). There is no explanation for hard edges causing a shift in the receptive field, but soft edges do not cause a shift in the receptive field.

Also Arnold, Thompson, and Johnston (2007) state that motion-induced position shift is not a result of a shift in receptive field. They measured illusory position shifts at the trailing edge, the leading edge, and the centre of luminance defined Gabors. If the motion-induced position shift was caused by a shift in the receptive fields, all regions of the stimulus that fall into the receptive field would be equally affected. However, they found large effects at trailing and leading edges of drifting Gabors, but the internal contour of the Gabor was not affected by motion. Arnold, Thompson, and Johnston suggested that a contrast modulation mechanism might effect the shape of the Gabor. More precisely, an increase of perceived contrast at the leading edge, and a decrease of perceived contrast at the trailing edge would cause the position shift.

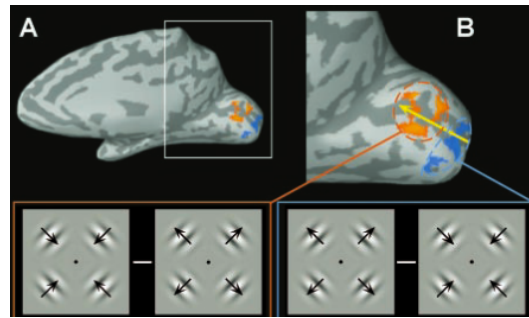


Figure 1.25: Results of one observer obtained in a fMRI study by Whitney et al. (2003). Panel A: The cortical surface, with the occipital lobe being activated (orange and blue colour). Panel B: A close-up view of the same surface as shown in panel A. The direction of the yellow arrow indicates increasing eccentricity in the visual field. Whitney et al. presented four Gabor stimuli around a fixation dot. Gabors were either drifting inwards (towards the fovea) or drifting outwards (away from the fovea). When the two conditions were subtracted, there was a significant resulting activation (inward-outward motion shown in orange, outward-inward motion shown in blue). From Whitney et al., 2003.

Chung et al. (2007) were more precise, when suggesting that a position shift might be due to a modulation of a motion activated gain field. They explain that the concept of a gain field is distinct from the concept of a receptive field in the following way: a visual receptive field defines a spatial region over which a neuron's response can be modulated by a visual input. The spatial

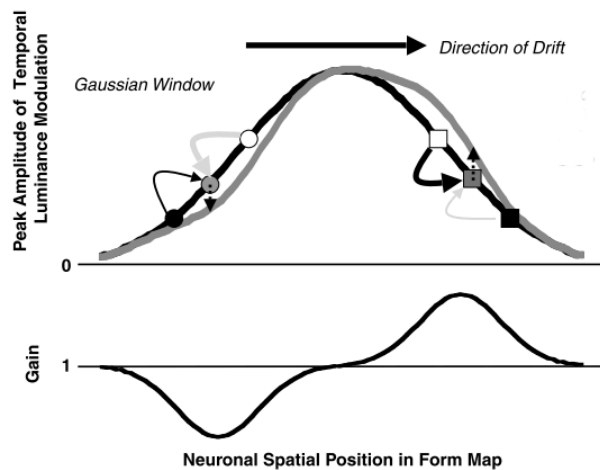


Figure 1.26: Motion-induced position shifts may be generated by a motion activated gain field. For more details read main text. From Chung et al., 2007.

interaction within a receptive field can produce activity in the target neuron. A gain field defines a spatial region over which a neuron's gain can be modulated by a visual input. The spatial interaction within a gain field can only modulate activity in the target neuron's on going activity. A neuron within a gain field receives a signal to increase/decrease its gain from neighbouring neurons, which are retinotopically to the left/right. The gain-decrease-signal removes persisting signals that would otherwise be left over from an object that has moved to another location, while a gain-increase-signal prepares neurons in the gain field that are likely to be excited by a moving stimulus in the future, in order to increase the speed to this response. Figure 1.26 (upper panel) illustrates the influence of a motion-activated gain field (thick grey curve) produced by a rightward drifting Gabor (thick black curve). The curved arrows represent the 'gain change' signals that a single neuron receives from its neighbours. The thickness of the arrow represents the magnitude of the gain change signal. Black arrows represent gain-increase signals, while grey arrows represent gain-decrease signals. Two example locations are illustrated: one at the leading edge (filled grey square) and another at the trailing edge (filled grey circle) of the Gabor. At the trailing edge, the gain-increase signal is lower than the gain-decrease signal, and thus, the net effect is to reduce the peak amplitude of luminance modulation at that location (downward dotted arrow). The opposite effect (upward dotted arrow) occurs for the location leading edge. The thick grey curve represents the peak amplitude of luminance modulation after the gain changes reach a steady state (lower panel).

However, a modulation in gain fields would not explain illusory shifts found in the study by Mussap and Prins (2002).

Another way to compensate for the neural delay was put forward by Ramachandran and Anstis (1990), who posited that motion signals from the internal motion are misapplied to the edges of the envelope, causing the envelope to appear shifted in the direction of motion. This is in contrast to the results of Mussap and Prins (2002), who found that illusory position shifts still arise when motion signals cannot be separated by local spatial signals, motion cues or luminance profiles. Furthermore, Chung et al. (2007) showed that illusory position shifts vary non-monotonically with velocity (see section 1.2.5), and therefore, concluded that shifts cannot be explained by a misapplication of motion signals to the edges of a moving stimulus. If the edges were misapplied, the magnitude of the shifts would be correlated with the velocities.

1.2.4.2 Prediction of the likely future

Roach, McGraw and Johnston (2011) put forward another hypothesis. They found evidence that the visual system uses a predictive signal at the leading edge of a drifting Gabor, generated by a forward model representing the likely future pattern of visual input. As shown in figure 1.27, they presented two high contrast inducer-Gabors on the right and on the left relative to a central fixation cross. A small low contrast target-Gabor drifting with the same speed and motion direction was presented at the leading

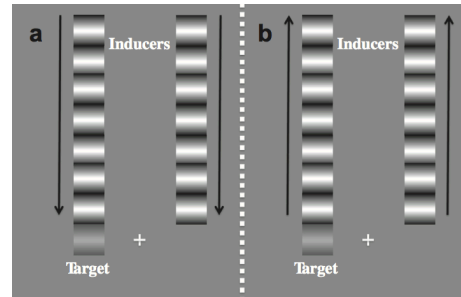


Figure 1.27: Stimulus to measure detection threshold at trailing and leading edges of a Gabor. Stimuli to measure detection thresholds of abutting target Gabors placed at the leading edge (panel on the left, a), and Gabors placed at the leading edge of drifting Gabor pattern (panel on the right, b). From Arnold, Marinovic & Whitney, 2014.

edge (see figure 1.27 a) or the trailing edge (see figure 1.27 b) of only one inducer-Gabor. Roach, McGraw & Johnston measured the ability of the observer to detect the target-Gabor containing varying phases in its sine waves. If a drifting low contrast target-Gabor was placed at the leading edge of a drifting high contrast inducer-Gabor, target sensitivity was enhanced when the target-Gabor was in-phase with the inducing-Gabor (see figure 1.28 a), relative to when they were out-of-phase (see figure 1.28 b). This effect was not found at the trailing edge of drifting Gabor edges. Hence, Roach,

McGraw & Johnston concluded that motion induces a forward prediction of spatial pattern that combines with cortical representation of the future stimulus.

This approach might be in contrast with a study by Eagleman & Sejnowski (2006), who investigated the flash-lag effect, wondering whether it was due to such a motion extrapolation mechanism that predicted the future location of a stimulus. If there is a mechanism extrapolating the object's position in the direction of motion, the flash-lag effect should also occur at the moment when the moving object reverses its direction mid-flight. Eagleman and Sejnowski presented a ring moving in a circular trajectory. When the ring reached the opposite side, a disc was presented briefly in the centre of the ring. After the flash, the ring either continued moving in the same direction, the opposite direction or stopped moving. Observers reported whether the flashed disc occurred above or below the ring. When the ring stopped moving no position shift was measured. When the ring continued moving in the same direction after the flashing of the disc, observers perceived the disc as lagging behind the moving ring. When the ring reversed its direction, however, observers perceived the disc as in front of the moving ring, resulting in a flash-lead-effect instead in a flash-lag effect. Thus, Eagleman & Sejnowski concluded that interpolation of the past, rather than a predictive model (motion extrapolation) would be a framework that explained the flash-lag phenomenon.

1.2.4.3 Spatial summation process

Arnold, Marinovic and Whitney (2014), suggest that target sensitivity adjacent to motion is modulated, not as a result of predictive signals, but because signals concerning proximate physical inputs summate everywhere except at the trailing edge. To assess whether the phase contingent target-inducer interaction reflects a process to predict the future location of the stimulus at the leading edge and not at the trailing edge, or whether it reflects a phase contingent spatial summation (Anderson and Burr, 1985), that is reduced at the trailing

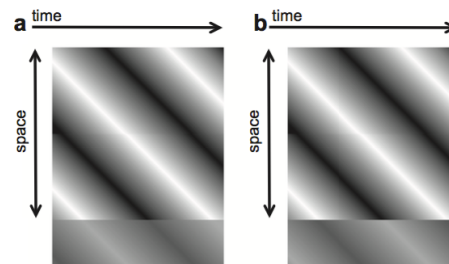


Figure 1.28: Space-time plots of a Gabor. Space-Time plots depicting high contrast waveforms of inducer-Gabors (above), and low contrast waveforms of the target-Gabors (below). The targets are placed at the leading edge of the inducer-Gabor. Panel A on the left shows the target-Gabor in-phase with the inducer Gabor, Panel B on the right shows the target-Gabor out-of-phase with the inducer Gabor. From Arnold, Marinovic & Whitney, 2014.

edges of Gabors, Arnold, Marinovic & Whitney (2014) used the same procedure as Roach, McGraw & Johnston (2011); two high contrast inducer Gabors were presented on the right and the left relative to a central fixation-cross, only one low contrast target-Gabor was presented at the trailing edge or leading edge of one inducer Gabor. Observers were asked to indicate where the ‘faint’ target-Gabor had been presented. As in experiments by Roach, McGraw & Johnston (2011), the target-inducer-phase relationship varied across trials. They found that if the two Gabors were in-phase, the detection threshold was higher than when they were out-of-phase, in both the trailing and the leading edge. The effect on the detection threshold was weaker along the trailing edge, but still significant. Arnold, Marinovic & Whitney state that this result is in contrast to results obtained by Roach, McGraw & Johnston. They tested Gabors with relative phase offsets of 0 deg, 90 deg, 180 deg and 270 deg, and conducted an ANOVA to find out whether there was a significant difference between the mean detection thresholds. A small p-value within an ANOVA indicates that at least one (also implying that maybe only one) mean value differs in respect to the other mean values. Multiple comparison of single datasets would be more convincing. However, they also found that the detection threshold changed with phase offsets when they used directionless flickering Gabors, which did not generate a predictive signal. Arnold, Marinovic & Whitney state that the strongest argument against a non-predictive phase contingent spatial summation process is based on results when observers were asked to detect the absence of a signal at the trailing and leading edge. If a predictive model caused changes in sensitivity threshold, the threshold to detect the absence of an object at the trailing edge would be higher than the threshold to detect the absence of an object at the leading edge. On the other hand, if a non-predictive phase-contingent spatial summation reflects a summation of physical inputs, the absence of a signal at the leading edge would not be harder to detect than at the trailing edge. They presented two Gabors; one was clipped while the other one was not. Observers were asked to indicate which of the two Gabors presented above or below a fixation dot had a clipped edge. Indeed, they found that the sensitivity threshold to detect the absence of a signal was even higher at the leading edge than at the trailing edges and the sides. Arnold, McGraw and Whitney suggested that there is no model involved that predicts the likely future, but a non-predictive phase contingent spatial summation process.

1.2.4.4 Motion deblurring mechanism

Another hypothesis for the basis of MIPS is related to the idea of motion smear (Burr, 1980). Marinovic and Arnold (2013) state that - to some extent - human vision can be thought of as a camera with a slow shutter speed (see figure 1.29). Visual information is integrated over ~ 100 ms (Barlow, 1958).



Figure 1.29: A photo when the camera had a shutter speed of 125 ms. Humans are assumed to integrate signals over a similar temporal interval. Surprisingly, they do not perceive motion streaks. From Burr, 1980.

Researchers asked whether images that move across the retina generate motion blur signals as a camera would do. It was shown that motion blur signals can be detected in the recording of brain activity (Geisler et al., 2001). The question of whether we ‘see’ motion blur has been controversial. For example, Burr & Morgan (1997) claim that humans are not able to discriminate if a moving object is sharply focused or blurred, while Burr, Ross and Morrone (1986) reported that our visual system suppresses motion blur from our awareness.

In the study by Whitney et al. (2003), a larger BOLD-Signal was found to stimuli in the opposite direction of motion. Larger BOLD Signals might not only signal increased neuronal activity, but a result of an inhibitory interaction to suppress visual responses (Mathiesen, Caesar & Lauritzen, 2000). Hence, Whitney et al. (2003) suggested that the larger BOLD-Signal to stimuli in the opposite direction of motion could be due to a suppression mechanism to reduce luminance contrast in order to diminish motion blur in the trailing edges of the drifting pattern. Arnold, Ross & Morrone (2007) and Tsui, Khuu & Hayes (2006) agreed with that approach after they measured illusory position shift at the edges and the centre of drifting pattern. Tsui, Khuu & Hayes (2006) found that the position shift effect is a consequence of a centroid shift of the Gabor envelope (described extensively in section 1.2.5); i. e. the leading edge was perceived to be further away from the mid point of a drifting Gabor compared to when the Gabor pattern was stationary. That effect was not found on the trailing edge of the Gabor. Thus, the whole pattern is perceived to be larger than an identical but stationary Gabor on the leading half of the stimulus. In other words, there

is a clearer percept at the trailing edge than on the leading edge. Tsui, Khuu & Hayes (2006) assumed that this result could be due to a reduction of motion smear at the trailing edge, or/and the elongated leading edge might be due to an extrapolation mechanism to compensate for the neural delay described above.

Assuming that the visual system does have a motion deblurring mechanism, it may account for the effect on the leading edge of a moving stimulus. The theory of motion extrapolation at the leading edge, however, is more controversial.

1.2.4.5 Bayesian Theory

Hisakata, Terao & Murakami (2013) suggested that a Bayesian approach would account for illusory position shifts. Bayesian theory is a concept in the field of statistics, in which the probability of a true object state is assessed using a ‘prior’ probability, and then refined with new measurements. As described in chapter 1.2.3, the authors did not study motion-induced position shifts by using static envelopes and static eye positions, but by using Gabors with the envelope moving or static, and the eyes either moving or static. When the carrier was drifting in the same direction as the retinally moving envelope (eyes are moving while the envelope was static), the shift decreased. Conversely, when the carrier was drifting in the opposite direction from the retinally moving envelope, the shift increased. Interestingly, when the retinal-relative velocity was cancelled out (eyes and envelope were moving simultaneously), no such asymmetry was found. Therefore, the authors concluded that: 1) Retinal motion has an effect on the motion-induced position shift. 2) The system interprets the motion-induced position shift induced by the carrier as being less reliable when it suggests a shift towards the future direction of the envelope’s retinal motion. Therefore, the system predicts the position of the envelope as being more likely somewhere along the previous trajectory than being somewhere along the extrapolated trajectory. As described by the authors, the Bayesian approach would explain these findings: The ‘prior’ containing information of stimulus position being somewhere along the previous trajectory, would have a higher probability than the probability of the stimulus position being somewhere along the path extrapolated for the future.

Hisakata, Terao & Murakami (2013) mention that the involvement of early visual areas (Whitney et al., 2003), a modulation of contrast sensitivity (Roach, McGraw &

Johnston, 2011), a shift in the centre of mass (Chung et al., 2007; Arnold, Thompson & Johnston, 2007) are not incompatible with the Bayesian approach.

Kwon, Tadin & Knill (2015) applied a mathematical model, which was invented by the mathematician Rudolf E. Kalman (1960). So far, previous sections show that motion and position coding mechanisms were investigated by numerous psychophysical experiments, fMRI and TMS studies. The data obtained offer great potential for understanding how the visual system processes visual motion and position information. But in order to fully discover that potential, we should also focus on developing mathematical models describing those data. We can learn from mathematical models, and furthermore, thereby transfer the knowledge into other research fields and into the commercial world.

Kwon, Tadin & Knill found that the Kalman Filter - an algorithm based on Bayesian statistics - was one approach to predict the effects of different positional illusions, such as the motion-induced position shift, perceptual speed biases (Stocker & Simoncelli, 2006), slowing of motions shown parafoveally (Tynan & Sekuler, 1982), and the curveball illusion (Shapiro et al., 2010). The Kalman filter has numerous applications, including the guidance of spacecraft. It uses a series of values over time, containing estimates to predict states using known physical conditions ('world model'), measured data ('sensory model'), and their inaccuracies. The optimal estimate of position and velocity is obtained by combining the estimates using the Kalman gain. The Kalman gain can be understood as a weighing factor between the two estimates depending on their inaccuracies. For example, if the predicted state variance is larger than that of the measurement state, the predicted state weight will be lower than that of the measurement. As stated by Kwon, Tadin & Knill (2015), motion information of e.g. a flying ball is created by the sum of two different motion signals: translation motion ('object motion') and rotation motion ('pattern motion'). The visual system has to attribute the different retinal pattern motion signals ('attribution problem'), applying the filter on the motion-induced position shift in our visual system. When positional uncertainty is low (e. g. Gabor with static envelope and hard aperture), the system accurately attributes the retinal texture motion to the actual sources (either object motion or pattern motion). When positional uncertainty is high (e. g. Gabor with static envelope and soft aperture), pattern motion and object motion strongly interact. This is also consistent with Kosovicheva, Wolfe and

Whitney (2014) who investigated luminance defined Gabors with soft-apertures and hard-apertures, and found comparatively small shifts in hard-aperture stimuli.

The system has to optimally weight current and past signals over time in order to track a current object's state. In other words, when sensory signal uncertainty is low, estimates of objects' states are largely determining by current signals, showing only little dependence on past signals. When signal uncertainty is high, the estimates of objects' states are strongly influenced by past signals. To the best of my knowledge, the Kalman-Filter is the first approach to predict the magnitude of positional illusions over time. Surely, there are reasons and possibilities to criticise and improve the algorithm. However, like all models it develops step-by-step.

1.2.5 Magnitudes of MIPS depending on characteristics

In the following I shall summarise how the magnitude of illusory position shifts depends on different stimuli characteristics.

Ramachandran & Anstis (1990), who investigated kinetic edges, found positional biases up to 0.43 deg when the background dots were twinkling, and positional biases up to 0.6 deg when dots in the background were static.

De Valois & De Valois (1991) measured the position shift induced by luminance-defined stimuli. Largest shifts were found in the temporal frequency range of 4 Hz to 8 Hz (up to ~ 0.22 deg), with curve fitting similar to the temporal contrast sensitivity function. The shift increased with decreasing spatial frequencies (peaking at 1 cyc/deg). Furthermore, they found that shifts increased with increasing eccentricity. De Valois & De Valois (1991) state that latter might be a result of decreasing spatial acuity in the periphery.

Tsui, Khuu & Hayes (2006) wondered whether the illusory position shift of a Gabor was a consequence of a shift of the whole Gabor, or a consequence of a shift of the centroid (centre of mass) of the Gabor. The two possible distortions have different influences on the perceived size of the Gabor: a simple shift in perceived position of the whole pattern would not influence the perceived size of the Gabor, while a shift in the centre of mass would either increase or decrease the size, depending on whether the trailing or leading edge was more affected. Tsui, Khuu & Hayes (2006) presented first order motion defined Gabors subsequently, which were either drifting (Test-Gabor), or stationary (Reference-

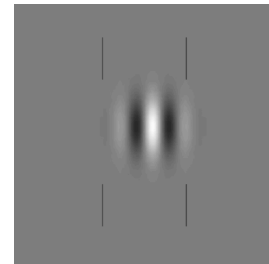


Figure 1.30: Experiment to test whether trailing and leading edges of moving Gabors are perceived as being displaced. From Tsui, Khuu & Hayes, 2006.

Gabor). Test-Gabors were of different carrier speed, moving randomly interleaved to the right or the left, and were of different sizes, manipulated by changing the standard deviation of the horizontal extents, but not the vertical extents. Observers were asked to judge - by key-press - whether the first or second interval contained a wider Gabor pattern. Tsui, Khuu & Hayes (2006) found that a moving Test-Gabor appeared to be wider than the stationary reference-Gabor, and that the effect increased (non-linear) with increasing carrier speed. Another experiment was conducted in order to verify

how far the leading edge and trailing edge were affected by motion. The stimuli were similar to those in experiment 1, but the size of the test-Gabor did not differ between trials. Instead of static reference-Gabors, two pairs of vertical bars were shown on the screen above and below the test-Gabor (see figure 1.30). Observers were asked to align the bars with the leading and trailing edge of the Gabor. When there was carrier motion, the leading edge was perceived as being further away from the centre of the Gabor as a function of carrier speed (non-linear) compared to when the Gabor was static, indicating shifts up to 0.2 deg. However, the perceived position of the trailing edge was only slightly (up to 0.03 deg) displaced in the direction of motion. When measuring the perceived centre of a moving bar with an adjustment task the authors found shifts up to 0.1 deg. Effects measured at the centre and leading edge were similar to effects measured by De Valois & De Valois (1991). In a third experiment, Tsui, Khuu & Hayes (2006) showed that displacing the centroid in the opposite direction of motion could eliminate the shifts. As already discussed in chapter 1.2.4, these findings are consistent with other studies (e.g. Arnold, Thompson & Johnston, 2007; Whitney et al., 2003).

Bressler & Whitney (2006) measured the position shift of first order and second order motion stimuli. First order motion stimuli resulted in position shifts up to ~1.05 deg, second order motion stimuli resulted in shifts up to 0.5 deg. Shifts for first order motion stimuli were larger than in the study of De Valois & De Valois (1991), with part of the difference possibly being due to different measurement methods. As described in chapter 1.2.1 and chapter 1.2.3, Bressler and Whitney (2006) presented two Gabors moving in opposite directions, while DeValois & DeValois (1991) presented three Gabors being vertically aligned, with only the central Gabor containing a right- or leftward sinusoidal pattern motion, while the two outer reference Gabors were flickering. Bressler & Whitney (2006) also found that first order motion influenced position assignments across a wide range of temporal frequencies (0 Hz - 26.7 Hz) and spatial frequencies of 0.18 cyc/deg, 0.35 cyc/deg, and 0.71 cyc/deg, with the peak (up to ~1.05 deg) occurring at lower spatial frequencies. In contrast, second order motion induced shift varied primarily as a function of temporal frequency over a narrow range, peaking at around 4 Hz, and cutting off at 12 Hz, and the shift did not vary as a function of spatial frequency.

As described in chapter 1.2.3, Durant & Zanker (2009) found position shifts in motion-defined-motion stimuli using spatial frequency of 0.1 cyc/deg and 0.7 cyc/deg.

Lower spatial frequency resulted in shifts up to 0.5 deg for orthogonal motion, and up to around 0.4 deg for parallel motion. A higher spatial frequency of 0.7 cyc/deg reduced the effect to a maximum of ~0.3 deg for orthogonal motion, and ~0.18 deg for parallel motion. The increasing effect with decreasing spatial frequency is consistent with the results of and Bressler & Whitney (2006) and De Valois & De Valois (1991) who found larger shifts in stimuli with a spatial frequency of 1 cyc/deg than in stimuli with a spatial frequency of 2 and 4 cyc/deg (see chapter 1.2.1).

McGraw et al. (2002) measured illusory position shifts after motion adaptation. The size of the position-after-effect was up to ~ 0.15 deg when stimuli (adapter and test) had the same orientation (parallel). The size of the position shift did not change with relative changes in spatial frequencies or differences in contrast between adaptation and test stimuli; but both are parameters that change the motion-after-effect.

DeValois and DeValois (1991) state that the magnitude in shifts depends on both spatial and temporal frequencies, but there is no proportional relationship between shifts and the speed of carrier motion, while Tsui Khoo & Hayes (2006), found increasing position shifts with increasing velocity. McGraw et al. (2002) showed that position-after effect does not vary with different spatial frequencies in adaption and test stimuli. Therefore, Chung et al. (2006) studied specifically the temporal and spatial properties of illusory position shifts induced by luminance-defined stimuli and also by random-texture patterns. Stimuli were placed either side of a central fixation-cross at different eccentricities, drifting in opposite directions (upwards and downwards). Observers were asked to indicate whether the stimulus on the right was perceived to be higher or lower relative to the left stimulus. Chung et al. (2006) found that position shifts were similar in both random texture patterns and Gabors at different eccentricities and velocities. Effects increased with increasing eccentricities. In order to test the temporal characteristics of illusory position shifts, they measured position shifts of a Gabor as a function of their drift speed for various stimulus presentation durations. They measured increasing position shifts for increasing durations. Shifts in stimuli with long presentation times (107 ms and 453 ms) reached an asymptotic value with a carrier velocity of 1 cyc/deg; shift in stimuli with short presentation times (53 ms) increased with increasing velocities. Comparison of these findings with the study by De Valois & De Valois (1991), and Tsui, Khoo & Hayes (2007) is not straightforward, because they used different experimental procedures. De Valois & De Valois (1991) presented the Gabor for 2 sec, and found – as mentioned

above - that the relationship between the effect size and velocity was non-monotone, which may be in contrast to Chung et al. (2007). Also Tsui, Khuu & Hayes (2006) used a comparatively long stimulus duration of 1410 ms; so their results may rather be consistent with Chung et al. (2007).

Kosovicheva, Wolfe & Whitney (2014) used a similar paradigm to De Valois & De Valois (1991) to compare position shifts of soft-aperture Gabors to hard-aperture Gabors. The size of the perceived shift in position was 0.55 deg in the soft-aperture condition, but only 0.14 deg in the hard-aperture condition. In order to find out whether the duration of the Gabor presentation had an influence on the magnitude of the position shift, Kosovicheva, Wolfe & Whitney (2014) also tested varying durations (20 ms, 40 ms, 60 ms, 80 ms, and 100 ms) of Gabor presentations. They observed no significant position bias with a 20 ms stimulus presentation, but the effect was significant for all other durations, reaching the maximum bias with duration of 80 msec. The authors claimed that their result supported the idea that the visual system uses motion to change the presented position of an object at early stages of visual processing.

Mather & Pavan (2009) investigated illusory position shifts of plaids in order to address the question of whether the effects arise before or after global motion integration. Type I plaids (single Gabors at an orientation of 45 deg), and Type II plaids induced shifts up to 0.3 deg and 0.21 deg across all observers, respectively. Hisakata & Murakami (2013) compared the illusion strength of oblique gratings to plaids (Type I) after perceived speed was equated to a vertically moving grating. They found slightly smaller shifts than Mather & Pavan (2009) between ~0.03 deg and ~0.23 deg when each single component of the plaid had an orientation of 45 deg.

Mather & Pavan (2009) also measured the position shifts of pseudo-plaids. When every single Gabor within the arrays was moving in a global motion direction, shifts were also between 0.8 deg and 0.27 deg across all observers. This result is consistent with Mussap and Prins (2002), who found position shifts of 0.08 deg in random dots, and consistent with shifts in pseudo-plaids measured by Rider, McOwan, and Johnston (2009) who found shifts of 0.8 deg to 0.22 deg across all observers.

Harp, Bressler and Whitney (2007) measured position after-effects occurring passively and remotely. When position shifts were determined following adaptation to local motion that was crowded out of awareness, shifts were up to 0.15 deg. In the

second experiment, where they measured whether local after-effects also resulted from global adaptation to the surrounding crowd, shifts of up to 0.11 deg were measured.

Tsui, Khuu and Hayes (2007) measured motion-induced position shifts in depth for three-dimensional stereo-defined objects. Dots forming a cylinder were moving either away or towards the observer. The end-plane and the near-plane of the cylinder were perceived to be displaced in the direction of the dots' motion, e.g. when dots moved towards the observer, the perceived distance of the far-end planes and near-end planes was closer than in the static dot condition. Shifts increased with increasing speed of dots. Murakami & Kashiwabara (2009) measured position shifts up to 0.12 deg when using cyclopean-defined motion stimuli, but much larger shifts up to around 1.3 deg when using first order motion defined stimuli. The cyclopean defined motion stimulus belongs to the category of second order motion, and therefore, Murakami & Kashiwabara (2009) summarised that the difference in effects might indeed reflect different processing pathways. The results are consistent with the results of Bressler and Whitney (2006), who found shifts of ~1.05 deg in luminance defined motion stimuli, and smaller shifts up to 0.5 deg in second order (contrast defined) motion stimuli when using the same measurement method.

Murakami & Kashiwabara (2009) also tested luminance defined Gabor stimuli with different contrasts (2% and 50%), finding that illusory shifts were invariant to contrast. That is consistent with the finding of McGraw et al. (2002), showing that the position-after-effect is invariant to contrast-differences in adapter- and test- stimuli.

The study by Hisakata, Terao and Murakami (2013) indicates that motion-induced position shifts depend on envelope relative velocity, rather than on display relative or retina relative velocities.

The difference in magnitude of effects measured by these studies are mainly due to different (1) measurement methods, (2) spatial frequencies, (3) temporal frequencies, (4) eccentricities, (5) sorts of motions, (6) velocities, (7) stimulus durations.

Table 1.1 summarises the key features affecting the magnitude of the motion induced position shift.

Measurement Method	Position of the reference stimulus at trailing edge, centre or leading edge (Chung, Khuu & Hayes, 2006).
Spatial Frequency	Low spatial frequencies induce larger shifts than high spatial frequencies in first order motion, but not in second order motion (Chung et al., 2007).
Temporal Frequency	First order motion: Largest shift at 4 Hz to 8 Hz, function describing the effect size shows strong similarity to contrast sensitivity function (De Valois & De Valois, 1991); Second order motion: Narrower than first order motion function describing the effect size (effect only arises at temporal frequencies of 4 Hz to 12 Hz; e.g. Chung et al., 2007).
Eccentricity	Increasing effect with increasing eccentricity (e.g. De Valois & De Valois, 1991).
Sort of Motion	First order motion (luminance defined) more affected than second order motion (contrast defined, cyclopean motion) (e.g. Bressler and Whitney, 2006; Murakami & Kashiwabara, 2009).
Velocity	Short stimulus presentation (50 msec): increasing shift with increasing velocity; Long stimulus presentation (107 msec and 453 msec): increasing shift with increasing velocity, reaching asymptotic values with carrier velocity of 1 cyc/deg (Chung et al., 2006).
Stimulus duration	Effect size saturates after 70 to 150 msec (Arnold, Thompson, Johnston, 2007; Kosovicheva, Wolfe & Whitney, 2014).

Table 1.1: Key features affecting the magnitude of MIPS.

1.2.6 Where do MIPS arise?

Many studies have investigated the physiological loci of motion-induced position shifts.

It is assumed that auditory transduction has a much shorter delay than visual transduction (Corey & Hudspeth, 1979), but both were found to project directly into the tectum or the colliculus superior, where a visual map of space is overlaid with an auditory map (Sparks, D. L., 1986; Knudsen 1982). Berry et al. (1999) suggested that if auditory and visual images of a moving object are aligned on a target map, the compensation for the delay in the visual pathway must occur very early in the visual processing stage. They found evidence for this theory when they recorded spike trains of ganglion cells in the retina of salamanders and rabbits. Berry et al. (1999) presented a drifting bar with a constant velocity, and a second bar briefly flashing up in alignment with the drifting bar. Ganglion cells just ahead of a drifting bar are excited as the edge begins to enter their receptive field centre, but then their response is reduced and the firing rate declines even before the edge is half way cross.

As stated in section 1.2.4, Roach, McGraw and Johnston (2011) measured detection thresholds of low contrast target-Gabors at trailing and leading edges of high contrast inducer-Gabors, suggesting a mechanism that predicts future location of a moving target. They also determined how far the prediction mechanism extended in space by measuring the effect on target detection threshold when the target-Gabor and the inducer-Gabor were spatially separated. Roach, McGraw, and Johnston (2011) stated that the effect persists over a narrow spatial range, and therefore concluded that motion-induced position shift is likely implemented at the early stage of visual processing where neuronal receptive fields are small and contrast polarity is retained. Furthermore, they presented target- and inducer- Gabors either to the same eye or to different eyes, asking whether predictions based on motion information presented to one eye can interfere with visual input from the other eye. Because signals from both eyes are assumed to converge after area V1, measurement of interocular transfer assesses the locus of illusory position shift induced by Gabors. They found similar detection thresholds when presenting stimuli to different eyes to when presenting stimuli to both eyes, suggesting that the effect occurred after the motion information of both eyes was combined. Based on their findings, Roach, McGraw & Johnston

(2011) suggested that a predictive mechanism responsible for MIPS probably arises in area V1, or very soon after V1.

Murakami & Kashiwabara (2009) found illusory position shifts induced by cyclopean motion, processed at binocular area V2 (Bredfeldt & Cumming, 2006), or in area MT (Bradley & Andersen, 1998; DeAngelis, Cumming and Newsome 1998). Since cyclopean and contrast defined motion both belong to second-order motion, Murakami & Kashiwabara (2009) stated that their finding was consistent with Bressler & Whitney (2006). Furthermore, they suggested a dual-process structure, with luminance-defined motion passing through monocular and binocular stages subsequently, and thus, the effect should be the sum of the independent effects of the lower and higher mechanisms. Second-order motion would only feed into higher mechanisms and thus induce a smaller effect. Murakami and Kashiwabara (2009) stated that the dual processing structure also had empirical support from the study by Bressler and Whitney (2006), who found different spatial and temporal characteristics for first- and second-order motion.

Mussap & Prins (2002) found illusory position shifts in random dot patterns, stating that the visual system must calculate motion trajectories over several motion steps and then applied to all dots underdoing motion, even if their direction of motion was not in the coherent motion. The authors stated that such a calculation could only be implemented by visual processes involved in global motion processing by neurons of area MT (V5). DeValois & DeValois (1991) found that radial movement (motion towards and away from the fovea) induced larger biases than the tangential movement. Based on a study by Albright (1989), who stated that cells in area MT and MST specifically responded to movement towards and away from the fovea, DeValois and DeValois suggested that these areas were a neurophysiological locus of illusory position shifts. Tsui, Khuu & Hayes (2007) agreed with this approach, after they found motion-induced position shifts in three-dimensional objects, which were defined by a random dot pattern. Mather & Pavan (2009) investigated plaid patterns, and found that MIPS are governed by the perceived direction of a plaid pattern, rather than the actual direction of its components, indicating that illusory position shifts arise at area MT as well. Rider, McOwan & Johnston (2009) investigated pseudo-plaid patterns, and stated that a MIPS cannot be accounted for by a local shift in the receptive field within V1, or a shift in responsivity within the retina. They assumed that the shift crucially depended on global motion information, processed in a stage

after the aperture problem was solved. Since Majaj, Carandini & Movshon (2007) found that MT neurons respond to plaid patterns, but not to pseudo-plaid patterns, Hisakata & Murakami (2009), suggested that illusory position shifts might occur even after area MT, within area MST. As stated in chapter 1.2.3, McGraw et al. (2002) investigated position-after-effects, and found evidence that they arise in higher visual areas, probably in MT.

Kohler, Cavanagh and Tse (2015) found that illusory position shifts were not determined by global motion alone, but that component motion played a larger role in determining objects' positions than global motion. Therefore, they suggested that the perceived position was influenced by processing at multiple stages, and that the influence of component motion occurred outside of area MT, such as in area V1; or that processing of component motion and global motion took place in the same area of the visual cortex. Nishida and Johnston (1999) suggested that motion and form information interacted at various levels in the visual system, maybe with information recurrently feeding from the cortical area MT to V1.

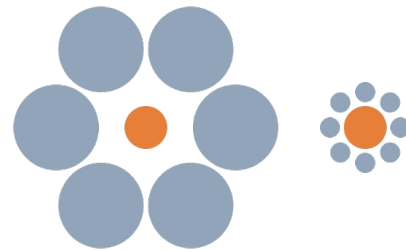
In general, the result of a study by Thompson et al. (2009) makes it controversial to assess the origin of MIPS by measuring and comparing effects induced by pseudo-plaids and gratings. They reported a double dissociation between the striate and extrastriate visual cortex for motion of pseudo-plaids: rTMS over striate cortex increased the coherent motion precepts, whereas rTMS over extrastriate cortex decreased the coherent motion precepts. Multiple studies showed that the neural representation of plaid motion might recruit multiple brain areas besides the extrastriate area MT. For example, Gegenfurtner, Kipper & Levitt (1997) found pattern sensitive V3 cells in monkeys. Also subcortical areas such as the superior colliculus in cats (Zhao, Chen & Li, 2005), and the pulvinar in cats (Merabet et al., 1998) and humans (Villeneuve et al., 2005) were found to respond to plaid motion.

As described in chapter 1.2.3, illusory position shifts can be induced by many types of motion, each with different characteristics, therefore, indicating that they may arise in different stages of visual processing. Also Bressler & Whitney (2006) posited that location assigned to an object depends on multiple motion pathways, and might occur at multiple stages within the visual system, with the perceptual system having access to all of them. Bressler & Whitney (2006) suggested that the redundancy of position information within several areas might be a by-product of efficient coding, or could

reflect the importance of position information relative to other types of visual information.

1.2.7 MIPS in action and perception

Goodale and Milner (1992) proposed that the visual processing mechanism is subdivided into two parallel processing streams. The delineation begins already within the retina after light is converted into neural signals. Small ('midget') retinal ganglion cells and large ('parasol') retinal ganglion cells project through the optic nerve, the optic chiasm, and tractus opticus into 'magnocellular' layers and 'parvocellular' layers within the lateral geniculate nucleus, respectively (Derrington & Lennie, 1984; Merigan, Katz & Maunsell, 1991). Next, the two streams project separately into the primary visual cortex (V1). The magnocellular pathway projected from V1 to the posterior parietal cortex (along dorsal areas) is assumed to be responsible for the analysis of motion and transforming information into visually guided actions (also called the 'Where'-Pathway), while the parvocellular pathway projects from V1 to the inferior temporal cortex (along ventral areas) and is assumed to be responsible for conscious awareness of objects and their surroundings (also called 'What'-Pathway by Ungerleider & Mishkin). Based on this approach, researchers studied whether matching perceptual tasks and visually guided actions could generate different object location signals. E.g. in the Ebbinghaus Illusion (see figure 1.31): both orange circles are exactly the same size.



The perceived sizes of the central target circles are affected by the size of the surrounding elements. The circle appears smaller when large elements surround it (circles on the left side) while the circle appears greater when small elements surround it (circles on the right side). But it was found, that grasping movements to the target circles remain accurate. Hence, Goodale and Milner found evidence for separate visual processing streams for perception and action tasks.

Figure 1.31: Ebbinghaus Illusion. Both orange circles are exactly the same size. The perceived sizes of the central target circles are affected by the size of the surrounding elements. The circle appears smaller when large elements surround it (circles on the left side) while the circle appears greater when small elements surround it (circles on the right side). But it was found, that grasping movements to the target circles remain accurate. (No author provided. Mond-vergleich [digital image] retrieved from https://en.wikipedia.org/wiki/Ebbinghaus_illusion)

The motion-induced position shift of a Gabor has also been reported as different when humans localise the Gabor's position with a motor task (e.g. hand movements towards

the perceived position of Gabors) instead of simple reporting the perceived position by, for example, calling it out. The next paragraph describes those studies.

Zimmerman, Morrone & Burr (2012) exploited the flash-lag effect to investigate whether there was a dissociation in action and perception tasks. A sinusoidal windmill rotated continuously clockwise and anticlockwise in the centre of the screen, changing direction every 2250 ms. In the motor task, observers fixated the centre of the windmill, and made a saccadic eye movement towards a briefly flashed probe bar as soon as it appeared. The probe bar appeared for 10 ms to the right or to the left of the windmill at different randomly selected heights. The presentation time of the bar was 1350 ms, 2250 ms, 3150 ms, or 4500 ms after trial onset. After execution of a saccade, the observers were instructed to fixate the centre of the windmill again. The next trial started when the windmill changed direction. Perceptual position shifts were measured in separate sessions. Observers were instructed to fixate the centre of the windmill for the entire session. After a probe bar was flashed at different randomly selected vertical positions, observers were asked to judge by key-press whether it was higher or lower than the fixation point inside the centre of the windmill. The windmill caused a position shift in the direction of motion, in both saccadic landing positions and perceived position of the flashed bar. Furthermore, they found that saccadic shifts depended on their latencies. Saccades made within 30 ms to 130 ms after bar presentation were not shifted in the direction of motion, while later saccades showed increasing shifts with increasing latencies. After excluding from analysis saccades that started within the first 130 ms, saccadic shifts and perceptual position shifts were found to be of the same magnitude, and largest at the moment when the windmill reversed its direction. Zimmermann, Morrone & Burr (2012) suggested that their results reinforced the assumption that different performances in action and perception tasks were the outcome of different reference frames for coding of object position.

As stated above, it may be that the illusory position shift reflects the compensation for neural delays in our perceptual system. Yamagishi, Anderson & Ashida (2001) suggested that grasping a moving object might require an additional temporal compensation for the delay caused by processing visual information into visually guided actions, and therefore investigated the ability to localise a stimulus using a motor task and a perceptual task with a Gabor stimulus. The Gabor was presented at different positions along the horizontal meridian in the right visual field, and drifting rightwards or leftwards or only flickering at the same frequency as the motion

stimulus speed (1.56 Hz, 3.13 Hz, and 6.25 Hz). In the perceptual task a ruler was displayed on the screen after the end of the Gabor presentation and observers spoke out the perceived location of the Gabor with reference to the ruler. In the motor tasks, observers marked the perceived position of the Gabor on a board using a pen held in their hand, but they were unable to see their own hand and arm. In both paradigms, observers were cued to disengage a central fixation by an audible tone and report the perceived position of the Gabor. Yamagishi, Anderson & Ashida (2001) considered that delayed actions directed towards a remembered target were thought to rely on perceptual memories (Milner, 1999). Therefore, the time difference between the disappearance of the Gabor and the cue to do a task was 200 ms for a short-delay condition, and 4200 ms for a long-delay condition.

In the short-delay condition Yamagishi, Anderson & Ashida (2001) found that Gabors were perceived as shifted along the direction of motion in both tasks, with increasing shifts for increasing temporal frequencies. The visuomotor task induced larger position shifts than the perceptual task. Furthermore, they found, that the magnitude of perceptual shift depended on the direction of interval motion: The effect of leftward drifting Gabors (toward the fovea) was greater than the effect of rightward drifting Gabors (away from the fovea). Yamagishi, Anderson & Ashida (2001) posited that a larger perceptual position shift induced by motion towards the fovea than shifts induced by motion away from the fovea might be related to differences in sensitivity in favour of centripetal motion (Raymond, 1994). Position shifts in the motor task did not show the same pattern. The authors suggested that the perceptual system used – due to a dual processing mechanism - different representation of objects from motor system.

Similar shifts were obtained in the long-delay condition, again, with largest shifts in high temporal frequency Gabors. No significant differences between both types of tasks were found. The authors stated that Gabors drifting towards the fovea induced larger biases than Gabors drifting away from the fovea.

Comparison between long- and short-delay conditions indicated no difference.

Kerzel & Gegenfurtner (2005) re-examined the study by Yamagishi, Anderson & Ashida (2001), criticising that both tasks were rather indirect. The Gabor in the study by Yamagishi, Anderson & Ashida (2001) had a size of 5.3 cm in diameter, while the tip of fingers is only 1.5 – 2 cm wide. Kerzel & Gegenfurtner (2005) believed that observers had to determine the centre of a stimulus before they could point to it. With

a Gabor of smaller size, however, observers would simply try to cover the stimulus with the finger instead of making a position judgement first. In the perception tasks of Yamagishi, Anderson & Ashida (2001), observers were using a ruler to judge the position, which was also criticised as being indirect.

Kerzel & Gegenfurtner (2005) measured motion-induced position shifts by 1) hand movements towards the centre of a Gabor stimulus. To trigger direct judgements, Gabor patches with diameters of 1.8 cm were presented in each trial. Observers were asked to make a finger point towards the perceived centre of the target-Gabor as soon as it appeared. This was done with full vision of the hand, and without vision of the hand by turning off the background luminance to eliminate visual feedback during the finger-point task. 2) key-press (perceptual task). Observers were asked to judge the central target Gabor position in respect to different reference stimuli. 3) Saccadic eye movements towards the centre of a Gabor. Kerzel & Gegenfurtner (2005) were interested in saccades because they were assumed to be ballistic in nature, that is, once they started, visual information would not be processed and saccade trajectory could not be changed mid-flight. Gabors were presented on the right side of the visual field in all three conditions.

Kerzel & Gegenfurtner (2005) found position shifts induced by drifting Gabors in the perceptual system, in finger points with visual feedback ('closed loop pointing'), and without visual feedback ('open loop pointing'). Also saccadic landing positions were shifted in the direction of motion. Saccadic errors were as large as motor errors (finger pointing), and thus, Kerzel & Gegenfurtner (2005) believed that motion-induced position shifts might originate very early in the processing stream, probably in V1. Perceptual errors were found to be more accurate. However, the authors stated that the choice of reference stimuli influenced the magnitude of the perceptual position shift, and therefore, the effects were not comparable with biases obtained in the finger pointing task and saccades.

Given all the visual illusions such as the motion-induced position shift, Caniard et al. (2011) wondered why our behaviour outside the laboratory was not more prone to error. They considered the possibility that – in everyday life – there was some action-related system involved, which compensated for errors arising during perception. The authors referred to a comment by Kerzel and Gegenfurtner (2005), that the magnitude of illusory position shifts tasks strongly depended on the measurement method, and therefore, comparison between perception and action tasks was deceptive. Instead of

measuring action and perception tasks, Caniard et al. (2011) designed an experiment to measure action and perceptual shifts together, while at the same time they tried to maximize the role of action (as in an everyday-life situation). Therefore, they created a computer game, and asked observers to continuously guide a Gabor along a randomly curving path (see figure 1.32) with a joystick. Results indicated that the illusion remained: when the Gabor drifted rightwards, the observers placed the Gabor to the left to guide it along the path.

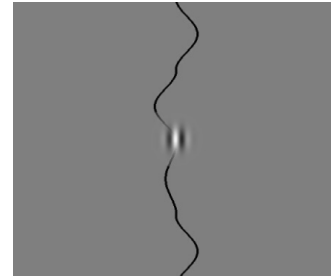


Figure 1.32. Experiment by Caniard et al. (2011). For more details read main text. From Caniard et al., 2011.

In 2015 Caniard, Bühlhoff & Thornton investigated illusory position shifts with an ‘active task’ and ‘passive task’, when observers had active control of the Gabors’ global position by using an iPad held in their hand. In experiment 1, the ‘active task’, observers were asked to change the horizontal position of the Gabors in order to guide them through the centre of gates. A

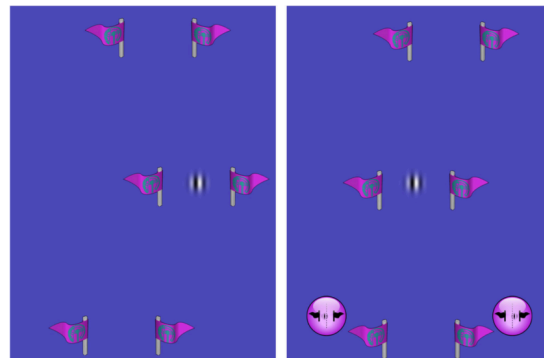


Figure 1.33: Experiment by Caniard, Bühlhoff & Thornton, 2015. ‘Active task’ to measure MIPS (left panel), and ‘passive task’ to measure MIPS (right panel). For more details read main text. Retrieved from Caniard, Bühlhoff & Thornton, 2015.

screen-shot of the experiment is shown in figure 1.33, left panel. The vertical position of the Gabor was fixed in the middle of the display. Physically tilting the iPad to the left or the right caused the Gabor to move in in the same direction, with increasing tilts resulting in increasing speed of patch movement. The patch was either drifting to the right or to the left at a constant speed, alternating its motion direction every 20 gates. A second experiment, the ‘passive tasks’ served as comparison. The observers had no active control of the Gabor’s global position, but were judging its position relative to two reference stimuli by pressing either the right or the left button (as shown in figure 1.32, panel on the right) once the patch had entered the gate. The alignment of the patch with the gate centre was parametrically varied at different offset positions. Caniard, Bühlhoff & Thornton found a clear shift in the direction of motion, confirming previous classical studies in MIPS. Secondly, active control of the Gabor’s position did not eliminate the effect, and third, they found that the magnitude of

illusory position shifts in the active task was larger than in the passive task. However, the authors themselves admitted that the experiment had some issues.

In general, investigation of a two-stream hypothesis in the context of visual illusions is controversial for at least two reasons: 1) Previous studies demonstrated strong interactions between both cortical streams. For example Niehorster & Cheng (2010) used the optic flow pattern to examine motion-streak-like form information and found that humans made optimal use of both form cues (processed by the ventral stream) and motion cues (processed by the dorsal stream), for heading perception. 2) Caniard et al. (2015) pointed out that the motion-induced position shift was not an eligible stimulus to investigate the two-stream hypothesis; one reason being the neural locus of motion-induced position shifts. As stated in section 1.2.6, researchers found that they might arise in the very early stages of visual processing within the retina (Berry et al., 1999) or the primary visual cortex (Roach, McGraw & Johnston, 2011), where there is no dissociation between ventral and dorsal stream processing anyway. Or motion-induced position shifts might arise in the extrastriate area MT/MST (e.g. Mussap & Prins, 2002; DeValois & DeValois, 1991, Mather & Pavan, 2009) located in the dorsal path. Milner & Goodale (2008), however, stated that dorsal stream tasks were an important prerequisite to studying whether actions escape the intrusion of ventral stream perceptual control.

The focus of contemporary research should be on the extent to which different action tasks are affected by different kinds of perceptual information.

1.3 Motivation

Scientists have been fascinated and challenged by the motion-induced position shift over the last 100 years. The widely discussed visual illusion raised a lot of diverse perspectives and opinions. For example, the cause of the motion-induced position shift might be lying in a mechanism that compensates the delay in visual processing (e.g. Yamagishi, Anderson & Ashida, 2001), by a mechanism predicts the likely future location of moving objects (e.g. Roach, McGraw & Johnston, 2011), by a motion deburring mechanism (e.g. Tsui, Khuu & Hayes, 2006), or by a spatial summation process (e.g. Arnold, Marinovic & Whitney, 2014). Furthermore, the investigation of the physiological locus is a heavily discussed topic. There is evidence that the motion-induced position shift arises already in the retina (e.g. Berry et al., 1999), in the first visual cortex (V1) (e.g. Roach, McGraw & Johnston, 2011), in area V2 (e.g. Murakami & Kashiwabara, 2009), in areas MT/MST (e.g. Mussap & Prins, 2002). However, it may also arise by processing the perceived position at multiple stages (e.g. Kohler, Cavanagh & Tse, 2015). Since Goodale and Milner published the ‘two-stream-hypothesis’ in 1992, a lot of studies on the motion-induced position shift were conducted in order to find a dissociation between the ventral and dorsal stream. As mentioned above and described extensively in section 1.2.6, the physiological locus of the motion-induced position shift arises either in very early stages of the visual processing path, such as in area V1, where there is no dissociation between ventral and dorsal stream processing, or in areas MT/MST, which are located in the dorsal-stream. However, Milner & Goodale (2008) stated that the dorsal stream tasks were an important prerequisite to studying whether actions (processed along the dorsal stream) escape the intrusion of ventral stream perceptual control. As a consequence, there is no relevant evidence to support the investigation of the two-stream hypothesis of Milner & Goodale by measuring and comparing the motion-induced position shift in perception and action tasks.

We intuitively assume that it is absolutely crucial to accurately compute our actions towards or away from moving objects in order to manage our every-day life. But to what extent is that true? If we are not operating accurately, how far do we have to compensate for this in the technology we develop? The current study investigated how we interact with objects in motion despite the fact that our perception is largely affected by the motion-induced position shift. In particular, the experiment studied the

effect of the motion-induced position shift on volitional and reflexive saccadic eye movements, as well as the effect of the motion-induced position shift on the perceptual system. It is important to note that volitional saccades are not as quickly initiated as reflexive saccades, are triggered internally and rely on high cortical areas such as the frontal eye field, while reflexive saccades are triggered externally and rely heavily on lower cortical and subcortical areas (e.g. Mc Dowell et al., 2008).

A few examples will be described briefly to provide ideas why research on the illusory position shift in perception tasks and saccadic eye movements may be important to society.

1.3.1 Camouflage

As introduced by Ramachandran & Anstis (1991), a leopard standing still within fluttering foliage may be almost completely invisible. However, as soon as the leopard moves it becomes visible as a result of kinetic edges (described in detail pp. 16-17). Also other researchers studied and claimed that animals, such as zebras and zebra seahorses (as shown in figure 1.34, left) may be camouflaged by their appearance (e.g. How & Zanker, 2014; Hughes, Troscianko & Stevens, 2014). The army made use of ‘razzle dazzle camouflage’ credited to the artist Norman Wilkinson (shown in figure 1.34, right). During the first and the second world war the army used razzle dazzle painting to prevent their boats from being located and attacked.

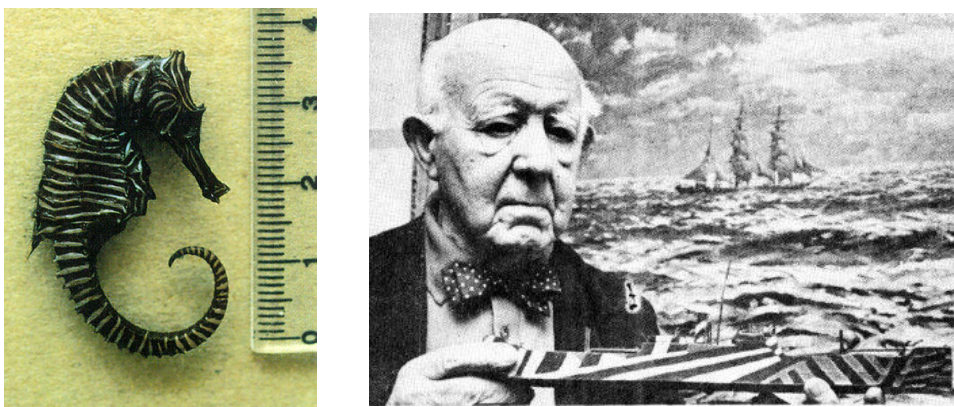


Figure 1.34: Camouflage. Left picture (Lourie, S. A, Hizeb_m0 [digital image] retrieved from <http://www.fishbase.org/summary/Hippocampus-zebra.html>): A hippocampus zebra may be camouflaged by its appearance. Right picture (no photographer provided [digital image] retrieved from <http://gotouring.com/razzledazzle/articles/dazzle4.html>): The British artist Norman Wilkinson poses in front of his painting with a model demonstrating his camouflage boat design. For more details read main text.

1.3.2 Human-Machine Interactions

As mentioned in the abstract many vehicles are equipped with control panels containing touchscreens. Figure 1.35 shows the on-board computer of the ‘Porsche Panamera S4’. Porsche advertises its first sport-limousine emphasising the extendable rear spoiler and the cockpit with its 12.3-inch touchscreens. The active control of this car requires hand



Figure 1.35: Porsche Panamera 4S (Fabian Meßner (Photographer) [digital image] retrieved from <http://autophorie.de/2016/09/07/test-2017-porsche-panamera-4s/>). Porsche advertises their first sport-limousine emphasising the new cockpit with their 12.3-inch touchscreens. The display depends on the driving situation; almost all functions are guided by the touchscreen.

movements. These actions, however, could be affected by perceptual illusions such as the motion-induced position shift, but also require time and attention while the driver is supposed to pay as much attention as possible to the changing environment. The display of the Porsche Panamera S4 is dynamic and depends on the driving situation; almost all functions are guided by the touchscreen. Even the airflow cannot be regulated haptically, but by modulators on the touchscreen. Porsche itself considered that too many functions available during driving posed the risk of more accidents. Therefore there are fewer functions available while the motor is running than when the motor is not running. As stated in the abstract, one alternative to finger points towards on-board computers is saccadic eye movements. The saccadic system is very fast, and therefore, would not require as much time and attention as a finger point task towards the touch screen. In that sense, investigations into how the saccadic system copes with dynamically changing screens are crucial.

2. GENERAL METHODS

All experiments in this thesis build upon each other. The third chapter, which describes the first experiment, introduces the methodical method and data analysis extensively and serves as a common background for following experimental sections. In this chapter the general methods for experiments will be described briefly.

2.1 Observers

This experiment was conducted according to the Helsinki Declaration, and was approved by the local ethics committee of the Max-Planck-Institute for Metabolism Research. Altogether, 12 different observers with an age range from 27 to 49 participated. JMF and BCD were female and non-naïve, NXN, DPW, KXE, SXX, SXE, LJR, AXS, were female and naïve, OGB and TXP were male and naïve. A medical check-up after the experiments showed that SXX has astigmatism of the right eye. All other observers had normal or corrected-to- normal vision.

2.2 Experimental Setup

All stimuli were displayed on a Cathode Ray Tube (CRT) monitor, and experiments were programmed with Psychtoolbox under Matlab (Mathworks). Experiments were displayed on a uniform grey background and eye movements were recorded with an Eyetracker, using forehead and chinrest to stabilise observers' heads. The observer's gaze direction was measured in pixels with x- and y-coordinates. Therefore, the unit of distance from one target to the next is the pixel. It is advantageous to

state the distance in units of visual angle (deg), as this unit is independent of distance d between the observer and the object. The variables d [mm] and the distance b between two targets (A and B) as shown in figure 2.1 are given. The following equation is used to find the angle that defines the distance between A and B:

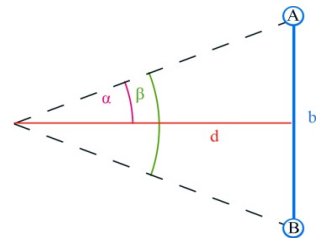


Figure 2.1: Angles define the distance between the two different target points A and B with viewing distance d . For more details read main text.

$$\beta = 2 \times \arctan\left(\frac{b}{2a}\right) \quad (2.1)$$

Stimuli were displayed on a CRT monitor (Sony GDM-F500) with screen resolution 1400x1050 pixels, a width of 40 cm and a refresh rate of 85 Hz. Experiments were programmed with Psychtoolbox 3 under Matlab R2009b (Mathworks). Analysis was conducted with Matlab R2009b (Mathworks). Eye movements were recorded by the Eyetracker (Eyelink 1000, SR Research) at 1000 Hz, using chin and forehead rest to stabilise the observer. Each experiment was started with a 9-point calibration (Eyelink) where fixations were accepted manually and supported by an inbuilt validation.

Experiments were conducted in a dimly lit room (Setup 1, shown in figure 2.2). In later experiments the whole setup (Eyetracker, camera, chair, head and chin-rest, monitor) were moved into a completely dark box (Setup 2), where observers were isolated from distractions, as for example people who were passing the Setup and different light conditions.

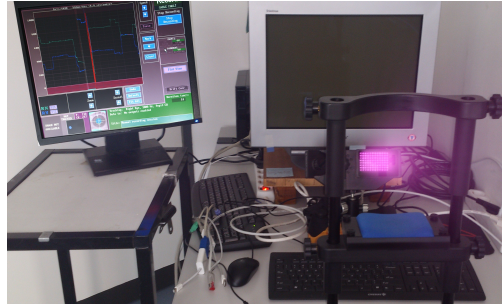


Figure 2.2: The Eyetracker, camera, chair, head and chin-rest, and CRT Monitor (Setup 1).

2.3 Monitor Calibration

As described by Dillenburger (2005), every monitor has individual properties, which depend not only on attributes such as the producer and production line, but also on its history and environment. Doing psychophysical tests, however, requires that we know the exact properties of stimuli. If no monitor is identical to another, identical input (RGB values) can generate different output, and thus, different perception. This makes comparison of psychophysical data which were gathered with different monitors impossible. Therefore, each monitor has to be gamma corrected by measuring the output at a given input. Identical numbers of R, G, and B generate the grey scale with RGB=[0,0,0] generating a black pixel, and RGB=[255,255,255] generating a white pixel. The monitor's output to each grey value should be described by a linear function. Therefore, a gamma correction has to be applied. Figure 2.3 shows the

luminance values before monitor calibration of a CRT Monitor used in my experiments. The y-axis indicates luminances (candela per square metre) at given grey values (RGB) indicated by the x-axis. The circles show luminances at given grey values measured with a photometer; the function is fitted with a gamma power function.

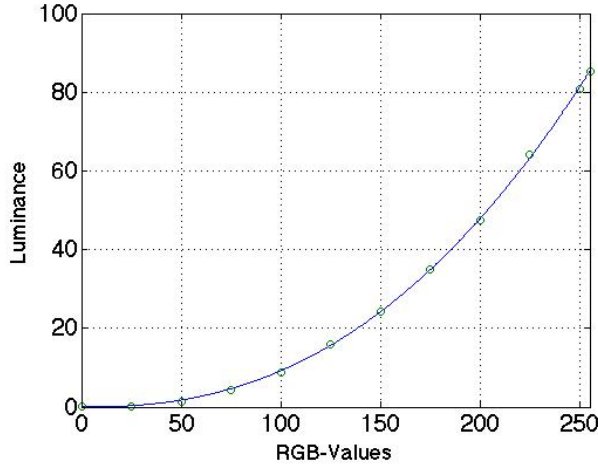


Figure 2.3: Luminance values before monitor calibration of a CRT Monitor used in my experiments. The y-axis indicates luminances (candela per square metre) at given grey values (RGB) indicated by the x-axis. The circles show luminances at given grey values measured with a photometer; the function is fitted with a gamma power function.

To luminances profile was corrected by using the following formula:

$$l_{out} = l_{in}^{\gamma} \quad (2.2)$$

with $\gamma = \frac{1}{2.38}$, and l_{out} and l_{in} being the corrected and uncorrected luminance profiles, respectively.

To properly describe experiments, we need to know the luminance of the screen, but also the contrasts of the stimuli presented on it. The definition of Michelson Contrast is:

$$\text{Contrast} = \frac{l_{\max} - l_{\min}}{l_{\max} + l_{\min}} \quad (2.3)$$

Stimuli in my experiments presented had a contrast of 0.39, 0.75, and 0.85.

3. MIPS IN PERCEPTION TASK AND VOLITIONAL SACCADDES

3.1 Introduction

The purpose of the first experiment was to measure the perceptual motion-induced position shift of a Gabor by asking observers to compare a target dot's position with the centre of a Gabor. Saccadic landing positions were recorded to determine if they were distorted by motion in a similar way to perceptual distortions. Saccades are interesting to study for different reasons: 1) they are, in contrast to perception tasks, not influenced by decisional biases and response biases, and 2) there is relatively little known about the interaction of visual illusions and saccadic eye movements.

The first experiment aims to answer following research questions:

- Is there a general effect of drifting Gabors in a static envelope on the perception of the location of a target dot superimposed on the Gabor?
- Is there a general effect in volitional saccadic eye movements to the Gabor stimulus?

3.2 Methods

3.2.1 Stimuli

The magnitude of the illusory displacement is greatest for eccentrically viewed stimuli (e. g. De Valois & De Valois, 1991) and high drifting rates. Yamagishi, Anderson & Ashida (2001) found greatest illusory effect for Gabor drift rates of 4 to 8 Hz. To make sure that I could also find a possible position shift of the Gabor and make our results comparable to results of Yamagishi, Anderson & Ashida (2001), I used a drift rate of 6.54 Hz and placed our Gabor at an eccentricity of 4.4° . On each trial the observer viewed sinusoidal Gabors of 2.25-cycles/deg periodicity and Michelson contrast of 39%, overlaid with a Gaussian function to blur the edges along the horizontal line. Each set of measures comprised a block of at least 80 trials, with 40

trials of rightward drifting and 40 trials of leftward drifting stimuli, which were presented randomly interleaved. At the beginning of every trial the Monitor displayed a white central fixation cross which was to be fixated by the observer. The fixation cross was 2° high and 2° wide.

3.2.2 Procedure

Each trial consisted of two parts – a saccadic effect measurement and a perceptual effect measurement. Figure 3.1 shows the stimulus presentation used to measure the saccadic effect by making a saccade to the centre of the drifting Gabor. The perceptual-effect was measured by judging whether a point superimposed on the Gabor was located to the left or right of the perceived centre of the Gabor. Each experiment was started with a 9-point calibration (Eyelink) where fixations were accepted manually and supported by an inbuilt validation. Each trial started by fixating a white central fixation cross. After 700 ms a drifting Gabor appeared in the upper-right quadrant of the visual field. Gabors were placed with the presentation order randomised with centres at eccentricities of $4.4^\circ \pm 1.5^\circ$ and $4.4^\circ \pm 0.7^\circ$. The disappearing of the fixation cross after 1200 ms was the observer's cue to make a saccade to the centre of the drifting Gabor. A white point appeared on the Gabor 1900 ms after onset of this trial (700 ms after fixation offset). The observer had to press a key to indicate whether the point was located left or right of the centre of the Gabor stimulus. The point's horizontal position was determined by the APE (Adaptive Probit Estimation) procedure (Watt & Andrews, 1981). Its vertical position was always aligned with the Gabor centre. The observer was asked to report the perceived position of the white point, when a noise-mask covered the Gabor. The mask consists of black and white dots that were randomised in their positions. If the observer did not answer within 700

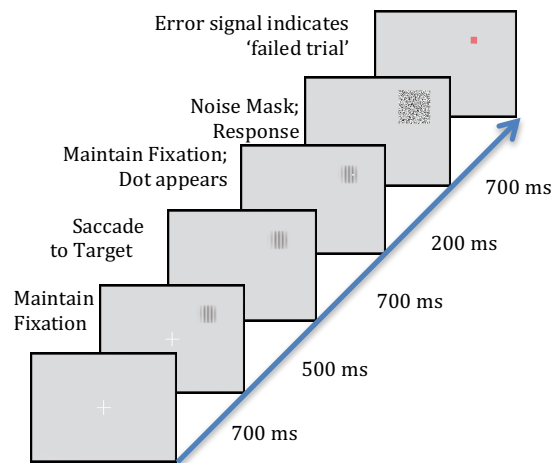


Figure 3.1: Procedure of experiment described in chapter 3. Paradigm to measure 1) saccades towards the centre of Gabor stimulus, 2) perceived position of a dot superimposed on a Gabor stimulus. For more details read main text.

ms after the mask onset, I counted it as a ‘failed trial’. ‘Failed trials’ were indicated by the brief appearance of a small red square placed at the position of the previously shown noise mask.

3.2.3 Observers and Setup

Seven observers participated in the experiment: BCD and JMF collected each 160 trials per motion direction. SXX collected 120 trials per motion direction and OGB collected 80 trials per motion direction. AXS collected 400 trials, SXE collected 480 trials and LJR collected 320 trials. They all used Setup 1. SXX was diagnosed with astigmatism of the right eye after the experiments. All other observers had normal or corrected-to-normal vision.

3.3 Data Analysis and Results

3.3.1 Perception bias

A psychometric function with two parameter cumulative Gaussian function of observers’ responses was fitted using a maximum likelihood method. The method is explained extensively in Appendix B. In this section I show one example of a psychometric function for one dataset. Figure 3.2 shows the data of one observer, which were gathered when the Gabors moved to the right. Red dots indicate the relative frequency of response ‘right’ (y-Axis) for each position of the target dot (x-Axis) relative to the true centre (position 0) of the Gabor stimulus. The red curve indicates a psychometric function φ , the green line is a cumulative standard-normal Gaussian function as a visual comparison to φ . The perceptual shift is shown as a blue horizontal line. Nonparametric bootstrapping (Efron & Tibshirani, 1993) was used to calculate the confidence intervals for mean perceptual shift. Each observer’s data was resampled 1000 times.

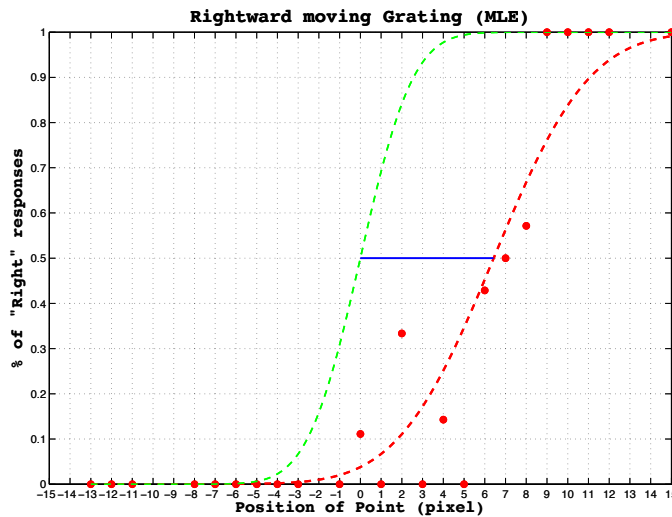


Figure 3.2: Psychometric functions for data gathered with rightward drifting Gabors. X-Axis indicates the position of the target point, y-axis indicates the percentage of 'right' responses. The green curve indicates a cumulative standard-normal distribution; the red curves indicate the psychometric function that was found to be the best fit of sampled data (red circles).

Observers had a similar perception-effect for each direction of motion: targets were perceived as shifted along the direction of motion (see figure 3.3). Specifically, observers perceived the target point as shifted rightwards with Gabors drifting to the right, and shifted leftwards with Gabors drifting to the left.

The confidence interval (CI) that includes the expected position shift with a probability of 95% does not include the value zero for all observers and drift directions, except that observers SXE. BCD and JMF had a larger perception shift for Gabors that moved away from the midline than for Gabors that moved towards the midline, while effect sizes of LJR and AXS showed an opposite pattern.

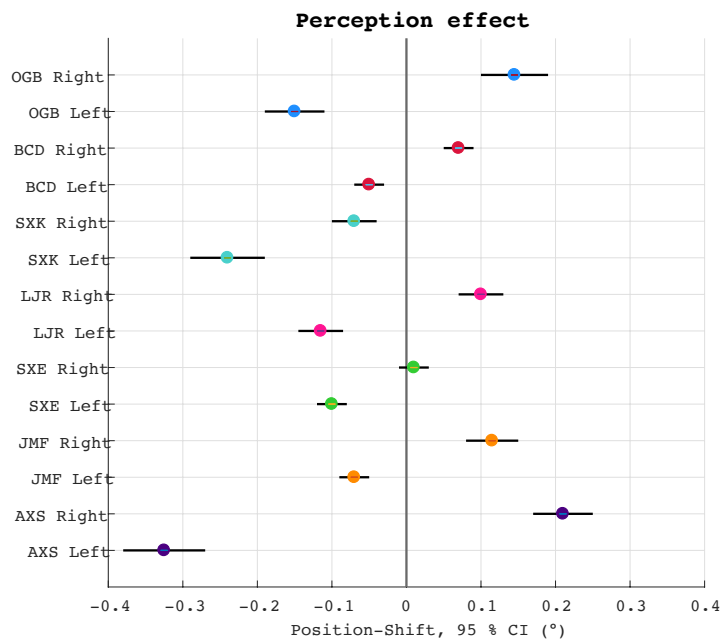


Figure 3.3: Perception effect. Results of observers OGB (blue), BCD (red), SXK (turquoise), SXK (turquoise), LJR (magenta), SXE (green), JMF (orange) and observer AXS (purple) are shown. Dots indicate mean values of a CDF and error bars represent bootstrapped 95% confidence intervals. The x-axis shows the perception-shift (degree), y-axis shows the observers and the direction of Gabors internal waveform. The vertical black line on position $x=0$ indicates the centre of the Gabor.

Effect sizes of OGB were found not to differ. SXK had a large effect for both directions of motion, but in the same direction. However, perceptual data showed the same pattern in leftwards and rightwards motion direction, i.e. the perceived centre in leftwards drifting stimuli appear to be leftwards of the perceived centre in rightwards drifting stimuli.

3.3.2 Saccadic landing positions

Filtering invalid saccades: End points of the saccades were assessed based on their velocity profile (see figure 3.4). Velocity profiles of raw data with 1000 Hz sample rate were filtered using a second order Butterworth filter. The very first minimum with a velocity < 40 deg/sec after velocity peak was defined to be the end of the saccade. Saccades, with velocity peak values that deviated more than their mean values ± 2 standard deviations, were excluded from analysis. The same procedure was followed for saccades where peak positions were too late (mean value +2 standard deviations) or too early (mean value -2 standard deviations) in time.

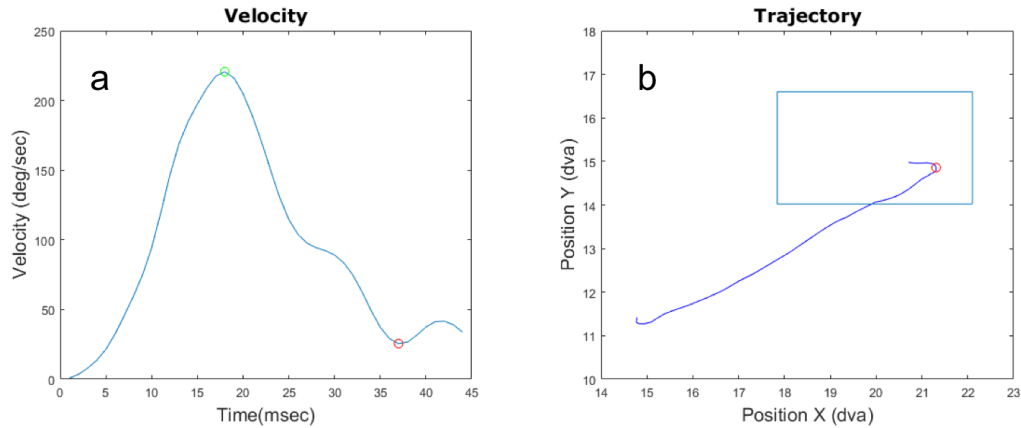


Figure 3.4: Saccade velocity profile and saccade trajectories. Saccade velocity profiles (a), plotted in deg/sec over time (ms), were filtered using a second order low pass Butterworth filter. Red circles indicate the minimum in the velocity profile with velocity < 40 degree/sec. In the saccade trajectory plotted in display coordinates (pixel) (b), red circles indicate the saccade end positions, which correspond to the first minimum in the velocity profile after the velocity peak. The blue rectangle in (b) indicates the location of the target-Gabor stimulus.

Saccadic start positions were not always at the centre of the fixation cross and saccadic end positions were not always on or close to the Gabor. There are several possible reasons for this:

- 1) Imperfect head stabilisation: The Eyetracker cannot distinguish if a change in position of the pupil and the purkinje reflex is due to eye movements or changes in head positions. Deviations from central fixation and/or saccade target may be due to the observer's head position stability.
- 2) Incorrect tracking of the eye due to e.g. pupil size artefacts: it is known that pupil size changes can affect eye movement tracking (Schreiber, Dillenburger & Morgan, 2014). This may affect estimates of where the observer is fixating at or saccading to.
- 3) Saccadic undershoot: If the first saccade does not land correctly, a second saccade will typically be made to correct the eye position (Becker & Fuchs, 1969). The inaccuracy is called 'saccadic undershoot' or 'Hypometria'. The degree of saccadic undershoots is typically only 10% of the amplitude of the saccade for non-predictable visual targets and is even smaller for small saccades. A drift in eyes at the end of saccades, called 'post-saccadic drift' or 'glissade', can also cause inaccurate landing positions. (Leigh & Zee, 2006).
- 4) Observer variability: no observer has a stable, perfect fixation to a single position across many trials. This inherent variability differs across observers.

To prevent issues 1) and 2), I used a chin rest, and used a stable illumination to, as far as possible, maintain a stable pupil size; especially for issue 2), which affects all eye trackers using pupil size information, there exists currently no satisfying solution. Issues 3) and 4) were corrected by normalizing saccadic end positions: I used an algorithm for robust clustering of eye-movements (Santella & DeCarlo, 2004) based on the mean-shift-procedure (Fukunaga & Hostetler, 1975). After finding the main cluster (the cluster that has the smallest Euclidian distance to the centre of the Gabor) of saccadic end positions, all saccadic end positions were shifted by the same amount s toward the true centre of the Gabor, where s is the distance between the weighted mean values of the cluster to the Gabor. Details about the cluster algorithm are stated in the Appendix A.

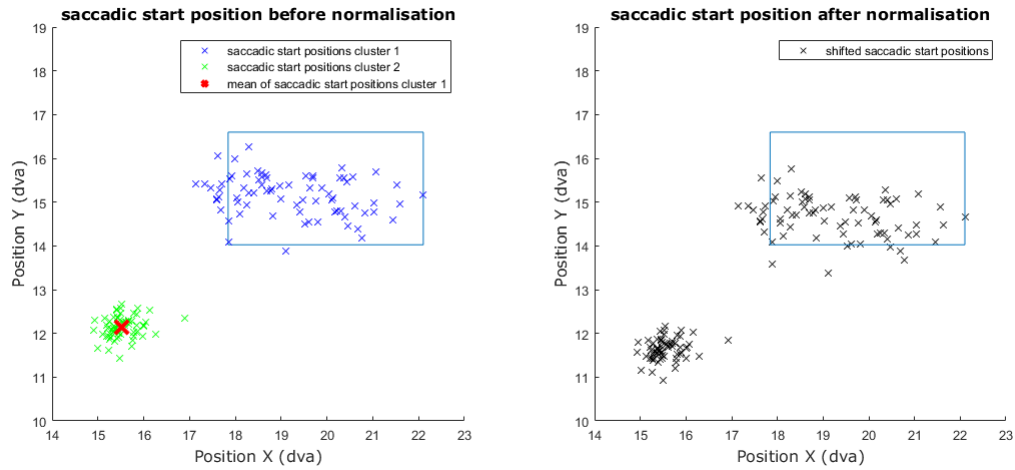


Figure 3.5: Cluster algorithm employed on saccadic start positions of observer AXS. Saccadic start positions (dva) along the x- and y-axes. The blue rectangle indicates the position of the Gabor. The plot on the left shows saccadic positions before normalisation-procedure, the panel on the right shows saccadic landing positions after normalisation process. The algorithm of Santella & DeCarlo found two clusters, which are indicated by green and blue colour. The start positions in green were found to be closest to the fixation cross, and therefore, the mean value s of this cluster was determined. Then, all saccadic start positions were shifted toward the fixation cross by the amount s .

Normalised saccadic end positions further away than ± 0.7 dva (horizontally) or ± 1.3 dva (vertically) from the centre of the Gabor were removed from analysis. The vertical dva was larger than the horizontal range because the saccadic undershoot was found to be larger in the horizontal than in the vertical direction across all observers. The same procedure was followed for saccadic start positions. Saccades that started further away than ± 1 dva (which is half of the size of the fixation cross) from the centre of the fixation cross in each direction were excluded from analysis. Furthermore, I calculated the ‘path length’ between each sample point and excluded the saccades that deviated by more than two standard deviations from the path length of all saccades. Visual input cannot influence saccade programming within 80–100 ms before saccade onset (Findlay & Harris, 1984). Therefore, saccades were included if onset was at least 80 ms after fixation offset, but also if they did not land before target dot onset. Trials without any saccades within this time interval were also removed.

Figure 3.6 shows the saccades of one observer after filter processing. To filter saccades, each experiment run was processed separately for each observer.

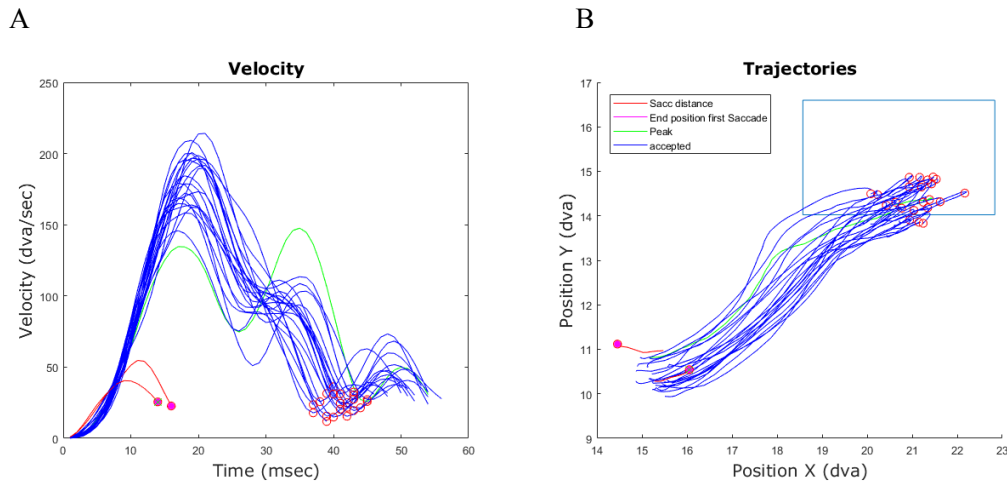


Figure 3.6: Saccade velocity profiles and saccade trajectories of one observer after applying filter.

Figure B (on the right) shows saccade trajectories of observer BCD (Gabor drifted to the right) after using filter options. Saccade velocity profiles on the left side (A), plotted in dva/sec over time (msec) and saccade trajectories in degree of visual angle (dva) on the right side. Red circles indicate the minimum in the velocity profile with velocity < 40 dva/sec, which were defined as saccadic landing positions. Blue coloured velocity profiles and their trajectories are found to be valid and therefore accepted for further data analysis. The saccades that were indicated by green colour (green trajectory or green cross at the end positions of saccades) were excluded from analysis, as the velocity peaks were not in the range of two standard deviations. Saccades indicated by red trajectories were removed from analysis because the path length between each measured sample point was too short (< 2 standard deviation) and saccades with end positions too far away from the Gabor were indicated by magenta filled circles at saccadic ends.

The number of valid saccades: LJR made 117 valid saccades to rightward drifting and 129 valid saccades to leftward drifting Gabors (23% of saccades were removed from analysis). SXE conducted 480 trials, after filtering there were 195 saccades to rightward and 196 saccades to leftward drifting Gabors found to be valid (19 % of saccades were not included in analysis). JMF made 130 valid saccades to rightwards and 124 valid saccades to leftward drifting Gabors (21 % of saccades were removed from analysis). Only for observer AXS, who initially conducted 400 trials, numerous saccades (63%) had to be removed from analysis. 99 saccades to rightward drifting and only 49 saccades to leftward drifting Gabors were included in analysis. Observer BCD made 105 valid saccades to rightward drifting Gabors, and 101 saccades to leftward drifting Gabors (36% of saccades were removed from analysis). 57 saccades to rightward and 58 saccades to leftward drifting Gabors were found to be valid in the

data of OGB (28% of saccades were removed from analysis). 49 saccades to rightward and 49 saccades to leftward drifting Gabors of observer SXX were included in analysis (18 % of saccades were removed from analysis).

Shift in saccadic landing positions: Arithmetic mean values were used as a first measurement to study whether horizontal and vertical positions of saccade endpoints in rightwards drifting conditions are different from leftwards drifting conditions. A two-sided Wilcoxon-Rank-Sum-Test at a Bonferroni-corrected alpha level of $0.05/\text{'number of observers'}$ was employed to test if the distribution of errors in saccades for rightward and leftward drifting Gabors were significantly different from each other. The advantage of this test compared to the t-test is that data do not have to follow the normal distribution. As shown in figure 3.7, datasets do not always come from a normal distribution. Because the Wilcoxon-Rank-Sum-Test indicates differences in distributions, but doesn't specify whether the difference is due to unequal variances or expectancy values, I applied the Brown-Forsythe-Test (BF-Test), which tests whether the variance of the sample data have the same variance. The Brown-Forsythe-Test has also been shown to be quite robust to non-normality (Algina, Olejnik & Ocanto, 1987).

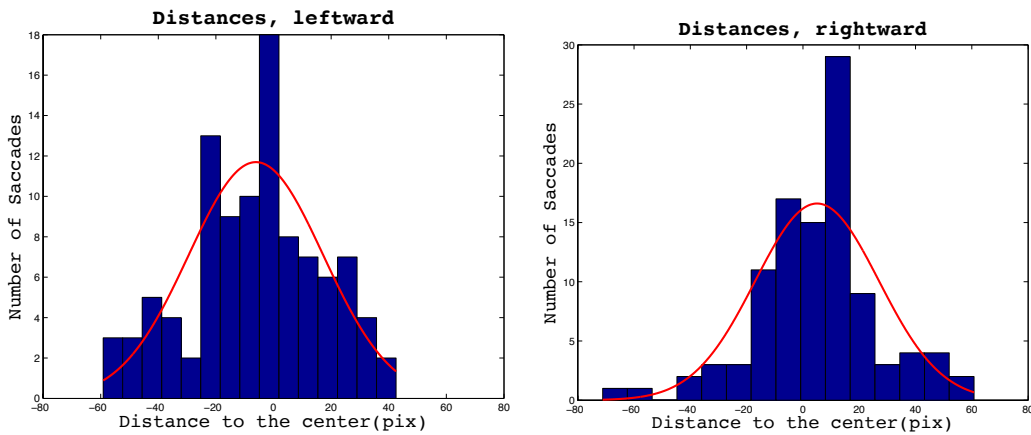


Figure 3.7: Histogram of distances of saccadic landing positions (pixel) to the centre of the Gabor in one experiment conducted by observer BCD. X-axis shows the distances in pixel and y-axis the number of saccades. Panel on the left shows the distances of saccadic landing positions to leftward drifting Gabors, Panel on the right shows distances to rightward drifting Gabors. The red curve shows the normal distribution with estimated expectancy value and standard deviation. The data shown in bars have a double peak, which clearly shows that the data do not follow any normal distribution.

Data sets for each observer were analysed after filtering invalid saccades and normalisation with the mean shift procedure. The effect was then measured by subtracting the arithmetic mean values of horizontal and vertical saccadic landing

positions from the true centre of the Gabor. As the Gabors were presented on the right side of the visual field, a saccadic effect, which should go along with the direction of motion and the perceptual effect, results in larger mean values of saccadic end positions to rightward drifting Gabors than saccadic end positions to leftward drifting Gabors.

Figure 3.8 shows saccadic landing positions and their mean values of observer LJR after the mean-shift procedure. X-axis and y-axis indicate the positions (pixel) of the monitor. More details are given in the legend of the figure.

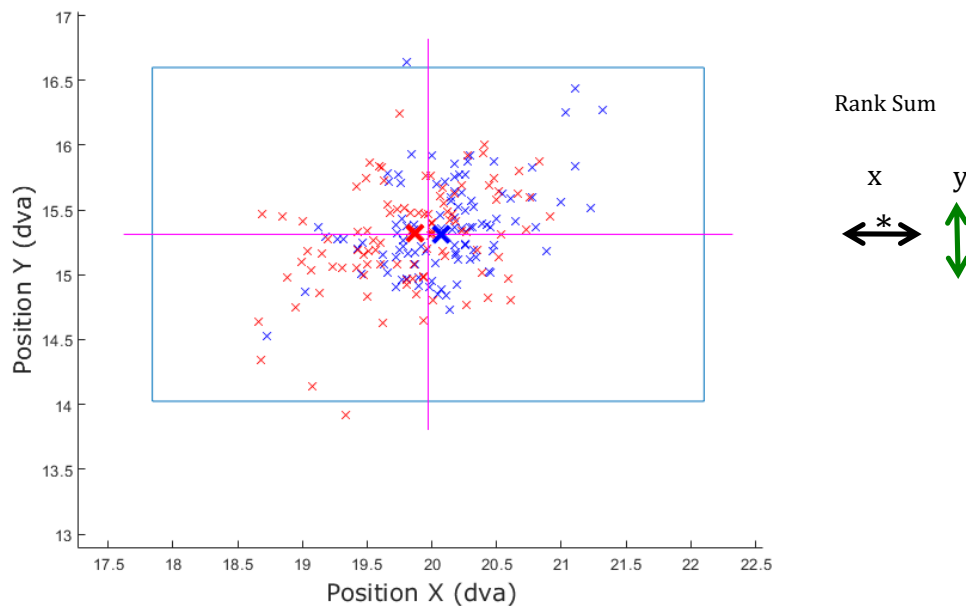


Figure 3.8: Saccadic effects of observer BCD. Individual saccade endpoints of all sessions are shown in display coordinates (x y, dva). A clustering algorithm (Santella & DeCarlo) was employed to estimate the centre of saccade endpoints within a condition. These central saccade endpoints are indicated by red (leftwards drifting stimuli) and blue (rightwards drifting stimuli) crosses. Blue rectangles indicate the location of the target Gabor stimulus and the magenta cross indicates the centre of it. Wilcoxon-Rank-Sum-Test was employed to test whether horizontal and vertical positions of saccade endpoints in rightwards drifting conditions were different from leftwards drifting conditions. Significance level ($p < 0.005$) is indicated in the figure.

As shown in figure 3.9, LJR had a significant shift in saccadic landing positions in the horizontal but not in the vertical direction. Only observer AXS, who reported that the experiment was running too fast, showed an opposite pattern. AXS conducted 400 trials, but only 148 trials were valid after using different filter options. Therefore, I consider the saccadic effect of AXS as an outlier. Saccades of observer SXK appeared to have a general bias towards the midline, but the general shift is also present in the

data. All other observers had a shift of saccadic landing positions in the direction of motion. Observer OGB had a larger shift when the Gabor drifted towards the midline (leftwards) than when the Gabor drifted away from the midline (rightwards). The opposite pattern of magnitudes in shifts to right, and leftward moving Gabors was found for observer BCD, LJR, SXE, and JMF. However, differences between the magnitudes in shifts for right and leftwards drifts were very small.

Wilcoxon-Rank-Sum-Tests indicate that the distribution of horizontal saccadic errors elicited by rightward drifting Gabors was significantly different from distributions of horizontal saccadic errors elicited by leftward drifting Gabors for observers OGB, BCD, LJR, SXE and JMF (p -values <0.005). The Wilcoxon-Rank-Sum-Test applied to the data of AXS resulted to a p -value of 0.042. Horizontal saccadic errors of observer SXX were not found to be significantly different ($p=0.68$) between right- and leftward drifts. Vertical distributions of errors in saccadic landing positions were not found to be significantly different in all observers. A BF-Test indicated no significant difference in variances for any observer, either for horizontal or for vertical directions.

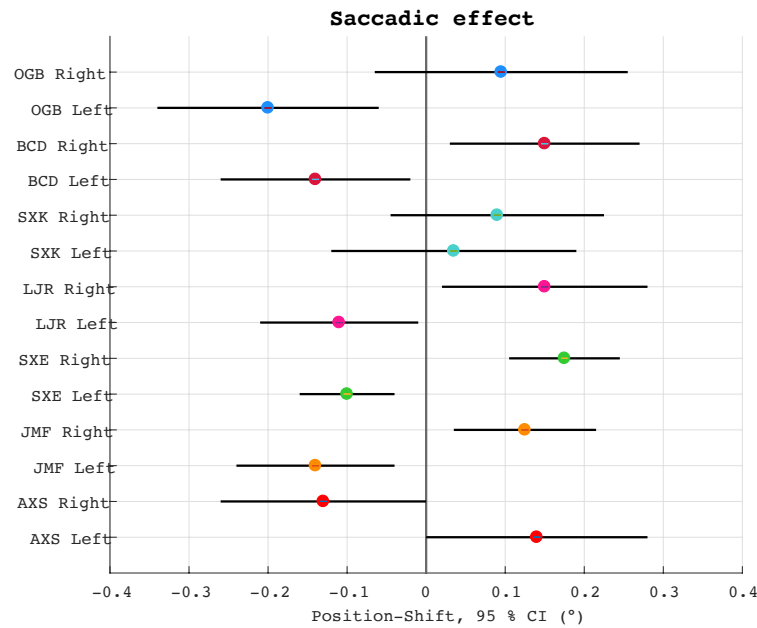


Figure 3.9: Saccadic effect. Mean values and bootstrapped 95 % confidence intervals of normalised saccadic landing positions for observer OGB (blue), BCD (red), SXX (turquoise), LJR (magenta), SXE (green), JMF (orange) and observer AXS (bright red) are shown. Dots indicate mean values of a CDF and error bars represent bootstrapped 95 % confidence intervals. The x-axis shows the saccadic-shift (degree), y-axis shows the observers and the direction of Gabors internal waveform. The vertical black line on position $x=0$ indicates the centre of the Gabor.

3.3.3 Fixations

It may be that the effect on saccades is due to drifting fixation in the Gabor's motion direction before saccade onset. Last fixations just before the saccade to the drifting Gabor started were taken into account. I made use of the same procedure as for saccadic landing positions: fixations were shifted by the cluster algorithm of Santella and DeCarlo to determine and exclude from analysis if they were too far away (± 1.5 dva) in a horizontal or vertical direction from the centre of the fixation cross. Afterwards valid fixations were normalised by shifting the centre of the whole cluster to the centre of the fixation cross. Finally I used statistical tests (BF-Test and Wilcoxon-Rank-Sum-Test) to investigate if there was a significant difference in horizontal or vertical directions between fixations that were made when the Gabor moved either to the right or the left. I found no consistent pattern of shifted fixations throughout all observers, which could indicate that fixations were influenced by the motion direction of the Gabors. Statistical tests to assess whether there was a significant difference in variances and mean values in horizontal or vertical direction, between both conditions (rightward versus leftward drifting Gabors) led to larger p-values than 0.06 for all observers except for AXS. The smallest p-value was obtained by employing the Wilcoxon-Rank-Sum-Test to the data of observer AXS ($p = 0.03$). However, the shifts went in the opposite direction to the Gabor's drifting direction. This means that fixations were shifted to the left when the Gabors moved to the right, and fixations were shifted to the right when the Gabors moved to the left. In summary, I did not find any influence of the Gabor on fixation just before saccade onset.

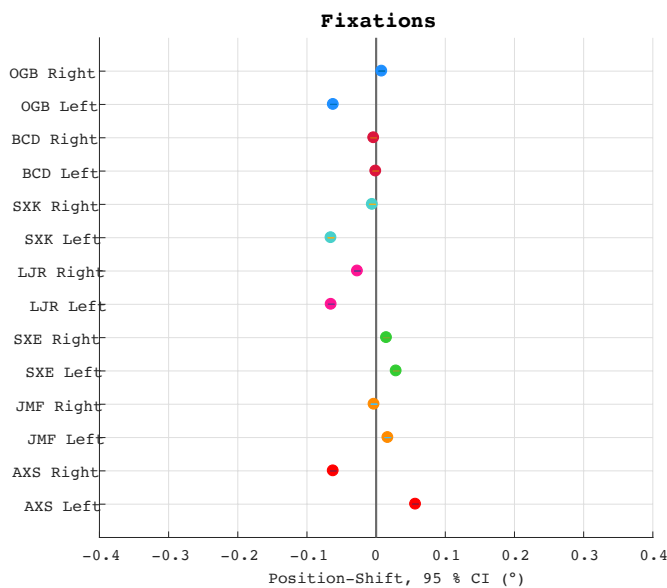


Figure 3.10: Last fixation before saccade onset. Results of observer OGB (blue), BCD (red), SXX (turquoise), LJR (magenta), SXE (green), JMF (orange) and observer AXS (red) are shown. X-Axis shows the position shift (dva), the y-axis shows the different observers and drifting direction of the Gabor.

3.3.4 Saccade trajectories

3.3.4.1 Averaged saccade trajectories

Averaged saccade trajectories (\bar{X}, \bar{Y}) in respect to each sample point (x, y) were determined by

$$\bar{X}_j = \sum_{i=1}^{n_j} \frac{x_i}{n_j} \quad (3.1)$$

and

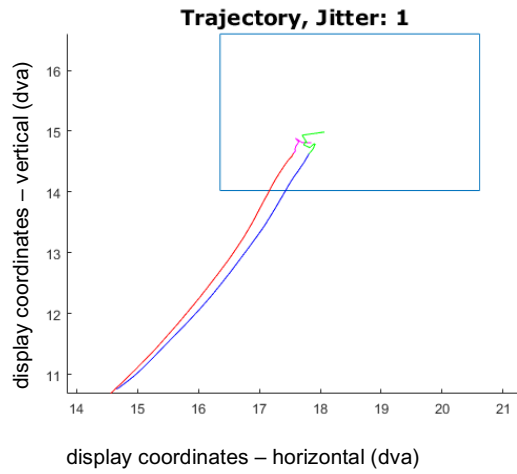
$$\bar{Y}_j = \sum_{i=1}^{n_j} \frac{y_i}{n_j} \quad (3.2)$$

where n_j indicates the amount of all valid saccades at time j to either rightwards or leftwards drifting Gabors.

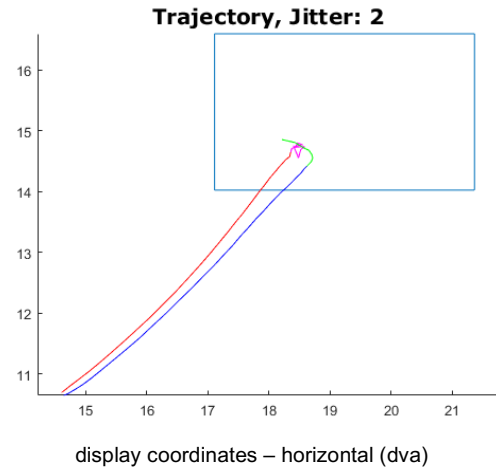
Figure 3.11 shows saccade trajectories plotted (in display coordinates [pixel]) as averages for observer SXE. Red traces are averages of trials in which the stimulus drifted leftwards; blue traces are averages of trials in which the stimulus drifted rightwards. As mentioned in the methods, averages were calculated by sample point, starting at the saccade start as defined by Eyelink; i.e. initially average trajectories were based on all saccades within a session and condition, but as some saccades were shorter than others, later parts of the trajectory were averages over fewer saccades. Red and blue traces were based on at least 90% of the saccades within the respective condition; sample points based on fewer saccades are coloured magenta and green in leftwards and rightwards drifting trials, respectively. Plots A, B, C and D represent trials where the Gabors were placed at an eccentricity of 2.9°, 3.7°, 5.1° and 5.9°, respectively.

Saccadic landing positions were shifted in direction of motion (see chapter 3.3.2). In accordance with this result, saccade trajectories are shifted into direction of motion (see figure 3.11).

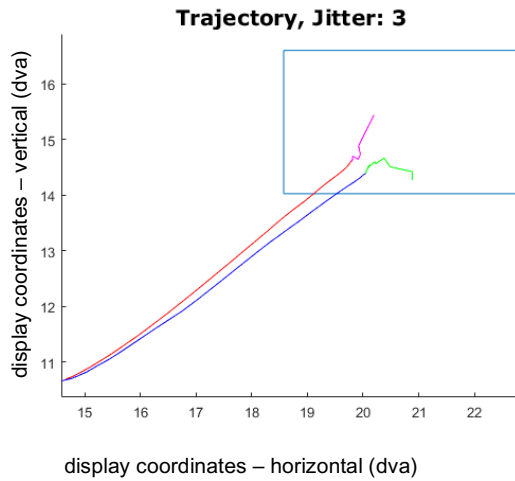
A



B



C



D

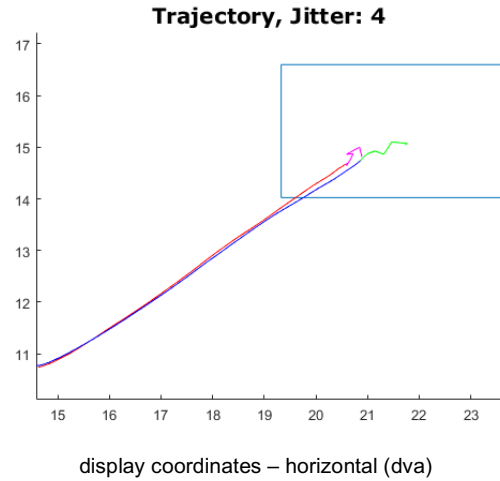


Figure 3.11: Average saccade trajectories. Saccade trajectories are plotted (in display coordinates [degree of visual angle]) for observer SXE. The blue rectangle indicates the positions of the Gabors. Red traces are averaged saccades to leftward drifting Gabors; blue traces are averaged saccades to rightward drifting Gabors. Averages were calculated by sample point, starting at the saccade start as defined by Eyelink; i.e. initially average trajectories were based on all saccades within a session and condition, but as some saccades were shorter than others, later parts of the trajectory are averages over fewer saccades. Red and blue traces are based on at least 90% of the saccades within the respective condition; sample points based on fewer saccades are coloured magenta and green. Each plot represents the four different Gabor positions. Plots A,B,C and D represent trials where the Gabors were placed at an eccentricity of 2.9° (Jitter 1), 3.7° (Jitter 2), 5.1° (Jitter 3) and 5.9° (Jitter 4), respectively.

To compare the saccadic trajectories data in various conditions, the slopes (gradients) of averaged saccades trajectories (\bar{X} , \bar{Y}) were determined by:

$$grad_i (\bar{X}, \bar{Y}) = \frac{\bar{Y}(t_{i+1}) - \bar{Y}(t_1)}{\bar{X}(t_{i+1}) - \bar{X}(t_1)}, \quad i = 1, \dots, 5 \quad (3.3)$$

where $t = [0, 10, 15, 20, 25, 30]$ indicates the time (msec) passed since saccade onset.

Figure 3.12 shows gradients averaged across all observers. X-Axes indicate time-intervals over which the gradient was computed as described in equation (3.3). Y-Axes indicate the averaged gradient across all observers. The blue and red dots represent averaged gradients when the Gabor drifted to the left and right, respectively. Each plot represents the four different Gabor positions. Plots A, B, C and D represent trials where the Gabors were placed at an eccentricity of 2.9° (Jitter 1), 3.7° (Jitter 2), 5.1° (Jitter 3), and 5.9° (Jitter 4), respectively. The Wilcoxon-Rank-Sum-Test was conducted to test whether gradients of averaged saccades to rightwards drifting Gabors were significantly different from averaged saccades to leftward drifting Gabors. No difference was found to be statistically significant (all p values > 0.39).

As shown in figure 3.12, the averaged gradients were larger (steeper) for leftward than for rightward drifting Gabors across all eccentricities and across all time intervals. This is consistent with the shift in saccadic landing positions in direction of motion of the Gabor (chapter 3.3.2). The difference between right- and leftward drifting Gabors was larger when the Gabor was placed at eccentricities of 2.9° (Jitter 1), 3.7° (Jitter 2) and 5.1° (Jitter 3) than when Gabor was placed at an eccentricity of 5.9° (Jitter 4), indicating that saccade targets are fully determined before saccade onset.

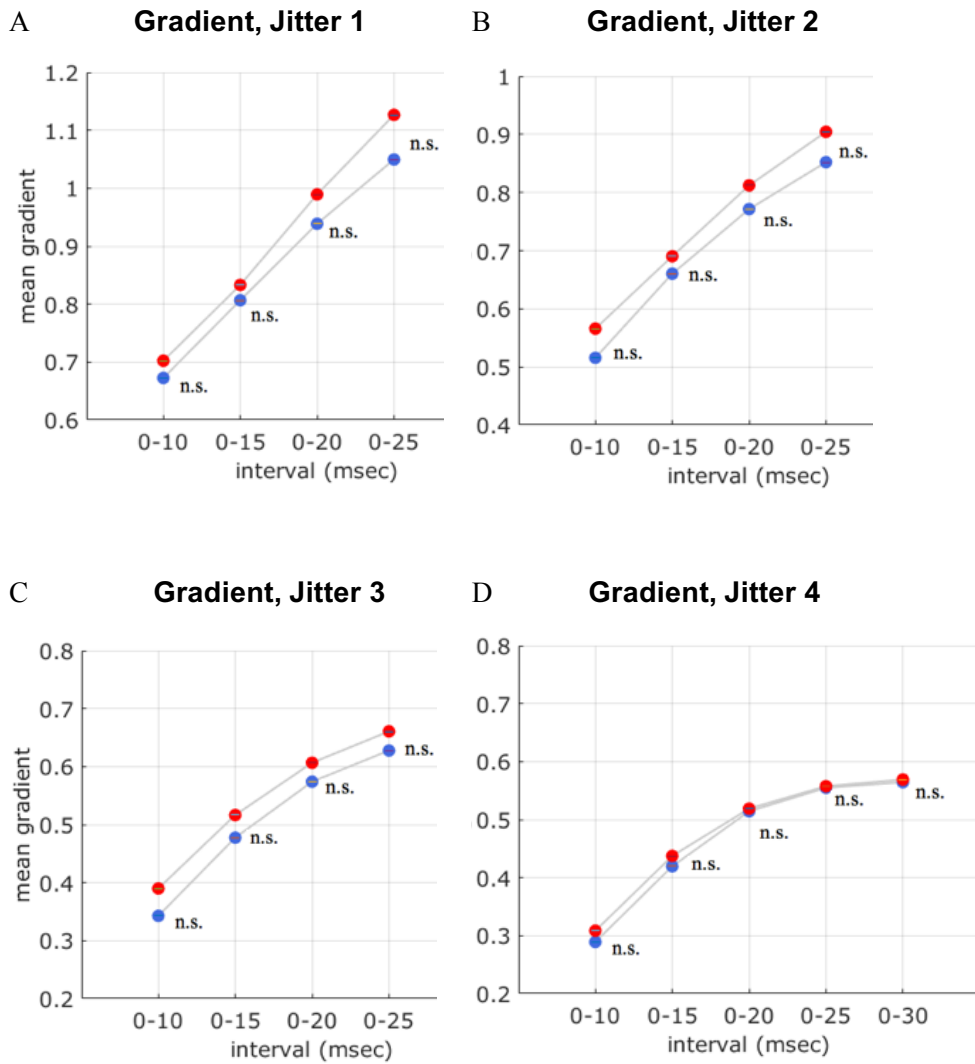


Figure 3.12: Averaged gradient of saccade trajectories. Gradient of saccade trajectories averaged across all observers. The x-Axes indicate time-intervals over which the gradient was computed as described in equation (3.3), y-Axes indicate the mean gradient over all observer. The blue and red dots represent averaged gradients when Gabor drifted rightwards and leftwards, respectively. Each plot represents the four different Gabor positions. Plots A,B,C and D represent trials where the Gabors were placed at an eccentricity of 2.9° (Jitter 1), 3.7° (Jitter 2), 5.1° (Jitter 3) and 5.9° (Jitter 4), respectively. For more details read main text.

3.3.4.2 Path length

Figure 3.12 and Figure 3.13 show the path length for each pair of sample points measured by the eyetracker. The Data of each observer, motion direction and Gabor position (2.9° , 3.7° , 5.1° , and 5.9°) were analysed separately. Titles of the plots indicate the observers; the X-axis represents the position of Gabors. Red and blue colours indicate mean values of saccade length when the Gabor drifted to the left and right, respectively.

When the Gabor was placed at eccentricities of 3.7° , 5.1° and 5.9° saccades to a rightward drifting (away from the midline) Gabor had larger mean saccadic lengths than saccades to a leftward drifting (toward the midline) Gabor for 4 out of 7 observers. LJR showed a larger mean path length in saccades to a rightward than to a leftward drifting Gabor for high eccentricities of 5.1° and 5.9° , but an opposite pattern when the Gabor was placed at 2.9° and 3.7° . SXX showed no consistent pattern in saccadic landing positions, but were – as stated before - considered outliers. Saccadic landing positions of observer AXS were shifted in the opposite direction of motion (see figure 3.9), a pattern that is also reflected in the path length of saccades.

The Wilcoxon-Rank-Sum-Test was applied to test whether distributions of saccadic length to rightwards drifting Gabors were significantly different from distributions of saccadic length to leftward drifting Gabors. No dataset was found to be significant.

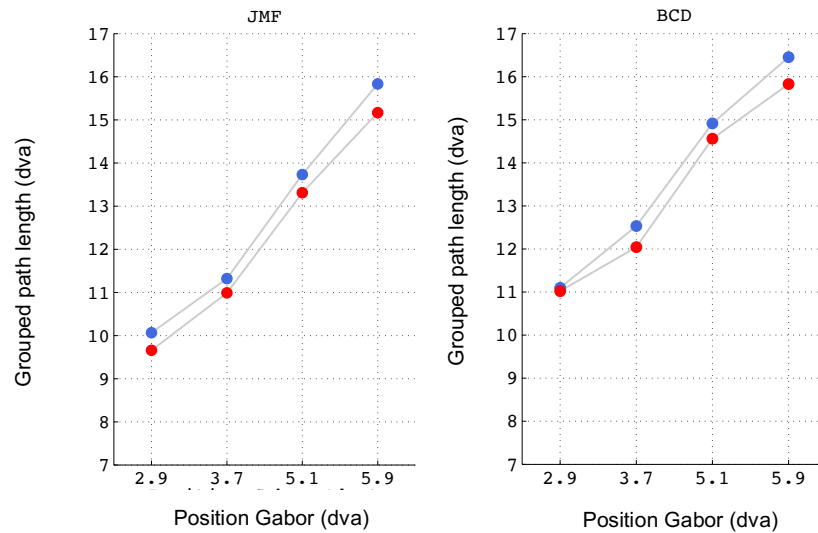


Figure 3.13: Resulting mean saccadic path length. Titles indicate the observers; Y-axes show the sum of path length for each pair of sample points measured by the eyetracker. X-axis represents the position of the Gabor. Red (leftward) and blue (rightward) colour indicates the Gabor's drift direction.

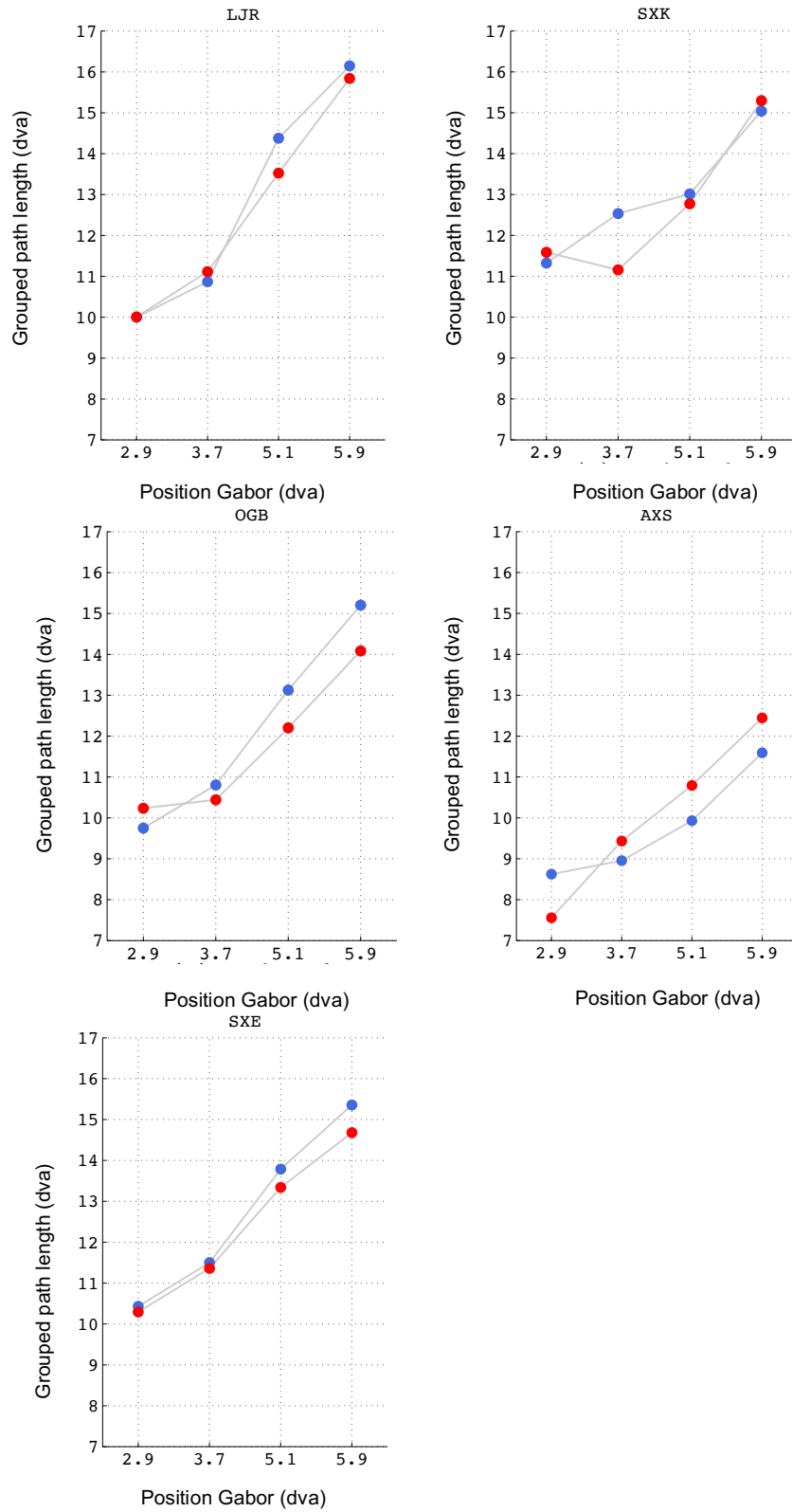


Figure 3.14: Resulting mean saccadic path length. Titles indicate the observers; Y-axes show the sum of path length for each pair of sample points measured by the eyetracker. X-axis represents the position of the Gabor. Red (leftward) and blue (rightward) colours indicate the Gabor's drift direction.

Figure 3.15 shows a summary graph of the path lengths over all observers (excluding one outlier, observer AXS). Path lengths were averaged across all observers. The Wilcoxon-Rank-Sum-Test was applied to test whether distributions of mean path lengths to rightwards drifting Gabors were significantly different from distributions of mean path lengths to leftward drifting Gabors. No difference was found to be significant (all p values > 0.31). However, there is a clear trend in data indicating that saccadic paths are larger for rightward than for leftward drifting Gabors when the Gabor was placed at high eccentricities of 3.7° , 5.1° and 5.9° .

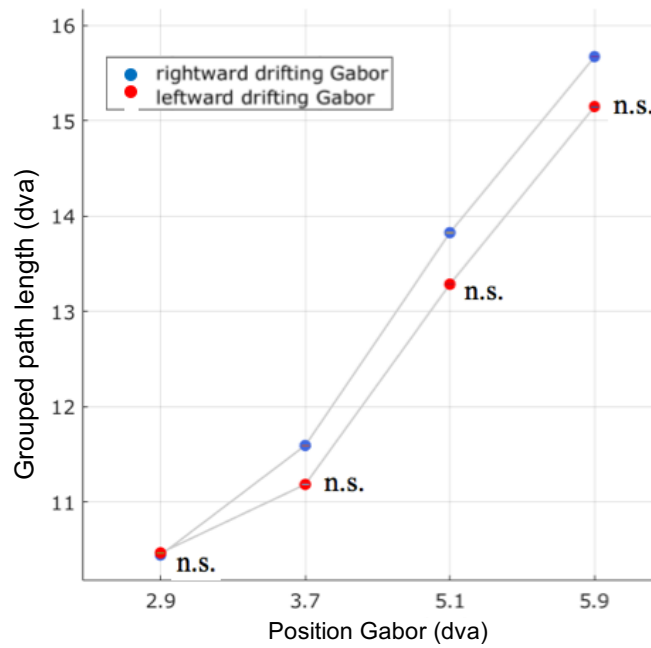


Figure 3.15: Grouped path length. Y-axes show the mean path length over all observers; X-axis represents the position (eccentricity) of the Gabor (dva). Red (leftwards) and blue (rightwards) colours indicate the drift direction of the Gabor.

3.3.4.3 Saccadic peak velocity

Because rightward drifting Gabors elicited saccades with a larger path length than leftward drifting Gabors for most datasets, peaks in velocity profiles should be larger for rightward than for leftward drifting Gabors, especially when the Gabor was placed at high eccentricities. As shown in figure 3.14 and figure 3.15, I found that peaks in velocities profiles were positively correlated with saccadic length; i. e. the larger the mean path length in saccade trajectory, the higher the mean peak velocity.

In summary, five out of seven observers had higher peak velocities in saccades to rightward than to leftward drifting stimuli at eccentricities of 5.1° and 5.9° .

The Wilcoxon-Rank-Sum-Test was applied to test whether distributions of velocity peaks to rightwards drifting Gabors were significantly different from distributions of velocity peaks to leftward drifting Gabors. No dataset was found to be significant.

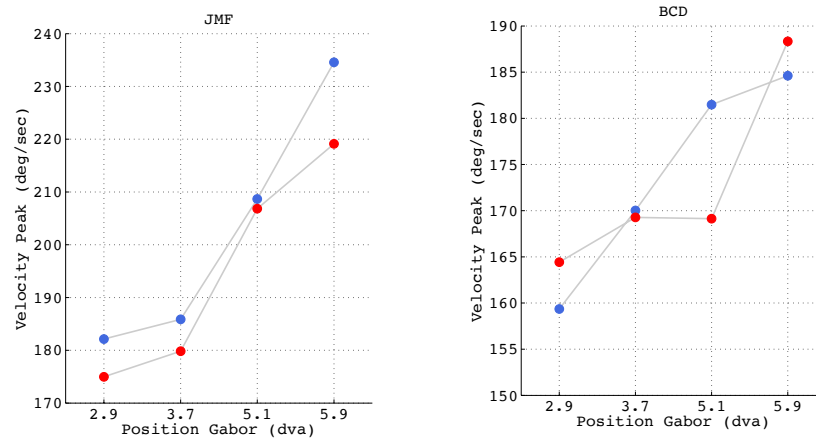


Figure 3.16: Resulting mean peaks of the velocity profiles. Titles indicate the observers; Y-axes show the mean peak velocity; X-axis represents the position of the Gabor. Red (leftwards) and blue (rightwards) colours indicate the drift direction of the Gabor.

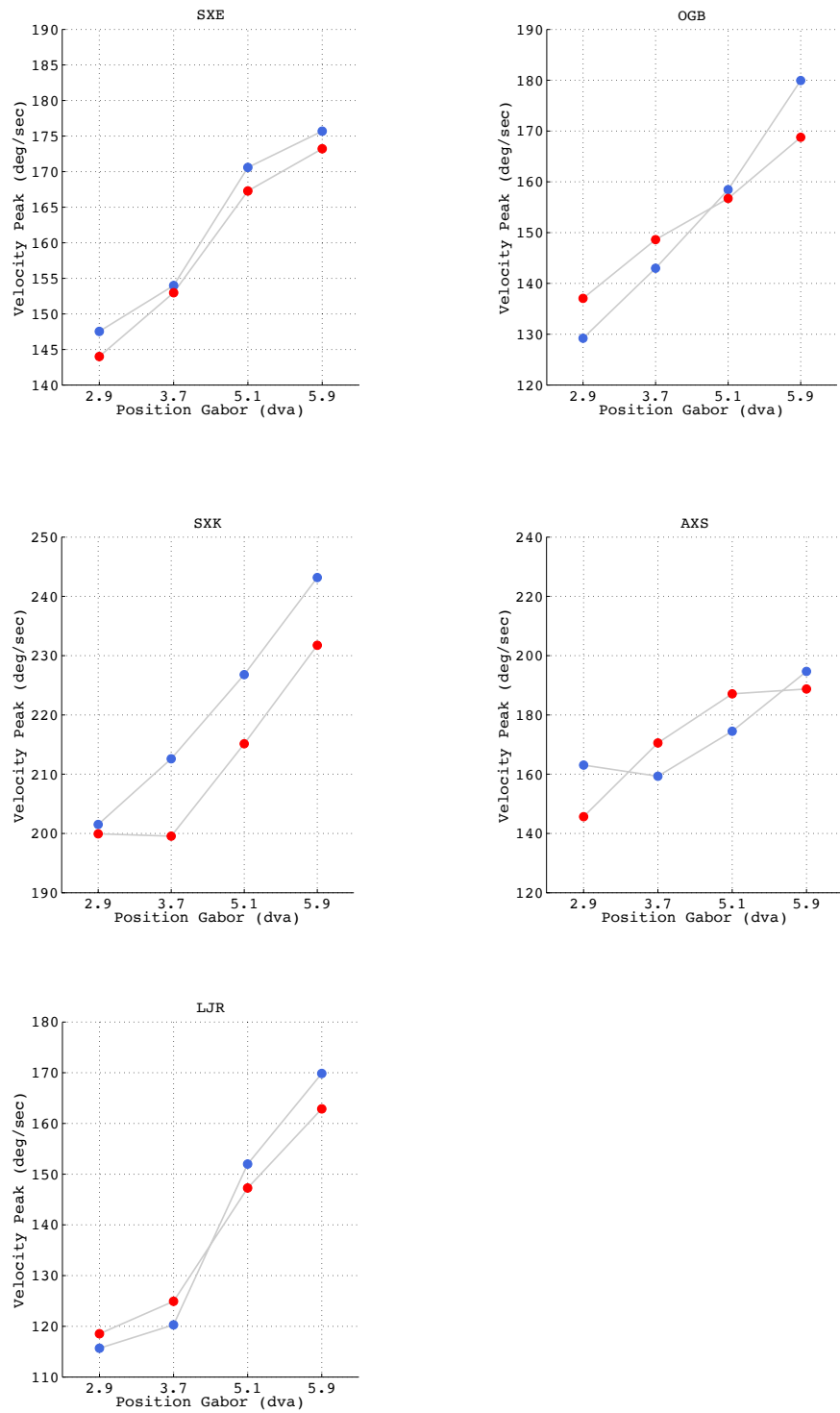


Figure 3.17: Resulting mean peaks of the velocity profiles. Titles indicate the observers; Y-axes show the mean peak velocity; X-axis represents the position of the Gabor. Red (leftwards) and blue (rightwards) colours indicate the drift direction of the Gabor.

Figure 3.18 shows a summary graph of saccadic peak velocities over all observers (excluding one outlier, observer AXS). Peak velocities were averaged across all observers. The Wilcoxon-Rank-Sum-Test was applied to test whether distributions of mean velocity peaks to rightwards drifting Gabors were significantly different from distributions of mean velocity peaks to leftward drifting Gabors. No difference was found to be significant (all p values > 0.59). Data show a clear trend indicating that saccadic velocity peaks are larger for rightward than for leftward drifting Gabors when the Gabor was placed at eccentricities of 5.1° and 5.9° .

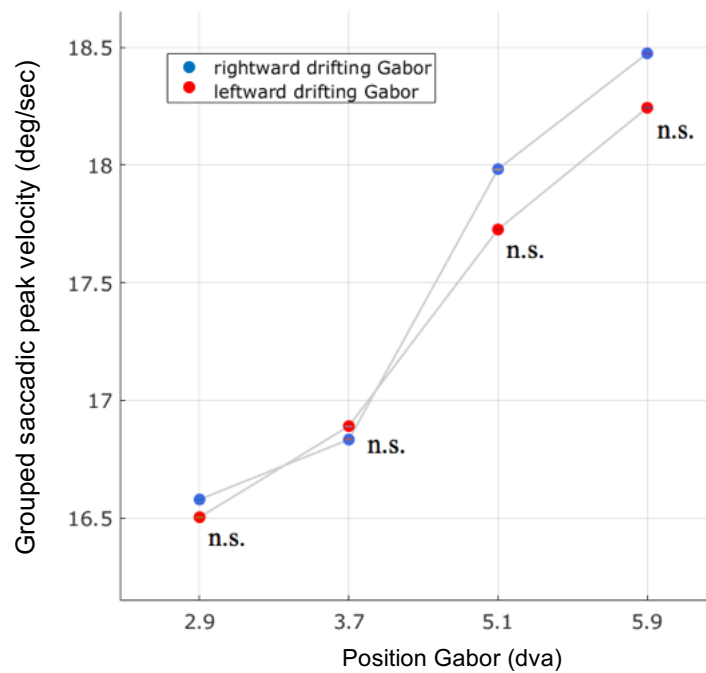


Figure 3.18: Grouped saccadic peak velocity. Y-axes show the averaged peaks of saccadic velocities (deg/sec) over all observers; X-axis represents the position (eccentricity) of the Gabor (dva). Red (leftwards) and blue (rightwards) colours indicate the drift direction of the Gabor.

3.4 Summary

I found that the perceptual shift depended on the Gabors' directional signature; more precisely, rightward drifting Gabors induced a perceptual shift to the right (up to 0.3°) and leftward drifting Gabors induced a perceptual shift to the left (up to -0.33°). Saccadic eye movements were influenced in the same way as perception. Only the effect of observer AXS showed an opposite pattern. However, data of AXS were considered to be outliers. These findings were consistent with previous studies (Kerzel & Gegenfurtner, 2004; De Valois & De Valois, 1991; Kosovicheva, Wolfe & Whitney, 2014). Detailed methodological comparison with these studies and a discussion of the results can be found in chapter 3.7.

I did not find that the magnitude of the effect was due to the drifting direction (away or toward the midline) of the Gabor, neither in saccades nor in perception.

I hypothesised that the shift in saccadic landing positions might be due to a drifting fixation before the onset of saccades. I investigated this by comparing the mean values of last averaged fixations just before saccade onset, but did not find evidence for this hypothesis: Statistical tests did not indicate a difference between fixations during right and leftward drifting Gabors.

As the fixations did not differ significantly, it can be assumed that averaged trajectories of eye movement to rightward and leftward drifting Gabors would not differ at the beginning of a saccade, but at the end. Therefore, trajectories were averaged, and were not found different at trial onset. Computing the slope (gradient) of saccade trajectories indicates that saccade targets are fully determined before saccade onset.

In regard to the 'main sequences relationships', amplitudes of saccades should be larger for rightward drifting than for leftward drifting Gabors. And therefore the peak velocity should be larger for rightward than for leftward drifting Gabors. I compared the path length of saccades to right and leftward drifting Gabors and found evidence that rightward drifting (away from the midline) Gabors induced saccades with larger amplitudes than leftward drifting (toward the midline) Gabors, particularly when Gabors were placed at eccentricities of 5.1° and 5.9° . Larger differences in saccade

amplitudes at eccentricities of 5.1° and 5.9° were consistent with a finding of DeValois & DeValois (1991) that the larger the eccentricity, the larger the perception shift. However, statistical tests did not indicate a significant difference in saccade amplitudes.

Averaged peak velocities were partly consistent with findings of saccade amplitudes (see figure 3.14, 3.15, 3.16 and 3.17); i.e. five out of seven observers had a higher averaged peak velocity for saccades with larger amplitudes than for saccades with comparatively small amplitude at eccentricities of 5.1° and 5.9° . I did not find a constant pattern for eccentricities of 2.9° and 3.7° .

3.5 Discussion

I measured the perceptual shift in a dot localisation task in a moving Gabor stimulus, and saccadic eye movements to the moving Gabor, to test whether saccades also showed a shift induced by the motion stimulus. In line with previous studies (Yamagishi, Anderson & Ashida, 2001; Kerzel & Gegenfurtner, 2004; De Valois & De Valois, 1991; Kosovicheva, Wolfe & Whitney, 2014) I found consistent perceptual and saccadic effects.

As stated in the literature review, Goodale and Milner (1992) proposed that visual information for perception and action are processed separately through the dorsal-stream and ventral-stream, therefore suggesting that perceptual tasks and visually guided motor tasks could generate different object location signals. Previous studies also used the motion-induced position shift in order to investigate the two-stream hypothesis. This approach is controversial for multiple reasons (see literature review), but might indicate other scientific insights besides the classical two-stream hypothesis. Furthermore, in contrast to perceptual tasks where observers are asked to judge the position of a Gabor by e.g. calling out the perceived position, motor-tasks - such as saccadic eye movements - are less likely to be affected by decisional biases or response biases. I will therefore compare publications that studied the motion-induced position shifts in action tasks and perception tasks.

3.5.1 Methodological comparison with previous studies

Yamagishi, Anderson & Ashida (2001) investigated the ability to localise a stimulus using a motor task and a perceptual task with a Gabor stimulus. The Gabor was presented at different positions along the horizontal meridian in the right visual field, and it was drifting rightward or leftwards or only flickering in the same frequency as the motion stimulus speed. In the perceptual task a ruler was displayed on the screen after the end of Gabor presentation and observers spoke out the perceived location of the Gabor with reference to the ruler. In the motor tasks, observers marked the perceived position of the Gabor on a board using a pen held in their hand. In both paradigms, observers were cued to disengage a central fixation by an audible tone and report the perceived position of the Gabor. Time difference between disappearing of the Gabor and the cue to do a task was 200 ms for a short-delay condition and 4200 ms for a long delay condition. In my experiment observers were only allowed to do the perceptual task within 700 ms. Otherwise the trial was counted as failed. Therefore, when comparing with the results from Yamagishi, Anderson & Ashida (2001), I focus on the results obtained in the short delay condition.

Yamagishi, Anderson & Ashida (2001) were able to confirm a previous study of DeValois & DeValois (1991): Gabors were perceived as shifted along the direction of motion. Furthermore, they found that the magnitude of both shifts depended on the direction of the interval waveform direction: The effect of leftward drifting Gabors (toward the midline) was for both observers greater than the effect of rightward drifting Gabors (away from the midline).

Confirming Yamagishi, Anderson & Ashida (2001) I also found consistent effects on perception. Instead of hand movements, I measured saccadic eye movements and found that the motion of Gabors also affected them. Visually guided hand movements may be driven by relatively late visual information from the posterior parietal cortex (Gardner et al. 2007), while eye movements are also driven by very early subcortical information such as that from the colliculus superior. Hence, it is unclear how comparable eye movements and hand movements are in this sort of paradigm, and it is not straightforward to interpret the differences.

Kerzel & Gegenfurtner (2005) investigated the motion effects of hand movements and also the effects of eye movements (see literature review): in the eye movements task, observers were invited to look at a fixation bull's-eye at the beginning of every trial and make a saccade to a right- or leftward moving Gabor on the right or left side of the visual field, appearing a hundred milliseconds after trial onset. Observers initiated a saccade as soon as they detected the Gabor. In my experiment, however, fixation offset was 500 ms after Gabor onset. Saccadic responses with latencies greater than 500 ms were considered late and saccadic responses with latencies smaller than 50 ms were considered anticipation. Both types were excluded from analysis.

Kerzel & Gegenfurtner (2005) used following analysis: the deviation of the true centre of the stimulus from the endpoint of the saccade was determined. Then the best estimate of the expectancy value was used, on the assumption that the measures were normally distributed. Positive values indicated that the moving object was localised too far in the direction of motion, while negative values indicated that the moving object was localised against the direction of motion. The average expectancy value for motion toward and away from the midline estimated the motion induced displacement: $(\mu(a) + \mu(t))/2$, while a consist of distances to the centre of the Gabor for trials with rightward moving Gabors and t consists of the distances to the centre of the Gabor for trials with leftward moving Gabors. Kerzel and Gegenfurtner found a significant motion induced visuomotor displacement. This measurement, however, was contaminated by saccadic undershoot. Additionally, Kerzel & Gegenfurtner (2005) defined a variable called foveal displacement to estimate whether the Gabor was mislocalised toward or away from the fovea relative to the centre of the Gabor: $(\mu(a) - \mu(t))/2$. The foveal displacement was significantly biased towards the fovea. But this may only show that observers made an undershoot relative to the true centre of the Gabor.

I analysed our data differently to truly allow comparison of motion toward and away from the midline. Furthermore, I designed our experiment such that eye movement direction and shift direction were approximately oblique. This was intended to improve detection of a shift effect independent of the undershoot.

While I conducted statistical analysis, Kosovicheva, Wolfe & Whitney (2014) published a study about saccadic eye movements to the perceived centre of Gabors in

comparison to perception-tasks of motion-induced position shifts in vertically aligned Gabors. Because the study is very similar to my study, I will describe and discuss it extensively in this section.

As mentioned briefly in the literature review, Kosovicheva, Wolfe & Whitney (2014) asked if the visual system used more sources of information to predict future target position, including changes in position of the object over time, or its motion. Alternatively, they hypothesized that motion information alone influenced the represented position of a moving object. To answer this hypothesis, they used drifting Gabors with soft-apertures and hard-apertures. The inclusion of the hard-aperture stimulus allowed them to present the same stimulus motion as in the soft aperture stimulus with a reduced shift in perceived position. With that stimulus they controlled stimulus motion while only generating a shift in perceived location in the soft aperture condition.

The experiment to measure saccadic eye movements started by fixating on a dark circle in the centre of the screen. Observers triggered the beginning of each trial by pressing a key on the keyboard. The fixation point then changed to black, and after a delay of 1500 ms to 2000 ms, the observers were presented a target either on the right or the left side of the visual field for 140 ms. Observers were instructed to make saccades to the target as soon as it appeared. The central position of the saccade target was jittered 10° to either the right or the left of the fixation. The range of possible jittered position spanned 3° horizontally and 3° vertically. The visual field location (left or right), motion direction of the target (left or right), and the aperture type (hard or soft) were randomised and counterbalanced across the whole block of 400 trials for each observer. Kosovicheva, Wolfe and Whitney (2014) also normalised saccadic landing positions by subtracting the mean landing location from the landing position on each trial. So, positive values indicated a shift in the direction of motion and negative values indicated a shift opposite to the direction of motion. In contrast to me, they did not compare saccadic landing positions to stimuli that were drifting away from the midline with saccadic landing positions to stimuli that were drifting towards the midline.

The paradigm to measure the perception shift was slightly different: On each trial observers were shown three targets for 140 ms: Either a drifting Gabor (soft aperture) or a drifting sinusoidal grating (hard aperture), and two stationary stimuli above and

below the drifting stimulus. The static stimuli had a 6.5° vertical centre-to-centre separation from the target. As in the paradigm to measure saccades, stimuli were presented at jittered positions 1.5° horizontally and vertically around the central location 10° to the right or the left of the fixation point. The horizontal position of the central stimulus was at one of seven possible offsets relative to the static stimuli, linearly spaced from 1.75° to the left to 1.75° to the right of the static stimuli. Observers maintained fixation throughout the whole trial and were to judge if shifts had occurred to the left or to the right relative to the two static stimuli. As in saccadic tests, there was a delay interval at the beginning of each trial that ranged from 750 ms to 1250 ms. The visual field location (left or right), the motion direction of the target (left or right), and the aperture type (hard or soft) were randomised and counterbalanced across the whole block.

The perception shift for hard aperture and soft aperture conditions was, as in my experiment, calculated as half the difference between the points of subjective equality of the two (right and leftward moving) fitted functions. Observers' responses were bootstrapped separately by resampling each observer's responses with 1000 samples and fitting each set of resampled data to a logistic function. Afterwards Kosovicheva, Wolfe & Whitney (2014) employed an ANOVA to test if bootstrapped data indicated a significant difference from zero for both motion directions in both the hard and soft aperture condition. Furthermore, the ANOVA tested if there was an interaction between hard and soft aperture conditions. I also used a bootstrap method, but resampled each observer's responses with the number of samples that were actually gathered. Matlab fitted each set of resampled data to a cumulative Gaussian function. To investigate if the perceptual shifts might be truly different from zero, I determined 95 % confidence intervals.

Another experiment by Kosovicheva, Wolfe & Whitney (2014) investigated if short stimulus presentation durations had a different effect on saccadic landing positions and perceived positions than longer durations. They used the same paradigm as in previous experiments, but only for the soft aperture condition, and showed the Gabor for 20, 40, 60, 80 or 100 ms.

In summary, they measured saccadic landing positions to Gabors with hard and soft-apertures and analysed whether the magnitude of the errors was due to saccade latencies or stimulus duration. Furthermore, they measured the perceived position of a

drifting Gabor in comparison to flickering Gabors. The perception shift was also measured for different Gabor presentation durations.

The comparison of perceptual error and saccadic error is more straightforward in my experiment, due to the experimental procedure. Kosovicheva, Wolfe & Whitney (2014) measured the perceptual shift of the whole stimulus, I measured instead the perception shift in the centre of the Gabor by placing a dot superimposed on it. As mentioned in the literature review, the shift of a Gabor may be due to a misperceived form of the patch, which in turn may be due to a motion deblurring mechanism at the trailing edges of the Gabor. Therefore it may be that the magnitude of the perception shift is different when measuring it at leading edges, trailing edges or the centre of the stimulus. Comparing saccades to the centre of the Gabor and to the perception shift within the centre of the Gabor may be more accurate. Furthermore, I presented only one Gabor in both tasks, while Kosovicheva, Wolfe & Whitney (2014) presented one Gabor in the saccade-task, but three Gabors in the perception-task.

Moreover, Kosovicheva, Wolfe & Whitney (2014) presented Gabors for up to 140 ms and observers made a saccade as soon as the Gabor appeared. I presented Gabors 500 ms before fixation offset, and the Gabor remained for 900 ms afterwards, triggering 'volitional saccades' which had not been investigated by any previous study.

3.5.2 Perceptual effect

I found consistent perceptual shifts for Gabors that appeared on the right side of the visual field with randomised Gabor positions. In most cases, perceived target positions were shifted leftwards with Gabors drifting to the left, and shifted rightwards with Gabors drifting to the right. These results are comparable to previous results of Yamagishi, Anderson & Ashida (2001). In the study of Yamagishi, Anderson & Ashida (2001) observers had a similar perception-effect for each direction of motion: targets were perceived as shifted along the direction of motion. The perception effect was larger for Gabors which moved toward the midline than for Gabors which moved away from the midline. In my experiment, magnitudes of perceptual shifts were not due to motion direction away from or towards the midline within my paradigm.

Kerzel & Gegenfurtner (2005) also investigated the perceptual effect and found consistent effects within different paradigms: targets were also perceived as shifted along the direction of motion.

DeValois & DeValois (1991) were also able to measure a perceptual shift for a moving stimulus up to 0.3° for both directions of motion.

Kosovicheva, Wolfe & Whitney (2014) found a perceptual shift of 0.55° in the soft aperture condition and a shift of 0.14° in the hard aperture condition. The authors suggested that one explanation for the significantly different shift to zero in the hard aperture condition might be due to the large stimulus eccentricity of 10° . The large eccentricity might result in a deblurring of the stimulus at the edges. Unfortunately, they did not state what sizes of shifts were obtained for motion direction towards and away from the midline.

As mentioned above, in another experiment they measured the perceptual shift of different Gabor durations in only the soft aperture condition. They found a significant effect on perception for all durations except 20 ms. The shift increased with stimulus duration and reached its asymptotic level with durations of 60-80 ms reaching 0.55 dva. In contrast to Kosovicheva, Wolfe & Whitney (2014) I analysed the data of each observer separately. I have found shifts up to 0.15° (OGB) for Gabors drifting towards the midline (rightwards), and shifts up to -0.24° (SXX) for Gabors drifting away from the midline (leftwards).

Table 3.1 summarises the key features of the methods and measured perceptual effects of the studies described in this section. In summary, perceptual shifts in my experiments are comparable with previous studies.

Author (Year)	Perceptual Measurement Method	Perceptual effect
De Valois & De Valois (1991)	Three Gabors vertically aligned, but only the middle one contained right or leftward sinusoidal drift, while the outer once where flickering; Eccentricity: 1° , 2° , ..., 8° ; Gabor presentation duration: 2000 msec; <i>Task</i> : Key-press to indicate whether the Gabor in the middle was to the right or the left relative to the outer Gabors (Method of Single Stimulus)	Up to 0.3° for both drift directions
Yamagishi, Anderson & Ashida (2001)	Single Gabor (drifting rightwards, leftwards); Eccentricity: 10° Gabor presentation duration: short-delay-condition (200 msec), long-delay-condition (4200 msec); <i>Task</i> : speak out the position of the Gabor with reference to a ruler (Method of Single Stimulus).	<i>Exact values are not stated in the study.</i> Gabors were perceived as shifted along the direction motion. Perception effect larger for Gabors which moved towards the fovea than for Gabors that moved away from the fovea. Short term-condition and long –term condition induced shifts of the same size.
Kerzel & Gegenfurtner (2005)	Three Gabors vertically aligned, the middle one contained right or leftward sinusoidal drift, while the outer once (reference stimuli) where drifting in opposite directions (Condition A); One central Gabor (drifting to the right or the left), continuously visible lines (Condition B) or flashed lines were used as reference stimulus (Condition C); Eccentricity: $6 \pm 0.55^{\circ}$; Gabor presentation duration: 500 msec <i>Task</i> : Compare the position of a flickering Gabor to the position of moving Gabor, stationary lines, or flashed lines (Method of Single Stimulus).	Mean motion displacement across observes: Condition A: $\sim 0.39^{\circ}$ Condition B: $\sim 0.2^{\circ}$ Condition C: $\sim 0.12^{\circ}$
Kosovicheva, Wolfe & Whitney (2014)	Three Gabors vertically aligned, but only the middle one contained right or leftward sinusoidal drift, while the outer once where flickering;	Up to $\sim 0.4^{\circ}$; The magnitude of shift is increasing with increasing

	Eccentricity: $10 \pm 3^\circ$; Gabor presentation duration: 20, 40, 60, 80, 100, 140 msec. <i>Task</i> : Key-press to indicate whether the Gabor in the middle was to the right or the left relative to the outer Gabors (Method of Single Stimulus).	stimulus presentation time.
This study	One Gabor (drifting rightward or leftwards), a single dot superimposed on the Gabor (reference stimulus); Eccentricity: $4.4 \pm 0.7^\circ$, $4.4 \pm 1.5^\circ$; Gabor presentation duration: 1400 msec <i>Task</i> : Indicate by key-press the perceived position of the dot relative to the centre of the Gabor (Method of Single Stimulus).	Perceptual shifts up to 0.15° for rightward drifting Gabor, and up to 0.33° for leftward drifting Gabors. No consistent pattern indicating that the magnitude of the shift depends on drift direction (rightwards vs. leftward)

Table 3.1: Key features of the methods and measured perceptual effects of the studies described in this section.

3.5.3 Saccadic eye movements

I measured consistent effects on saccadic landing positions up to -0.2° (OGB). After the normalisation procedure, saccadic landing positions to rightward drifting Gabors were for almost every observer (except SXX and AXS) shifted to the right relative to the true centre of the Gabor and shifted to the left for leftward drifting Gabors. SXX had a general bias of saccadic landing positions away from the midline, but the same pattern as with other observers was still found; i. e. saccades were shifted rightwards to saccadic landing positions of leftward drifting Gabors. Data from one observer were not included, because too many saccades were started too late. AXS reported that it was too difficult to do saccadic eye movements in time, because the trials repeated too quickly. In general, her results were in the opposite direction from the other observers' results.

Furthermore I analysed whether shifts in saccadic end positions were due to drifting fixations in the Gabors' motion direction before saccade onset. However, last fixations just before saccade onset to Gabors were not found to be affected by the motion.

I analysed the length of saccade trajectories, and the peak of the velocity profiles for saccades to right- and leftward drifting Gabors. When a Gabor was placed at eccentricities of 5.1° and 5.9° saccades to a rightward drifting (away from the midline) Gabor had larger mean saccadic lengths than saccades to a leftward drifting (toward the midline) Gabor for five out of seven observers. One observer showed a larger mean path length in saccades to a rightward than to leftward drifting Gabor for high eccentricities of 5.1° and 5.9° , but an opposite pattern when the Gabor was placed at 2.9° and 3.7° . This is consistent with the study by DeValois & DeValois (1991) which found that the larger the eccentricity, the larger the perceptual shift. Peaks in velocity profiles were correlated with saccadic length; i. e. the larger the path length of the saccade trajectory, the higher the average peak velocity. Five out of seven observers had higher peak velocities in saccades to rightward than to leftward drifting stimuli at eccentricities of 5.1° and 5.9° . These results indicate that saccades are truly affected by the motion-induced position shift. Measured shifts in saccadic landing positions cannot be caused by e.g. a statistical artefact.

An example of saccadic effects in humans by Kerzel and Gegenfurtner (2005) has already been mentioned above: they stated that they had found a significant net motion induced visuomotor displacement, as described above. Unfortunately, because of their analysis method it was unclear whether motion induced saccadic displacements were greater for Gabors which moved away from the midline than for Gabors which moved toward the midline. Using a different analysis method I found no consistent pattern in magnitudes of shifts when the Gabor drifted away or towards the midline. Furthermore the differences between the magnitudes in shifts for right and leftwards drifts were very small.

Schafer and Moore (2007) tested the saccadic shift in macaque monkeys using comparable stimuli to the ones I used. They found significant differences in monkey eye movements to differently moving Gabors. The means of saccade angles to differently moving Gabors differed by 1.8° (polar angle). Note, that the monkeys had been trained specifically and for a long time to do this visuomotor task, and thereby were possibly able to conduct the task more precisely than our observers.

Kosovicheva, Wolfe & Whitney (2014) found a general shift of saccadic landing positions in the direction of motion of $\sim 0.50^\circ$ to soft aperture Gabors and $\sim 0.20^\circ$ to hard aperture Gabors. As in the perceptual results, they did not differ between motion

direction towards the midline and away from the midline. Soft versus hard aperture conditions were compared, and the authors concluded that motion alone was not sufficient to induce an error in saccadic landing positions.

Kosovicheva, Wolfe & Whitney (2014) also investigated the error in saccadic landing positions with different Gabor presentation durations (20-100 ms). They found larger saccadic errors with shorter saccadic latencies for all Gabor durations except the shortest (20 ms). Pooling single trial data into latency bins of 100-170 ms, 171-240 ms, and 241-380 ms indicated that early saccades (with latencies of 100-170 ms) were shifted significantly in the direction of motion for all Gabor durations. No significant effect was found for the other latency ranges for any Gabor duration. However, consistent with the perceptual effect for different Gabor durations (see above), Kosovicheva, Wolfe & Whitney (2014) showed for all latencies that the longer the Gabor duration, the larger the error. The largest shift was found for short latency saccades and long Gabor durations. They suggested that the visual system might use motion information to change the position of an object at early stages of visual processing.

3.6 Conclusion

In the introduction of this chapter I asked two main questions:

First, is there a general effect of drifting Gabors in a static envelope on the perception of the location of a target dot superimposed on the Gabor?

I found a clear effect on the perceived position of the dot superimposed on a drifting Gabor. Target dots were perceived as shifted along the direction of motion: When the Gabors were drifting rightwards, target dots were perceived to be shifted to the left, and when the Gabors were drifting leftwards, target dots were perceived to be shifted to the right relative to the true centre of the Gabor. Note that the measured position of the target-dot does not indicate an illusory position shift of the target-dot itself, but it does indicate the illusory position shift of the Gabor placed underneath. I measured perceptual shifts up to 0.15° (observer OGB) for Gabors drifting toward the midline (rightwards), and shifts up to 0.33° (observer SXX) for Gabors drifting away from the midline (leftwards).

Secondly, is there a general effect in volitional saccadic eye movements to the Gabor stimulus?

Volitional saccadic eye movements are also distorted by the motion-induced position shift of a Gabor. The effect is consistent with the perceptual effect: After the normalisation process, saccadic landing positions were shifted to the left (up to -0.20° , observer OGB) in leftward drifting Gabors, and shifted to the right (up to 0.175° , observer SXE) in rightward drifting Gabors. In addition, I found a non-significant trend that the peaks of saccadic velocity profiles were larger for rightward drifting than for leftward drifting Gabors. This is consistent with the finding that saccades elicited by rightward drifting Gabors had a larger path length than saccades elicited by leftward drifting Gabors. In summary, I can conclude that the saccadic system is truly affected by the motion of the Gabor, and the result is very unlikely be due to a statistical artefact. Furthermore, I compared the slopes of saccade trajectories towards right- and leftward drifting Gabors. The results are consistent with the widely investigated hypothesis of a mechanism preventing an inflight-correction after saccade onset (e.g. Purves et al., 2001).

4. COMPARISON OF MIPS IN PERCEPTION TASKS AND VOLITIONAL SACCADES

4.1 Introduction

The results of the experiment described in chapter 3 showed that saccadic eye movements are misled by the internal drifting texture of Gabors with a static envelope. Rightward drifting Gabors elicited saccades with landing positions shifted to the right, and leftward drifting Gabors elicited saccades with landing positions shifted to the left. The same effect of internal motion on object localisation was found in the perceptual system. After saccade landing a dot was presented superimposed on the Gabor, and observers were asked to indicate whether the dot was located on the right or the left relative to the centre of the Gabor. The dot was perceived displaced in the opposite direction to the direction of motion: rightward and leftward drifting textures elicited mislocalisation of the dots' position to the left and right, respectively. In other words, the whole patch was perceived shifted in the direction of motion.

Comparison of the effect on the saccadic system and the perceptual system is controversial. The saccadic localisation task was done while fixating a central fixation cross (Gabor was shown parafoveally), but the perception task was done after saccade landing while fixating the centre of the Gabor (foveally). As stated in the literature review, the position of the Gabor relative to the retina has a large influence on the magnitude of the effects (e.g. De Valois & De Valois, 1991); i.e. the illusory position shift was found to increase with increasing eccentricities. In contrast to a possible saccadic inflight correction mechanism, many researchers suggest that saccade targets have to be determined before saccade onset, and once they start, a saccadic suppression mechanism prevents an inflight correction (e.g. Purves et al., 2001). In other words, saccade trajectories cannot be influenced inflight. Therefore, researchers speak about 'ballistic saccades'.

To cancel out differences in magnitudes of effects that may be due to different stimulus locations, the current experiment measures the perceptual effect parafoveally, and attempts to answer the question:

What is the relation between saccadic eye movements and perceptual shifts in Gabors?

4.2 Methods

Observers BCD, and JMF each performed 80 trials per motion direction in Setup 1. All methods were identical to those used in the experiment described in chapter 3, but the fixation cross did not disappear triggering observers to saccade to the Gabor.

4.3 Data Analysis and Results

4.3.1 Perceptual shifts

Perceptual shifts were analysed as described in chapter 3. Both observers showed a perceptual shift in the direction of motion: In leftward drifting Gabors, BCD and JMF had a perceptual shift of -0.30 dva and -0.18 dva, respectively. In rightward drifting Gabors, BCD had a perceptual shift of 0.19 dva, and JMF had a perceptual shift of 0.20 dva.

4.4 Summary

The experiment described in chapter 3 showed that the horizontal error elicited by leftward drifting Gabors was -0.14 dva in saccades of observer BCD, and -0.14 dva in saccades of observer JMF. Perceptual biases measured parafoveally (-0.30 dva in BCD, -0.18 dva in JMF) were comparatively large for leftward drifting Gabors in both observers.

The same pattern was found in rightward drifting Gabors. Horizontal saccadic errors (chapter 3) elicited by rightward drifts were 0.15 dva, and 0.12 dva for observer BCD and observer JMF, respectively. Perceptual biases measured parafoveally were comparatively large in both observers (0.19 dva in BCD, 0.20 dva in JMF).

In summary, I found that the magnitudes of saccadic errors were smaller than the magnitudes of perceptual shifts in both observers and in both conditions, right- and leftward drifts.

4.5 Discussion

Comparison of saccadic shifts and perceptual shifts indicates that the perceptual system induces a larger shift in the direction of motion than the saccadic system.

In the literature review I pointed out that other scientists also measured motion-induced position shifts in perception and saccades (Kerzel & Gegenfurtner, 2004; Kosovicheva, Wolfe & Whitney, 2014). In contrast to them, I asked observers to judge the perceived centre of a single Gabor in both tasks: 1) saccades towards a single Gabor, and 2) perceptual position judgement of a dot superimposed on a single Gabor. Kerzel & Gegenfurtner (2005), and Kosovicheva, Wolfe & Whitney (2014) used a single Gabor when observers were asked to make a saccade towards the centre of it. In the perception tasks, however, two additional reference stimuli above and below the target-Gabor were presented. Kosovicheva, Wolfe & Whitney (2014) used two reference Gabors, Kerzel & Gegenfurtner (2005) used two reference Gabors, or two lines. In both studies, reference stimuli were not at the centre of the drifting target-Gabor, but in the surrounding environment. Thus, it was impossible to know whether observers used the centre, trailing edge, or leading edge of the drifting Gabor to judge its position relative to the references. Many studies, however, showed that the motion-induced position shift varies at the trailing edge, leading edge and the centre of the Gabor (e. g. Arnold, Thompson & Johnston, 2007; Chung et al., 2007). In my experiments, observers fixated the centre of the Gabor, and judged a dot's position superimposed around the perceived centre of it.

In contrast to other studies, I asked observers to conduct both tasks within one experiment and within each trial. Hence, biases were not affected by changing performance over time.

The timing in my experiment could be controversial. Saccades were found to be valid when they started 800 ms after Gabor onset, while perception tasks were made after 1200 ms. Studies showed that the illusory position shifts in Gabors saturates after 150 ms (Arnold, Thompson & Johnston, 2007), and they last for at least 2000 ms (De Valois & De Valois, 1991). However, no study was conducted to investigate the relationship between motion-induced position shifts in saccades in perception over a time interval of 1200 ms. The difference in saccadic and perceptual shift may be

caused by different timings, a hypothesis which needs to be investigated in future experiments.

The smaller bias in saccades than in perception might also be due to 1) dissociation between saccades and perceptual tasks, or 2) a decisional-bias in the perception task. In the perceptual task, the key indicating 'dot seen on the right' was pressed with the right hand, while the key indicating 'dot seen on the left' was pressed with the left hand. Results may be manipulated by the observer's decisional criterion, such as that the observer may have decided in favour of one alternative when unsure. In my experiments, for example, a larger shift could have been elicited when observers chose to press 'dot seen on the left' when the Gabor was drifting rightwards, chose to press 'dot seen on the right' when the Gabor was drifting leftwards. To find out whether a decisional bias might affect perceptual shifts, one could design an experiment such that it was difficult for the observer to influence the effect of drifting direction with a decisional criterion. Morgan, Melmoth, & Solomon (2013), for example, suggested using a 2-Alternative Forced Choice (2AFC) method instead of the Method of Single Stimuli. So far, a 2AFC method has not been used to investigate illusory position shifts in Gabors. Kerzel, & Gegenfurtner (2005) and Kosovicheva, Wolfe & Whitney (2014) referred to a 2AFC method within their experiments, although they actually made use of MSS. In both studies observers had to choose between two different responses (right versus left), which could be the reason why they referred to as a 2AFC method. But the distinction between MSS and 2AFC is defined by the external noise source; i.e. 2AFC has two external noise sources, MSS has one external source of noise (Morgan, Watamaniuk, & McKee, 2000).

4.6 Conclusion

Both systems, the perceptual and the saccadic system, are influenced by the internal motion of a Gabor. Saccadic landing positions were shifted in the direction of motion, the target dot was perceived displaced opposite the direction of motion.

5. SACCADIC ADAPTATION IN MIPS

5.1 Introduction

McLaughlin (1967) showed that saccadic eye movements are adaptable; i.e. if a saccade towards a stationary target fails multiple times within a ‘double step paradigm’, the parameters to bring the eye toward the target will be adapted (see chapter 1.1).

Semmlow, Gauthier & Vercher (1989) studied mechanisms of saccadic adaptation within a double-step paradigm that either increased or decreased saccade amplitudes, when stimuli were presented randomly interleaved on the right or the left side of the visual field. Although the localisation (right or left hemifield) of stimuli in each trial was not predictable, the responses to reduction-training stimuli induced a decrease in saccade amplitude, whereas the response to augmentation-training stimuli induced an increase in saccade amplitude.

In previous experiments described in chapter 3 and chapter 4, each dot superimposed on the Gabor was determined by an APE Procedure depending on observers’ previous perceptual responses, and observers had a perception bias to the internal motion direction of the Gabor. It might be that the drift direction (right or left) of the Gabor was used as a cue to engage saccadic adaptation mechanisms in different directions, and the shift in saccadic landing position could be due to an error signal arising from the position of the target dot relative to the eye position after saccade landing.

Therefore, the present experiment measured saccadic eye movements without showing the target dot superimposed on the Gabor answering the question:

Were saccades affected not by the internal motion of the Gabor, but by the dot giving some error-signal to the saccadic system?

5.1 Methods

5.1.1 Stimuli and Procedure

All stimuli were identical to those used in the experiment described in chapter 3. Figure 5.1 shows the experimental procedure. Each trial consisted only a saccadic-effect measurement, and started by fixating a white central fixation cross. After 3000 ms a drifting Gabor appeared above the fixation cross on the right side of the visual field. The long duration was

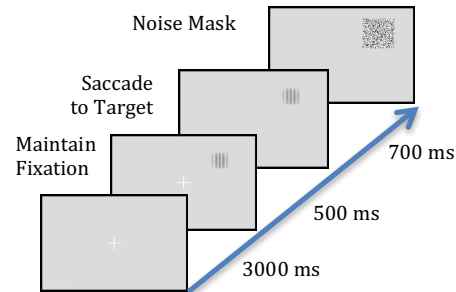


Figure 5.1: Procedure of experiment described in chapter 5. For more details see main text.

chosen to make sure that observer AXS, who failed to do saccades in time in chapter 3, would be able to keep up and complete the saccades for each trial. The Gabors were placed on the right side of the visual field with the presentation order randomised at eccentricities of 2.9°, 3.7°, 5.1° or 5.9°. The disappearing of the fixation cross after 3000 ms induced the observers to disengage the fixation cross and make a saccade to the centre of the drifting Gabor. A noise-mask was shown 4200 ms after trial onset, covering the drifting Gabor. The next trials started automatically after showing the mask for 700 msec.

5.1.2 Observer and Setup

Three observers (JMF, LJR and SXE) conducted the experiment with 160 trials in Setup 2; one observer (AXS) conducted 240 trials in Setup 1.

5.2 Data Analysis and Results

Shifts in saccadic landing positions and perceptual shift were filtered and analysed as described in chapter 3: Trials on which observers made a saccade too early (earlier than 100 ms after fixation offset) were excluded from the analysis. In addition, I excluded trials on which the saccade landing locations and saccade starting locations deviated by more than 2° horizontally or vertically from the centre of the saccade

target and fixation cross, respectively. Also saccades were excluded if they had velocity peaks that were not in the range of two standard deviations. If the path length between each measured sample point was not in a range of two standard deviations, they were excluded.

Each observer made at least 54 valid saccades for each motion direction. Due to the slower timing, observer AXS was able to saccade to the perceived centre as well and made 100 valid saccades to leftward drifting Gabors and 105 saccades to rightward drifting Gabors.

5.2.1 Saccadic landing positions

Confirming results described in chapter 3, I found that all observers had saccadic landing positions shifted in the direction of motion (see figure 5.2). The Wilcoxon-Rank-Sum-Test indicated that the distribution of horizontal errors in saccades of AXS, SXE and LJR were significantly different between right- and leftward drifts (all p-values < 0.01). For observer JMF, the test did not indicate a difference in distributions of horizontal saccadic errors elicited by rightward drifts from horizontal saccadic errors elicited by leftward drifts. BF-Tests showed that the differences in distributions of saccades were not due to different variances for any observer.

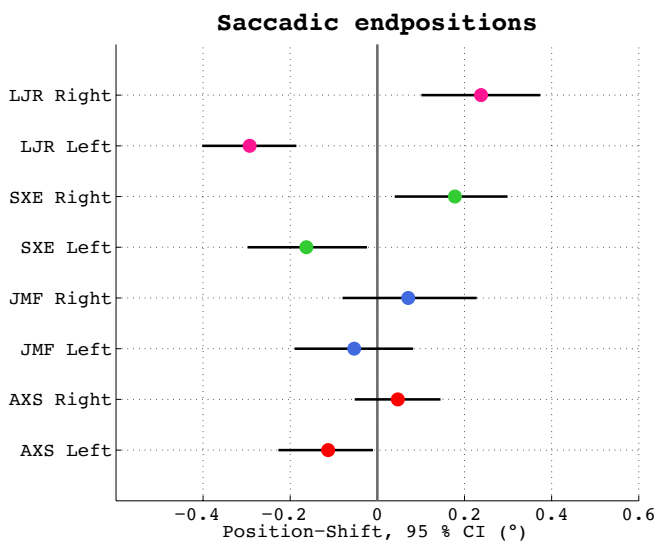


Figure 5.2: Saccadic effect. Results of observer LJR (blue), SXE (magenta), JMF (green) and AXS (red) are shown. Y-Axis indicates the observers and the direction of Gabors' internal waveform. X-Axis shows the perception-shift (degree), the vertical black line on position $x=0$ shows the centre of the Gabor.

5.4 Summary

Confirming previous experiments, I found saccadic shifts in the direction of motion across all observers. Statistical tests confirmed that the horizontal errors in saccades elicited by rightward drifts were significantly different from horizontal errors in saccades elicited by leftward drifts for three out of four observers.

5.5 Discussion

In the current chapter I showed that the saccadic system does not apply an adaption mechanism based on the drift direction of the Gabor and the target dot location.

It might also be that the visual system does not use the dot's' location as an error signal, but the motion-induced position shift of the perceptual system triggers a saccadic adaptation mechanism, and therefore, saccadic landing positions are shifted in the direction of motion. Future experiments could test this hypothesis by presenting a single Gabor moving in only one direction throughout all trials. If my hypothesis is correct, analysis of saccades over a time (trials) would confirm the pattern of a saccadic adaptation process; e.g. for reduction-training stimuli and augmentation-training stimuli both modifications were reported to be proportional to error-step size; i.e. modifications caused by reduction stimuli approached 70% of the error step, and modifications in saccadic amplitudes by augmentation stimuli approached 25 % of the error step (Semmlow, Gauthier & Vercher, 1989). Hence, saccadic amplitudes towards Gabors would approach 70% (in leftward drifts) and 25% (in rightward drifts) of the size of the error signal.

5.6 Conclusion

Confirming previous experiments, I found saccadic shifts in the direction of motion, indicating that saccadic shift is not due to an error signal caused by the dot superimposed on the Gabor.

6. MIPS IN REFLEXIVE SACCADDES: COMPARISON OF WITHIN-OBSERVER STATISTICS AND GROUP-LEVEL STATISTICS

6.1 Introduction

As described in previous chapters, a Gabor with an internal waveform moving to the right or the left induces a shift in landing positions of saccadic eye movements. Rightward drifting Gabors induce saccades with landing positions shifted to the right relative to landing positions of saccades towards leftward drifting Gabors.

A study by Kosovicheva, Wolfe & Whitney (2014) found that the magnitude of errors in reflexive saccades (onset of saccade is triggered simultaneously with target onset) was negatively correlated with saccadic latencies. More precisely, saccades with latencies of 100-170 ms and 171-240 ms resulted in an averaged position shift of ~ 0.55 dva and ~ 0.18 dva, respectively. Landing positions of saccades that started after 241-380 ms were not shifted in the direction of motion at all. Only landing positions of short latency saccades (100 – 170 ms) had a significant error in the direction of drift.

Kosovicheva, Wolfe & Whitney (2014) analysed the aggregated data of six observers. However, by aggregating datasets, they could not exclude the possibility that the resulting correlation between saccadic latencies and saccadic shift was due to a coincidence, with slow observers being less accurate than comparatively fast observers, or an indirect relationship between saccadic errors and saccadic latencies. In other words, the correlation between position shifts and latencies might be due to an artefact of group-level statistics.

The experiments described in chapters 3, 4 and 5 differed from the experiment of Kosovicheva, Wolfe & Whitney (2014). Two main differences were: 1) I investigated volitional saccades; i.e. the target (Gabor) was presented before fixation offset. In contrast, Kosovicheva, Wolfe & Whitney (2014) investigated reflexive saccades; i.e. the target (Gabor) appeared simultaneously with fixation offset. 2) I placed the Gabor on the right side of the visual field in all trials. Kosovicheva, Wolfe, & Whitney

(2014) presented the Gabor on the right or the left side of the visual field randomly interleaved.

Reanalysing the data of previous chapters would not be straightforward for at least two reasons: 1) reflexive saccades and volitional saccades involve different cortical streams and (described in chapter 1.1) and 2) the analysis of saccadic errors and saccadic latencies might indicate a negative correlation, but I cannot exclude the possibility that the negative correlation was due to a saccadic undershoot, whereas presenting the Gabor on the right and left side of the visual field cancels out saccadic undershoots.

Therefore, the following experiment attempts to replicate the study of Kosovicheva, Wolfe & Whitney (2014), and to compare resulting data with group-level statistics and within-observer statistics.

6.2 Methods

6.2.1 Stimuli

Like the stimulus used by Kosovicheva, Wolfe & Whitney (2014), the Gabors had a drift rate of 4 Hz, a spatial frequency of 0.75 cycles/deg, and a Michelson Contrast of 85%.

The standard deviation of the contrast envelope was 0.62° . At the beginning of every trial the Monitor displayed a white central fixation cross which was 2° high and 2° wide.

6.2.2 Procedure

Each experiment was started with a 9-point calibration (Eyelink) where fixations were accepted manually. Figure 6.1 shows the experimental procedure. Each trial started by fixating a white central fixation cross for 1250 ± 250 ms. A Gabor appeared simultaneously with fixation offset. Gabors were centred between 5 and 7 deg of visual angle (azimuth between 53 deg to 60 deg) to the right (shown in figure 6.1) or the left (not shown in figure 6.1) of the fixation. Drift directions

(rightwards/leftwards) of sinusoidal waveforms were randomly interleaved. Observers did not know in advance on any trial whether the saccade target would have a drift direction to the right or the left, or whether it would be in the left or the right visual field. The disappearance of the fixation cross was the observer's cue to make a saccade to the centre of the stimulus. After 300 ms a grey uniform screen was presented and observers started the next trial by a key-press.

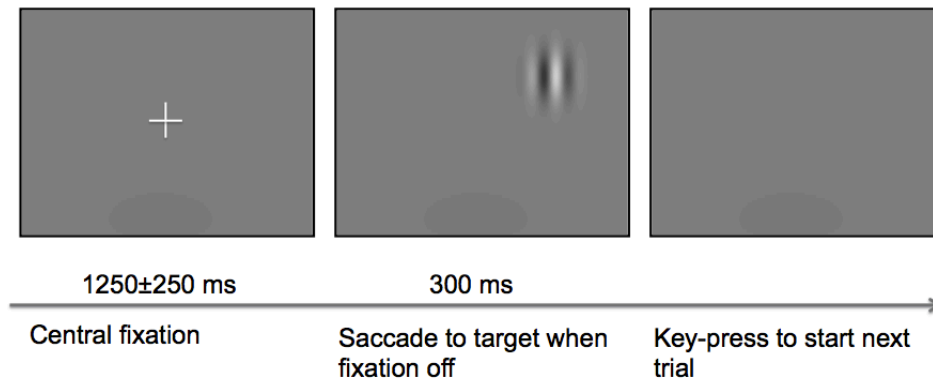


Figure 6.1: Experimental procedure to measure saccadic landing position to a single Gabor (chapter 6). For more details see main text.

6.2.3 Setup

Experiments were conducted in Setup 2, displayed on a uniform grey background (luminance 38 cd/m²), with viewing distance of 70 cm. At this distance, 43 pixels subtended approximately 1° of visual angle.

6.2.4 Observers

Altogether six trained observers with an age range from 28 to 35 participated. JMF was female and non-naïve. DPW, KXE, SXE, NXN were female and naïve. TXP was male and naïve. All observers had normal or corrected-to-normal vision.

6.3 Data Analysis and Results

Trials on which observers made a saccade too early (earlier than 100 ms after stimulus onset) were excluded from the analysis. Valid saccades were normalised individually for each observer to correct for saccadic undershoot. Next saccades were excluded from analysis if the velocity peaks were not in the range of two standard deviations, or the path length between each measured sample point was too short or long (smaller or larger than 2 standard deviation). Also, I excluded trials on which the saccade landing locations and starting location deviated by more than 2 deg horizontally or vertically from the centre of the saccade target and fixation cross, respectively.

The number of valid saccades ranged between 134 and 183 for rightward drifts, and between 138 and 185 for leftward drifts. QQ-Plots indicate the data from each observer and motion direction do follow the normal distribution. Figure 6.2 shows the data of one observer (TXP), which were gathered when the Gabors moved to the right (left plot) and when the Gabor moved to the left (right plot).

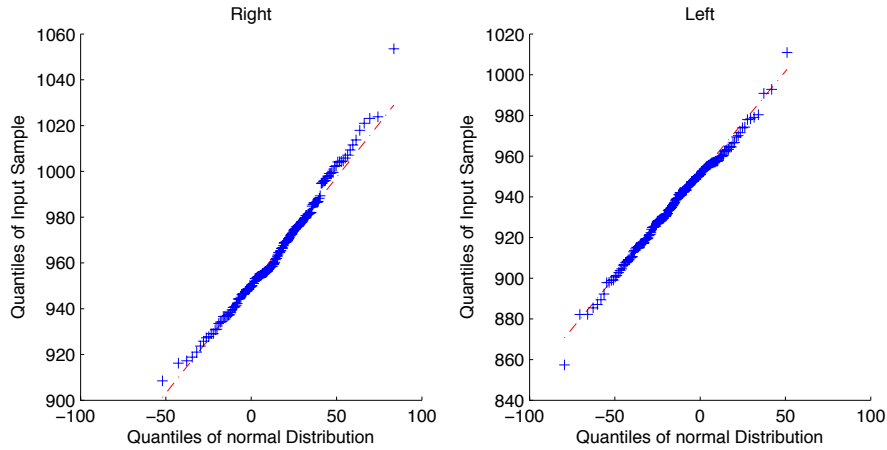


Figure 6.2: QQ-Plots. QQ-Plots for data gathered with rightward drifting Gabors (left panel) and for data gathered with leftward drifting Gabors (right panel). X-Axes indicate the quantiles of the normal distribution; Y-Axes indicate the quantiles of the input samples.

Figure 6.3 shows mean saccadic landing position (dva) and their 95 % confidence intervals of normalised saccadic landing positions for all observers (indicated by different colours). T-tests were employed to test whether horizontal mean saccadic errors in rightwards drifting conditions were different from leftwards drifting conditions. Six out of six observers produced saccades with landing positions shifted in the direction of motion, with mean values being significantly different for right and leftward drifts (all p-values <0.001).

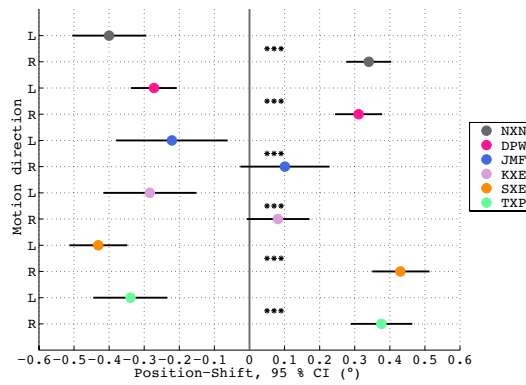


Figure 6.3: Perception effect. Mean values and their 95 % confidence intervals of normalised saccadic landing positions for all observers indicated by different colours. The x-axis shows the saccadic- shift (degree), the y-axis shows the observers and the direction of Gábors' internal waveform. The vertical black line on position $x=0$ indicates the centre of the Gábor. T-test was employed to test whether horizontal positions of saccade endpoints in rightwards drifting conditions were different from leftwards drifting conditions. Stars indicate p-values ($p < 0.001$: ***)

6.3.1 Group-Level Statistics

When single trial data were pooled across all observers, 1002 saccades to rightward drifting Gabors were found to be valid (11 % of saccades were excluded from analysis), and 1012 saccades to leftward drifting Gabors were found to be valid (10 % of saccades were excluded from analysis).

To test the relationship between saccade latency and the effect of motion on landing position, Spearman's correlation factor was applied. Saccadic errors to leftward and rightward drifting Gabors resulted in a correlation of $r = -0.15$ ($p\text{-value} < 0.001$) and $r = -0.18$ ($p\text{-value} < 0.001$), respectively.

Like Kosovicheva, Wolfe & Whitney (2014), I binned data for three latency bins: 100–170 ms (containing 335 saccades and 378 saccades to rightward and leftward drifting Gabors, respectively), 170–240 ms (containing 575 saccades to rightward, and 544 saccades to leftward drifting Gabors), and 240–380 ms (containing 92 saccades

and 90 saccades to rightward and leftward drifting Gabors, respectively), and calculated the saccade error by averaging the single-trial saccade errors within each bin. Figure 6.4 shows the saccade errors at each latency bin separately. Consistent with the Spearman's correlation analysis, shorter saccade latencies were associated with larger saccade errors. A Wilcoxon-Rank-Sum-Test confirmed that the distribution of horizontal errors elicited by leftward drifts were (for saccades with latencies of 100-170 ms, and latencies of 171-240 ms) significantly different from the distribution of errors elicited by rightward drifts (p-values <0.001). A Brown-Forsythe test showed that differences in distributions were not due to differences in variances (all p-values > 0.19). Distributions of saccadic errors in rightward drifting Gabors were not found to be significantly different from the distribution of saccadic errors in leftward drifting Gabors when saccades started later than 241 ms after fixation offset (Wilcoxon Rank Sum Test: p-value = 0.41).

Figure 6.4 indicates that variances in saccadic landing positions increase with increasing latencies. In particular, long latency saccades starting 241 ms after fixation offset show large variance relative to saccades starting within 100-240 ms after fixation offset. This could be due to an error-compensation mechanism that results in larger variance.

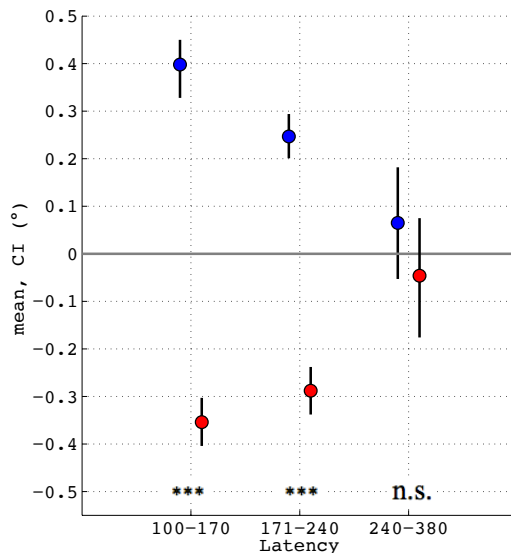


Figure 6.4: Saccadic effect group-level statistic. Mean shifts in saccade landing positions (stimulus moved rightwards: blue, stimulus moved leftwards: red) as a function of saccade latency. Single-trial data were pooled across observer, then sorted into three latency bins (ms). X-axis represents the latency bin edges. Error bars represent bootstrapped 95 % confidence intervals on the y-axis. Wilcoxon Rank Sum test was applied to test whether distributions of horizontal saccadic errors elicited by rightward drifts were different from distributions of horizontal saccadic errors elicited by leftward drifts (p < 0.001: ***; p > 0.05/6: ns).

As described above, Kosovicheva, Wolfe & Whitney (2014) found shifts of up to ~0.55 dva that continuously decreased with increasing latencies. So far, my results

replicate their study. However, it is important to establish whether the saccadic landing positions of each observer show the same statistical pattern as single trial saccadic landing positions pooled across all observers. Therefore, I analyse the same dataset with within-observer statistics in the next section.

6.3.2 Within-Observer Statistics

In rightward drifting Gabors the correlation between saccadic errors and saccadic latencies ranged between $r = -0.18$ and $r = -0.10$ for five out of six observers (all p -values > 0.05). One observer had a positive correlation of $r = 0.07$ ($p = 0.35$).

In leftward drifting Gabors one observer showed negative correlation between saccadic errors and saccadic latencies ($r = -0.22$, $p = 0.003$). Three out of six observers had a negative correlation ranging between $r = -0.11$ and $r = -0.08$ (all p -values > 0.16), and two observers showed a positive correlation of $r = 0.05$ ($p = 0.50$) and $r = 0.02$ ($p = 0.76$).

In summary, nine out of twelve datasets showed a negative correlation between saccadic errors and saccadic latencies. The comparatively small number of saccades may be the reason for non-significant correlation factors.

Next I binned the data of each observer in two latency bins. For four out of six observers (JMF, DPW, SXE, TXP) I binned data into saccades that started between 100-170 ms, and into saccades that started between 171-380 ms. Two observers made saccades comparatively late. The data of KXE were binned into saccades with latencies of 100-220 ms, and saccades with latencies of 221-380 ms. Saccades of observer NXN were separated into latency bins of 100-190 ms, and 191-380 ms. In both latency bins, the number of valid saccades ranged between 54 and 113 for rightward drifts, and between 48 and 127 saccades for leftward drifts.

QQ-Plots indicate that data of each observer and motion direction follow the normal distribution. I calculated saccade error by averaging the single-trial saccade errors within each bin for each observer. Figure 6.5 shows that for all observers shorter saccade latencies were associated with larger saccade errors in both conditions, right-

and leftward drifts. T-tests confirmed that, for early saccades, the mean of horizontal errors elicited by leftward drifts were (for all observer and short latency saccades) significantly different from the mean of horizontal errors elicited by rightward drifts (all p-values < 0.002). In long latency saccades, analogous tests indicate a difference between the means of horizontal errors in saccades for observer DPW, SXE, TXP, and NXN (all p-values < 0.001). Errors to right- and leftward drifting Gabors of observers KXE and JMF were not found to be significantly different (p-values > 0.06).

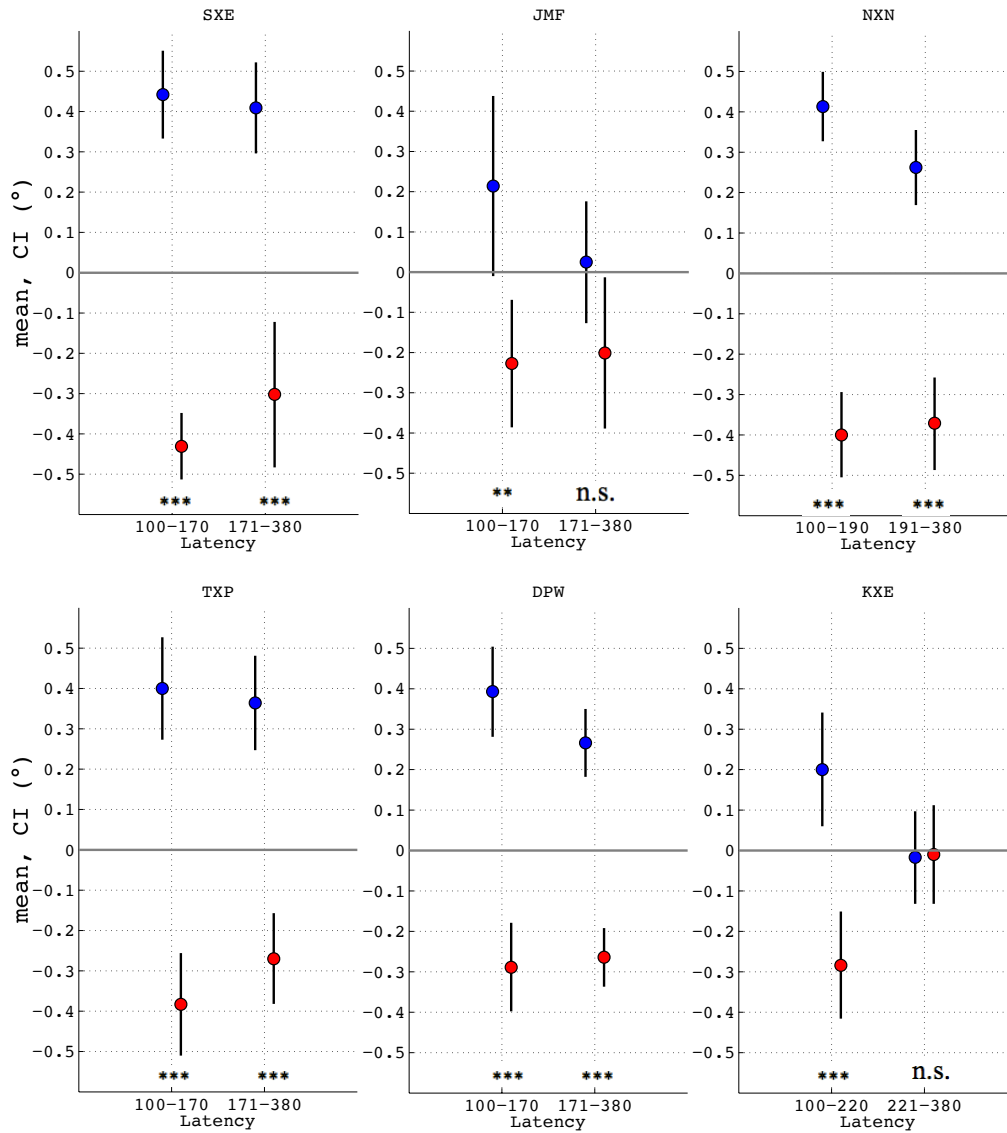


Figure 6.5: Saccadic effect within-observer statistic. Mean shifts in saccade landing positions (stimulus moved rightwards: blue, stimulus moved leftwards: red) as a function of saccade latency. Single-trial data for each observer sorted into two latency bins (ms). X-axis represents the latency bin edges. Y-Axis indicates mean error and its 95 % confidence intervals. T-test was applied to test whether distributions of saccades elicited by rightward drifts were different from distributions elicited by leftward drifts (p < 0.001 : ***, p > 0.06 : n.s.). For more details read main text.

6.4 Summary

As shown in figure 6.3, all observers showed a significant shift in saccadic landing positions in the direction of carrier motion (rightward drifts elicited shifts up to 0.44 dva, leftward drifts elicited shifts up to 0.43 dva).

Spearman correlation between saccadic errors and saccadic latencies was found to be negative and significant when combined over all observers. In within-observer statistics the Spearman correlation factors were found to be negative in nine out of twelve datasets, but not significant in one out of these nine negatively correlated datasets.

When saccades that started 100-170 ms after fixation offset were binned in latency bins, group-level statistics resulted in saccadic shifts of 0.40 dva in rightward drifting Gabors, and saccadic shifts of -0.35 dva in leftward drifting Gabors (figure 6.4). Within-observer statistics resulted in averaged saccadic errors of up to 0.44 dva for rightward drifts, and averaged errors up to -0.43 dva for leftward drifts (figure 6.5). In both statistical approaches, group-level statistics and in within-observer statistics showed that the magnitudes of saccadic errors decrease with increasing saccadic latencies.

In summary, I confirm that horizontal errors in saccadic landing positions are negatively correlated with saccade latencies. However, I cannot exclude the possibility that pooling single data trials across all observers results in a different statistical pattern from analysing data for each observer separately. Long latency saccades (241-380 ms) in group-level statistics (see figure 6.4) indicate a very small and non-significant horizontal error in landing positions, but this result might be biased by the data of observer KXE, who made a lot of long latency saccades and had no significant horizontal error in those saccades.

6.5 Discussion

6.5.1 Methodical comparison with previous studies

The experimental procedure I used was very similar to the procedure of Kosovicheva, Wolfe & Whitney (2014). However, I elaborate three differences as follows:

1) Kosovicheva, Wolfe & Whitney (2014) placed the central position of the Gabor around a point 10° to either the left or right of fixation, with the range of possible jittered positions spanned 3° horizontally and 3° vertically. I, in contrast, placed the stimuli around a point 6° to either the left or right of fixation, with the range of possible jittered positions spanned 1° horizontally. It is well known that perceptual position shifts increase with increasing eccentricity (De Valois & De Valois, 1991). The difference in the stimulus localisation might have influenced the magnitude of saccadic errors. However, I found saccadic errors induced by Gabors with low eccentricities of 2.95° to 5.92° (see chapter 3), and therefore, had no reason to assume I would be unable to measure an effect on saccadic landing positions when placing the Gabors at $6^\circ \pm 1^\circ$.

2) Kosovicheva, Wolfe & Whitney (2014) presented the stimuli for 140 ms (experiment 1), or for 20 ms, 40 ms, 60 ms, 80 ms, 100 ms randomly (experiment 2). In both experiments, saccades were only considered to be valid when the onset was 100 ms after fixation offset. Thus, in experiment 1 some saccades started before stimulus offset, while other saccades started after stimulus offset, and therefore, were memory-guided.

At the beginning of my study, observers reported feeling discomfort and discouraged when they were asked to make a saccade to a target which disappeared before saccades landed. That is why I presented the stimulus for 300 ms and at comparatively small eccentricity, allowing observers to actually land with their saccades on the stimulus in most of the trials.

3) I and Kosovicheva had different samples sizes. In my study every observer conducted 300 – 400 trials, which resulted – as stated above - in at least 54 valid saccades for each condition. In experiment 1, Kosovicheva, Wolfe & Whitney (2014) asked observers to make 1040 saccades in total for all stimulus durations of 20 ms, 40

ms, 60 ms, 80 ms, 100 ms and motion direction to the right and left. For every observer 104 saccades for each motion direction and stimulus durations were gathered. Binning 104 single trials into three latency bins for each observer separately, may not have contained a big enough sample from which to draw significant conclusions. That might have been the reason for group-level statistics in the study of Kosovicheva, Wolfe & Whitney (2014).

6.5.2 Comparison of effect sizes

Kosovicheva, Wolfe & Whitney (2014) found that saccadic errors were negatively correlated with saccadic latencies in both experiments (all $r < -0.14$; for the 20-ms condition, $r = 0.003$). Spearman rho correlation factors were of the same magnitude in my data (rightward drifts $r = -0.18$, $p < 0.001$; leftward drifts $r = -0.12$, $p < 0.001$).

In experiment 2 of Kosovicheva, Wolfe & Whitney (2014), saccades with latencies of 100-170 ms resulted in an averaged position shift of ~ 0.55 dva. No significant effect was found at any duration in either the 170- to 240-ms latency bin or the 240- to 380-ms bin. I found that saccades to rightward drifting Gabors, with latencies of 100-170 ms and 171-240 ms resulted in an averaged position shift of ~ 0.40 dva and ~ -0.35 dva, respectively. Saccades to leftward drifting Gabors, with latencies of 100-170 ms and 171-240 ms resulted in an averaged position shift of ~ 0.25 dva and ~ -0.29 dva, respectively. Statistical tests indicated that mean errors in saccades elicited by rightward drifts were significantly different from errors in saccades elicited by leftward drifts for latency bin of 100-170 ms, and also for latency bin of 171-240 ms. As stated above, Kosovicheva, Wolfe & Whitney (2014) did not find a shift for saccades starting between 170-241 ms and 240-380-ms after fixation offset. I cannot confirm that saccades of both latency bins were not affected by motion, even though I cannot find an effect in group-level statistics for saccades starting 240-380 ms after fixation offset. As stated above, this result might be biased by the data of observer KXE, who made many high-latency saccades and had no significant horizontal error in those saccades.

6.6 Conclusion

Group level statistics might be biased by slow observers, who may be less accurate than fast observers. In other words, the negative correlation in group-level statistics might be due to a coincidence, with slow observers being less accurate than comparatively fast observers. Therefore, I can conclude group-level statistics does not necessarily represent the true pattern in underlying data.

Within-observer statistics showed that only two (KXE and JMF) out of six observers did not show a significant shift in direction of motion for long latency saccades. For JMF, the large variance in data (see figure 6.5) might be the reason why statistical tests did not indicate a significant difference between long latency saccades towards right and leftward drifting Gabors.

However, although not statistically detectable, there is a small decrease in mean saccadic landing positions with increasing latencies across all observers. Different approaches to explain this pattern will be described extensively in the next two chapters.

7. MIPS IN REFLEXIVE SACCADDES TOWARDS PSEUDO-PLAIDS

7.1 Introduction

Kosovicheva, Wolfe & Whitney (2014) found the landing positions of reflexive saccadic eye movements towards a single Gabor to be biased in the direction of motion. The magnitude of this bias was negatively correlated with saccadic latencies. The visual system may confuse motion inside an object with motion of the object itself, especially when viewing time is short. I hypothesised that short-latency saccades were programmed to intercept a feature of the drifting carrier. To test this hypothesis I compared saccadic errors induced by a drifting Gabor with saccadic errors induced by a pseudo-plaid as shown in figure 7.1. The pseudo-plaid comprised randomly oriented single Gabors arranged in an annular array. Each Gabor had a static envelope, the carrier was moving in the direction normal to their carrier orientation. The drift velocity of each carrier was consistent with its rigid horizontal motion, so that the Gabors cohere into a single surface that appeared to move in a global motion direction (Amano et al., 2009); i. e. to the right or the left. This pseudo-plaid did not have a feature which could be used by early saccades to guide saccadic landing positions further in the direction of motion than comparatively late saccades.

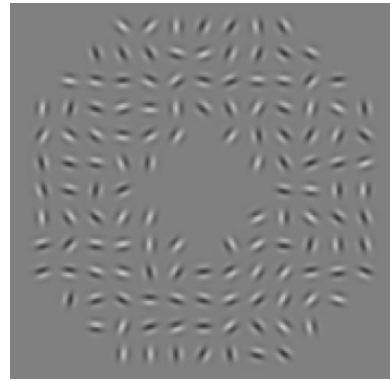


Figure 7.1: Example of the stimulus I used in my experiment (described in chapter 7). Pseudo-plaids were composed randomly oriented Gabors in an annular array. Each Gabor in the pseudo-plaid had a drift velocity consistent with rigid horizontal motion.

If my hypothesis was correct, errors in landing positions of saccadic eye movements would not be negatively correlated with saccadic latencies.

7.2 Methods

7.2.1 Setup

Experiments were conducted in Setup 2, displayed on a uniform grey background (luminance 38 cd/m²), with viewing distance of 70 cm. At this distance, 43 pixels subtended approximately 1° of visual angle.

7.2.2 Observers

Altogether five trained observers with an age range from 30 to 35 participated. JMF was female and non-naïve. DPW, KXE, SXE were female and naïve. TXP was male and naïve. All observers had normal or corrected-to-normal vision.

7.2.3 Stimuli

Pseudo-plaids were composed 128 randomly oriented Gabors in an annular array. Each Gabor in the pseudo-plaid had a drift velocity consistent with rigid horizontal motion. Single Gabors had a Michelson Contrast of 85 %, the spatial frequencies of single sinewaves were 2.25 cpd, a standard deviation of the Gaussian function was 0.1 dva, and each patch was restricted to a 0.65 dva square. At the beginning of every trial the Monitor displayed a white central fixation cross which was 2° high and 2° wide.

7.2.4 Procedure

Each experiment was started with a 9-point calibration (Eyelink) where fixations were accepted manually. Figure 7.2 shows the experimental procedure. Each trial started by fixating a white central fixation cross for 1250±250 ms. A pseudo-plaid appeared simultaneously with fixation offset. Pseudo-plaids were centred between 5 and 7 deg of visual angle (azimuth ranged between 53 deg to 60 deg) to the right (shown in figure 7.2) or the left (not shown in figure 7.2) of the fixation cross. Drift directions (rightwards/leftwards) of sinusoidal waveforms were randomly interleaved. Observers did not know in advance on any trial whether the saccade target would have a drift direction to the right or the left, or whether it would be in the left or the right

visual field. The disappearance of the fixation cross was the observer's cue to make a saccade to the centre of the stimulus. After 300 ms a grey uniform screen was presented, and observers started the next trial by a key-press.

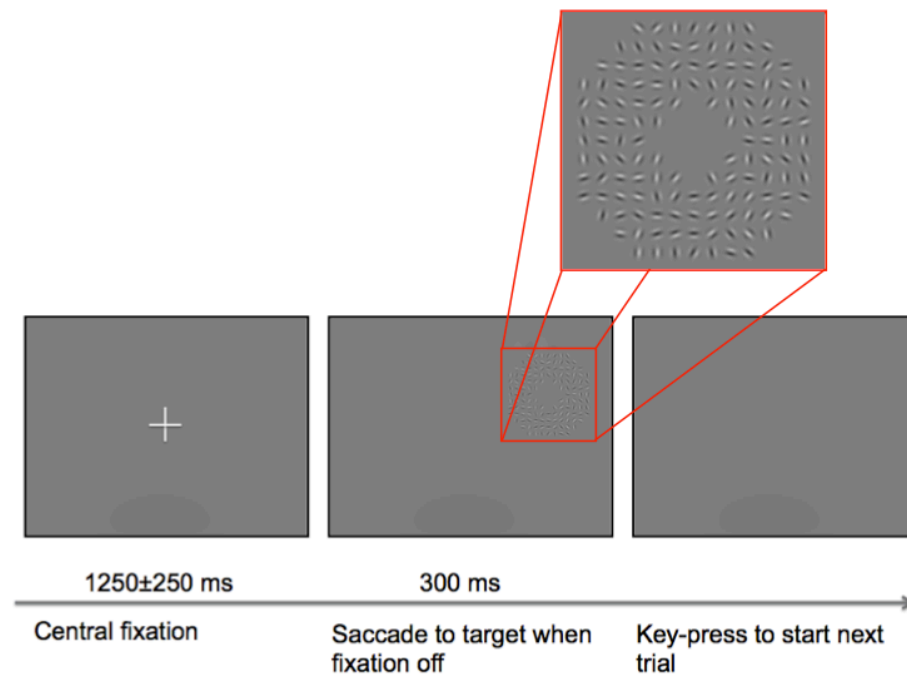


Figure 7.2: Experimental procedure to measure saccadic landing positions to a pseudo-plaid (chapter 7). For more details read main text.

7.3 Data Analysis and Results

7.3.1 Within-Observer Statistics

As described in previous chapters, trials on which observers made a saccade too early (earlier than 100 ms after fixation offset) were excluded from the analysis. In addition, I excluded trials on which the saccade landing locations and saccade starting locations deviated by more than 2° horizontally or vertically from the centre of the saccade target and fixation cross, respectively. Also saccades were excluded if they had velocity peaks that were not in the range of two standard deviations, or the path length between each measured sample point was not in a range of two standard deviations.

Numbers of valid saccades over all observers ranged between 81 and 90 for rightward drifts, and between 81 and 92 saccades for leftward drifts. QQ-Plots indicate that data of each observer and motion direction follow the normal distribution.

Figure 7.3 shows mean errors in saccadic landing positions (dva) and their 95 % confidence intervals for all observers (indicated by different colours). T-tests were employed to test whether horizontal mean saccadic errors in rightwards drifting conditions were different from leftwards drifting conditions. Five out of five observers made saccades with landing positions shifted in the direction of motion. Three observers made saccades with mean saccadic errors being significantly different for right and leftward drifts (DPW and SXE p-value < 0.001, TXP p=0.0037)

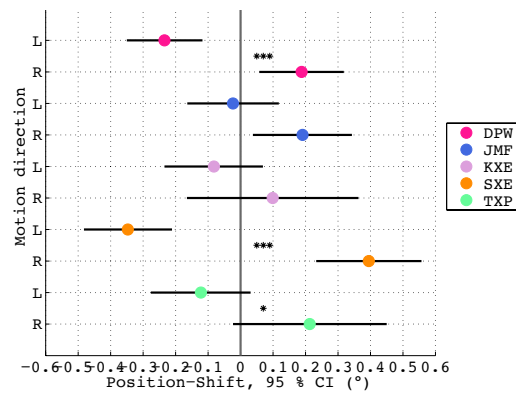


Figure 7.3: Perception effect. Mean values and 95 % confidence intervals of normalised saccadic landing positions for all observers indicated by different colours. The x-axis shows the saccadic- shift (degree), y-axis shows the observers and the direction of global motion. The vertical black line on position $x=0$ indicates the centre of the pseudo-plaid. T-tests were applied to test whether horizontal mean saccadic errors elicited by rightward drifts were significantly different from horizontal mean errors elicited by leftward drifts ($p<0.001$: ***; $p<0.005$: *).

To study whether the magnitude of saccadic errors was negatively correlated with saccadic latencies, I binned the data of each observer in two latency bins (see figure 6.4). Latency intervals were based on individual latencies of observers, so that each

latency bin contained approximately 50% of all valid saccades. In both latency bins, the number of valid saccades ranged between 31 and 55 for rightward drifts, and between 31 and 57 saccades for leftward drifts. QQ-Plots indicate that data of each observer and motion direction follow the normal distribution.

T-tests were applied to test whether mean values of errors elicited by rightward drifting pseudo-plaids were different from mean values of errors elicited by leftward drifts. Alpha levels were corrected by Bonferroni-Correction. Figure 7.3 shows mean saccadic errors for each motion direction (blue dots: rightward drifts; red dots: leftward drifts) and their 95 % Confidence intervals against saccadic latencies bins for each observer separately. Stars (***) indicate highly significant differences in mean values ($p < 0.001$), whereas 'n.s.' indicates that there was no significant difference ($p > 0.01$) between mean values in saccadic errors to right- and leftward drifting pseudo-plaids.

In short latency saccades, all five observers showed a shift in direction of global motion. The mean errors elicited by rightward drifts were significantly different from mean errors elicited by leftward drifts for three out of five observers (p -values < 0.001). T-test applied to data of observer JMF resulted in a p -value=0.019, and for observer KXE in $p=0.43$.

In long latency saccades, I found shifts in direction of motion for only three out of five observers, and only saccades of two observers (SXE and DPW) showed a significant difference in mean values between right and leftward drifts ($p < 0.001$). SXE showed a clear decrease of saccadic errors with increasing latencies in both conditions, right- and leftward drifts. For observer DPW, the error decreased with increasing latencies in leftward drifting Gabors, but increased with increasing latencies in rightward drifting Gabors.

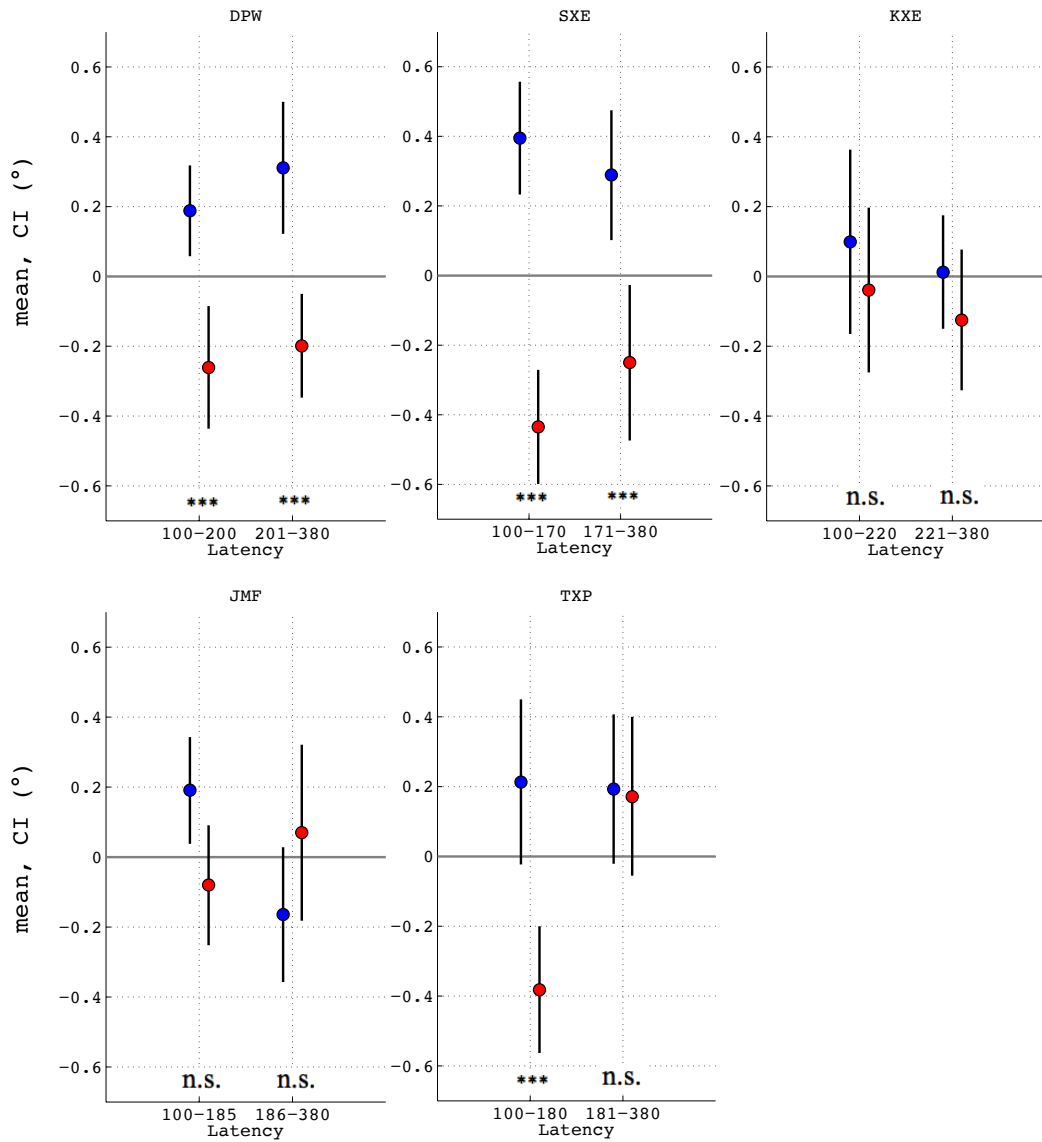


Figure 7.4: Saccadic effect within-observer statistic. Mean shifts in saccade landing positions (stimulus moved rightwards: blue, stimulus moved leftwards: red) as a function of saccade latency. Single-trial data were sorted into three latency bins (ms) for each observer. X-axis represents the latency bin edges. Y-axis indicates mean errors and their 95% confidence intervals. T-test was applied to test whether mean saccadic errors elicited by rightward drifts were different from mean saccadic errors elicited by leftward drifts ($p < 0.001$: ***; $p > 0.01$: n.s.). For more details read main text.

7.3.2 Group-Level Statistics

In order to compare saccadic landing positions to pseudo-plaids with saccadic landing positions to Gabors, single trial data were pooled across all observers and binned into the same latency bins as in chapter 6 (see x-axis of figure 7.4).

433 saccades to rightward drifting pseudo-plaids were found to be valid (13 % of saccades were excluded from analysis), and 433 saccades to leftward drifting pseudo-plaids were found to be valid (13 % of saccades were excluded from analysis).

Spearman's correlation factors were applied to determine whether saccadic errors were negatively correlated with saccadic latencies. Saccadic errors to leftward and rightward drifting Gabors resulted in a correlation of $r = -0.14$ (p-value = 0.003) and $r = -0.10$ (p-value < 0.038), respectively.

As in chapter 6, I divided data into three latency bins: 100–170 ms (containing 64 saccades and 87 saccades to rightward and leftward drifting pseudo-plaids, respectively), 170–240 ms (containing 335 saccades and 326 saccades to rightward and leftward drifting pseudo-plaids, respectively), and 240–380 ms (containing 34 saccades and 20 saccades to rightward and leftward drifting pseudo-plaids, respectively), and calculated the saccade error by averaging the single-trial saccade errors within each bin. Figure 7.5 shows the saccade errors at each latency bin. A Wilcoxon-Rank-Sum-Test confirmed that the distribution of horizontal

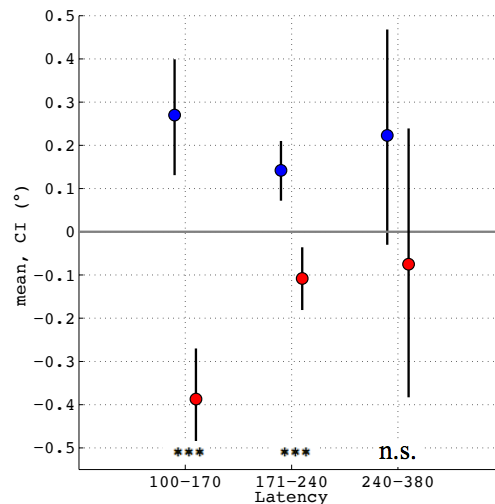


Figure 7.5: Saccadic effect group-level statistic. Mean shifts in saccade landing positions (stimulus moved rightwards: blue, stimulus moved leftwards: red) as a function of saccade latency. Single-trial data were pooled across observers, then sorted into three latency bins (ms). X-axis represents the latency bin edges. Error bars represent bootstrapped 95 % confidence intervals on the y-axis. Wilcoxon Rank Sum tests were applied to test whether distributions of saccades elicited by rightward drifts were different from distributions elicited by leftward drifts ($p < 0.001$: ***, $p > 0.1$: n.s.). For more details read main text.

errors elicited by leftward drifts were (for saccades with latencies of 100-170 ms, and latencies of 171-240 ms) significantly different from the distribution of errors elicited

by rightward drifts (both p-values <0.001). A Brown-Forsythe test showed that differences in distributions were not due to differences in their variances (both p-values > 0.32). In latencies of 241-380 ms, landing positions of saccades to rightward drifting pseudo plaids were not found to be significantly different from saccades to leftward drifting pseudo plaids (Wilcoxon Rank Sum Test: p-value = 0.11).

7.4 Summary

I measured errors in saccadic landing positions to a pseudo-plaid. Especially for short latency saccades I found large shifts in the direction of global motion across all observers, with three out of five observers having a significant difference in mean values of saccadic landing positions elicited by right- and leftward drifting pseudo-plaids. For long latency saccades, only two out of five observers showed a shift in direction of motion (both significant).

Pooling single trial data across all observers resulted in negative correlations between saccadic errors in saccadic landing positions of -0.14, and -0.10 for right- and leftward drifts, respectively. Binning the data into a latency interval of 100-170 ms, resulted in saccadic shifts of 0.27 dva in rightward drifting Gabors, and saccadic shifts of -0.39 dva in leftward drifting pseudo-plaids. A second interval with saccades that started 171-240 ms after fixation offset, resulted in averaged saccadic errors of 0.14 dva for rightward drifts, and averaged errors of -0.11 dva for leftward drifts. Mean shifts were significantly different between right and leftward drifts in both latency intervals, 100-171 ms, and 171-240 ms. Long latency saccades of 241-380 ms were not found to have had significantly different mean values between right- and leftward drifting pseudo-plaids.

In summary, I found the magnitude of this bias was negatively correlated with saccadic latencies.

7.5 Discussion

7.5.1 Comparison of saccadic shift to Gabors and pseudo-plaids

Comparing mean saccadic errors induced by leftward drifting and rightward drifting stimuli (figure 6.3 and figure 7.3) indicated that errors were smaller in pseudo-plaids than in Gabors. The smaller error does not necessarily indicate that the saccadic system tried to intercept a feature of the moving carrier, but might be due to other differences in stimulus attributes; e.g. the pseudo-plaid was arranged in an annular array with the centre having no Gabors; hence, observers had to target a localisation defined by surrounding objects instead of targeting the object's centre itself. In both experiments, saccadic shifts were negatively correlated with saccadic latencies.

7.5.2 Does the size of the saccadic shift depend on the motion processing stage?

As stated above, Mather & Pavan (2009) applied a two-stage motion processing model to investigate the loci of motion-induced position shifts. I feel I need to add my body of thoughts on this matter, even though it is not related to the hypothesis stated in the introduction.

As described in chapter 1.2 Literature Review, it may be that we process visual information through a two-stage motion processing mechanism (Adelson & Movshon, 1982): after light is converted into neural signals by the retina, signals are processed in subcortical areas, such as the pulvinar and lateral geniculate nucleus, and next sent to different cortical areas, such as the primary visual cortex V1. The first stage of visual processing - selective to speed, motion direction, and orientation - computes local motion signals, which are ambiguous because orientation selective receptive fields can only process motion signals orthogonal to their preferred direction of motion (Nakayama & Silverman, 1988, Hubel and Wiesel, 1962), and do not solve the aperture problem. Local motion signals feed into the second stage of visual motion processing, where mechanisms generate a global motion percept of complex objects (Adelson & Movshon, 1982). The neural loci for first- and second-stage motion processing are presumably based in striate area V1 and extrastriate area MT, respectively (Movshon et al., 1985; Rodman & Albright, 1989; Movshon & Newsome, 1996). Neurons in area V1 were found to respond well to stimuli like

Gabors (Hubel & Wiesel, 1962), whereas neurons in area MT and MST were found to respond well to plaids (e.g. Movshon & Newsome, 1996) and pseudo-plaids (Majaj et al., 2007), respectively. Based on this theory, it has been suggested that illusory position shifts arise in area MT or even MST (e.g. Mather & Pavan, 2009; Rider, McOwan & Johnston, 2009).

Errors of landing positions in reflexive saccades towards a Gabor were found to decrease with increasing saccadic latencies (Kosovicheva, Wolfe & Whitney, 2014) suggesting that saccades might be accurate if the visual system has enough time to process visual information within higher visual areas. One interpretation might be that early saccades were guided by local motion processing mechanisms, while late saccades could have been guided by higher order motion integration mechanisms. However, this relies on a strictly feed-forward model of processing from V1 to MT, which has been questioned.

It was traditionally believed that destructions of the visual cortex or the optic radiations would lead to areas of blindness ('scotomata') within the corresponding visual field. Pöppel, Held & Frost (1973) reported, however, that patients with lesions in area V1 were able to move their gaze towards stimuli presented in their destructed visual field, despite reporting a lack of conscious visual experience. This phenomenon (called 'blindsight' by Sanders et al., 1974) is therefore, a challenge for a strict feedforward two-stage motion processing mechanism as described above. Instead, visual information might bypass the first visual cortex, sending information directly into higher visual areas. Comparison of fMRI studies with behaviour data before and after inactivation of the lateral geniculate nucleus in monkeys with chronic V1 lesions, demonstrated that the lateral geniculate nucleus has a causal role in V1-independent processing of visual information (Schmid & Mrowka, 2010).

Thus, blindsight challenges a strictly hierarchical two-stage processing mechanism where V1 feeds visual information into extrastriate areas. As discussed in the literature review, the approach is also controversial because multiple cortical areas have been found to respond to plaids (Thompson et al., 2009).

In summary, a strictly two-stage feedforward hierarchical model is challenged by such studies. If such a model existed, the saccadic error in the direction of pseudo-plaid motion would not be as large as saccadic errors in the direction of Gabors' motion. As stated above, pooling saccades across all latencies (figure 6.3 and figure 7.3) showed

that errors in saccades to pseudo-plaids were slightly smaller than saccadic shifts to a Gabor. However, shifts decreased with increasing latencies when presenting plaids and also when presenting pseudo-plaids. Therefore, I cannot conclude that the negative correlation between saccade error and latency occurred because the visual motion integration system had not had time to influence saccade programming.

7.6 Conclusion

In summary, I found that 1) saccades towards a pseudo-plaid were more accurate than saccades towards a single Gabor, and 2) the magnitude of saccadic bias was negatively correlated with saccadic latencies in both Gabors (chapter 6) and pseudo-plaids, with late saccades (241-380 ms) not being significantly shifted in the direction of motion.

The saccadic shift was smaller in pseudo-plaids than in single Gabors. However, saccades in pseudo-plaids were still negatively correlated with saccade latencies. Thus, my results indicate that saccadic errors in the direction of pseudo-plaid motion cannot be explained by attempts to intercept drifting textures. I could not explain the negative correlation between saccadic errors and saccadic latencies by attempts to intercept a feature of the moving carrier inside the Gaussian blob. Thus, the question why reflexive saccades resist the perceptual motion-induced position shift remains unanswered.

7.7 Further Investigations

As stated in my literature review, Arnold, Thompson and Johnston (2005) measured illusory position shifts at the trailing edges and leading edges and the centre of luminance-defined Gabors. They found 1) that the perceptual effect increased over 150 ms and 2) the envelope appeared to shift, but the contours of the internal waveform did not appear to shift. Therefore, Alan Johnston (personal communication, AVA Meeting, December 19, 2016) suggested the envelope might drive low latency saccades, whereas for the long latency saccades, there was enough time to target a particular feature within the carrier and the saccade was more accurate.

8. CIRCULAR DATA ANALYSIS

8.1 Introduction

Rightward drifting Gabors elicited saccades with landing positions shifted to the right, and leftward drifting Gabors elicited saccades with landing positions shifted to the left. Kosovicheva, Wolfe & Whitney (2014) found that saccadic errors were negatively correlated with saccadic latencies, and that the motion of a Gabor affected high-latency saccades, whereas low-latency saccades were not affected by motion. I suggested that the result might be due to a statistical artefact. Therefore, I replicated their experiment and confirmed that the horizontal shift in saccadic landing positions was negatively correlated with saccadic latencies (see chapter 7).

Because the Gabors in previous studies (e.g. Kosovicheva, Wolfe & Whitney, 2014; Kerzel & Gegenfurtner, 2005) and in this thesis drifted to the right or the left, only horizontal errors in saccadic landing positions relative to the horizontal centre of the Gabor were determined. Depending on the distribution of saccadic landing positions, this method could indicate small saccadic shifts although eye movements were largely affected by motion.

Figure 8.1 shows an example of two sets of saccadic landing positions that followed different distributions. The large black crosses indicate the centre of the Gabors, small red and blue crosses represent saccadic landing positions when the Gabor drifted to the left and the right, respectively. The green lines represent the horizontal distance to the horizontal centre of the Gabor for rightward drifting Gabors. The ellipses indicate the two-dimensional distributions of all saccadic landing positions. The sum of horizontal errors in saccadic landing positions on the upper panel was larger than the sum of horizontal errors in saccadic landing position on the lower panel. However, saccadic landing positions indicated in both panels would be affected by motion.

I hypothesise that the negative correlation in saccadic landing positions and saccade latencies might not be caused by a smaller error in saccades for high-latency saccades than in low-latency saccades, but by a change in the two dimensional distribution of saccadic landing positions.

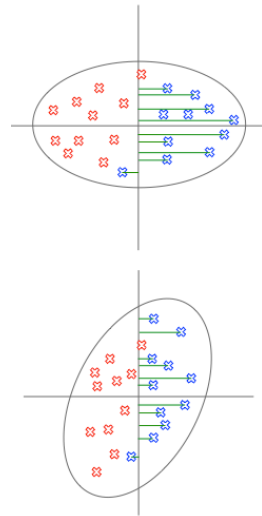


Figure 8.1: Example of two sets of saccadic landing positions that follow different distributions. Black crosses indicate the centre of the Gabors. Small red and blue crosses represent saccadic landing positions when the Gabor drifted to the left and the right, respectively. The green lines represent the horizontal distance to the horizontal centre of the Gabor for rightward drifting Gabors. The ellipses indicate the two dimensional distributions of all saccadic landing positions. For more details read main text.

This chapter introduces an alternative approach to assessing landing positions of saccadic eye movements. Applying this method attempts to answer the question: Is the negative correlation between horizontal saccadic shifts and saccadic latencies an artefact caused by considering only the horizontal errors relative to the horizontal centre?

8.2 Methods

In this chapter I re-analyse valid data gathered and filtered for chapter 6 (replication of Kosovicheva, Wolfe & Whitney, 2014). Figure 8.2 shows the experimental paradigm. For more details read the methods in chapter 6.

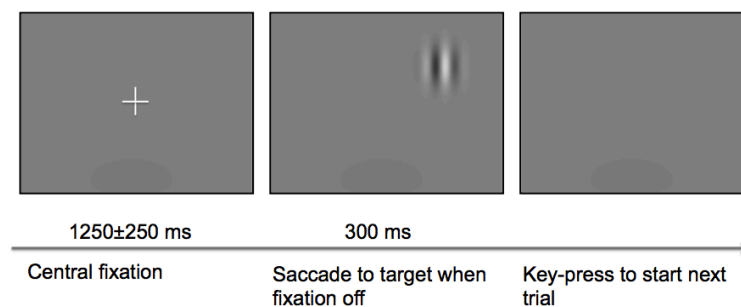


Figure 8.2: Paradigm of the experiment described in chapter 6. The present chapter re-analyses saccadic landing positions.

8.3 Data Analysis and Results

To figure out whether the negative correlation between saccadic landing positions and saccadic latencies was caused by accurate saccades in high-latencies or by a change in the two-dimensional distributions, I introduced a statistical method called circular data analysis, described in Fisher (1995). Circular data analysis measures deg from 0 deg to 360 deg in order to assess data occurring around a circle. Consequently, they do not have a beginning or end along a real axis, but they indicate a direction in two dimensions. For example, an angle of 190 deg indicates the opposite direction to an angle of 10 deg.

See figure 8.3 for illustration: this shows a circular histogram (also called rosediagram) of saccadic landing positions towards leftward drifting Gabors (left panel, red bars) and rightward drifting (right panel, blue bars) Gabors. The numbers arranged around the circle indicate the deg, starting with 0 at 3 o'clock and increasing in mathematical positive direction. The numbers arranged inside the graphs indicate the total number of saccades that landed within a predefined interval. In figure 8.3 each interval contained 10 deg, splitting each circle into 36 intervals. Leftward drifting Gabors elicited saccades mainly landing between 140 deg and 220 deg, while rightward drifting Gabors elicited saccades mainly landing between 310 deg and 40 deg.

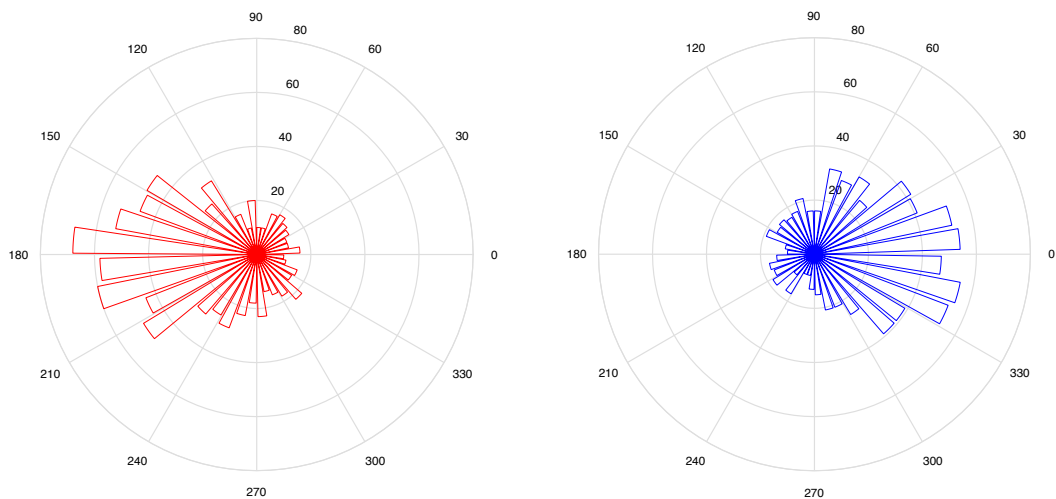


Figure 8.3: Two rosediagrams presenting saccadic landing positions towards leftward (left diagram) and rightward (right diagram) drifting Gabors. Numbers around the circle indicate deg, starting with 0 at 3 o'clock and increasing in mathematical positive direction. The numbers arranged inside the graphs indicate the total number of saccades that landed within a predefined interval. Each interval contained 10 deg, splitting the each circle in 36 intervals. For more details read main text.

I determined two variables: 1) the average direction of saccadic landing positions (φ) and 2) the mean Euclidian distance of saccadic landing positions relative to the horizontal/vertical centre of the Gabor (r). Both variables can be expressed in polar coordinates by (r, φ):

$$r = \frac{\sum_{i=1}^n \sqrt{x_i^2 + y_i^2}}{n} \quad (8.1)$$

where n is the total numbers of saccadic landing positions in one condition (right or leftward drifts).

$$\alpha_i = \begin{cases} \arctan\left(\frac{y_i}{x_i}\right); & x_i > 0 \\ \arctan\left(\frac{y_i}{x_i}\right) + 180; & x_i < 0, y_i \geq 0 \\ \arctan\left(\frac{y_i}{x_i}\right) - 180; & x_i < 0, y_i < 0 \\ 90; & x_i = 0, y_i > 0 \\ 270; & x_i = 0, y_i < 0 \end{cases} \quad (8.2)$$

$$S = \sum_{i=1}^n \sin(\alpha_i) \quad (8.3)$$

$$C = \sum_{i=1}^n \cos(\alpha_i) \quad (8.4)$$

$$\varphi = \begin{cases} \frac{S}{C}; & S > 0, C > 0 \\ \frac{S}{C} + 180; & C < 0 \\ \frac{S}{C} + 360; & S < 0, S > 0 \end{cases} \quad (8.5)$$

Figure 8.4 shows an example of a vector defined by (r, φ). Both variables are important to assess the error in saccadic landing positions. The direction of the vector (red) represents the mean direction (φ) and the length (r) represents the mean Euclidian distance of saccadic landing positions to the centre of the Gabor.

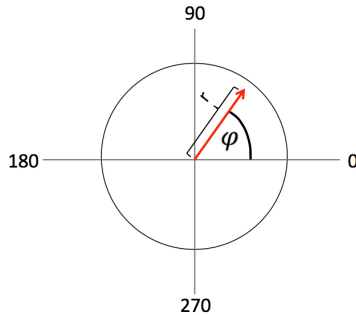


Figure 8.4: An example of a vector defined by direction and angle (r, φ). The direction of the vector (red) represents the mean direction (φ) and the length (r) represents the mean Euclidian distance of saccadic landing positions to the centre of the Gabor. For more details read main text.

I suggest that low-latency saccades are as much affected by motion as high-latency saccades if: 1) the mean directions (φ) point in the direction of motion in high- and low-latency saccades, and 2) the mean Euclidian distances (r) are not smaller in low-latency saccades than in high-latency saccades.

As stated in chapter 6 the number of valid saccades ranged between 134 and 183 for rightward drifts, and between 138 and 185 saccades for leftward drifts.

Figure 8.5 shows the mean direction of saccadic landing positions for each observer and each direction of motion. The red and blue vectors represent mean directions of saccades elicited by leftward and rightward drifts, respectively. Rightward drifts elicited saccades with mean directions to the right. More precisely, all vectors had an orientation between of 1 deg and 24 deg. Leftwards drifting Gabors elicited saccades with mean directions to the left. All vectors had an orientation between 169 deg and 195 deg. As described above, the lengths of each vector represent the mean Euclidian distance to the horizontal/vertical centre of the Gabor. In all observers, the lengths of vectors in both conditions varied only very little. Figure 8.6 shows vector lengths for each observer and each condition in order to simplify comparison.

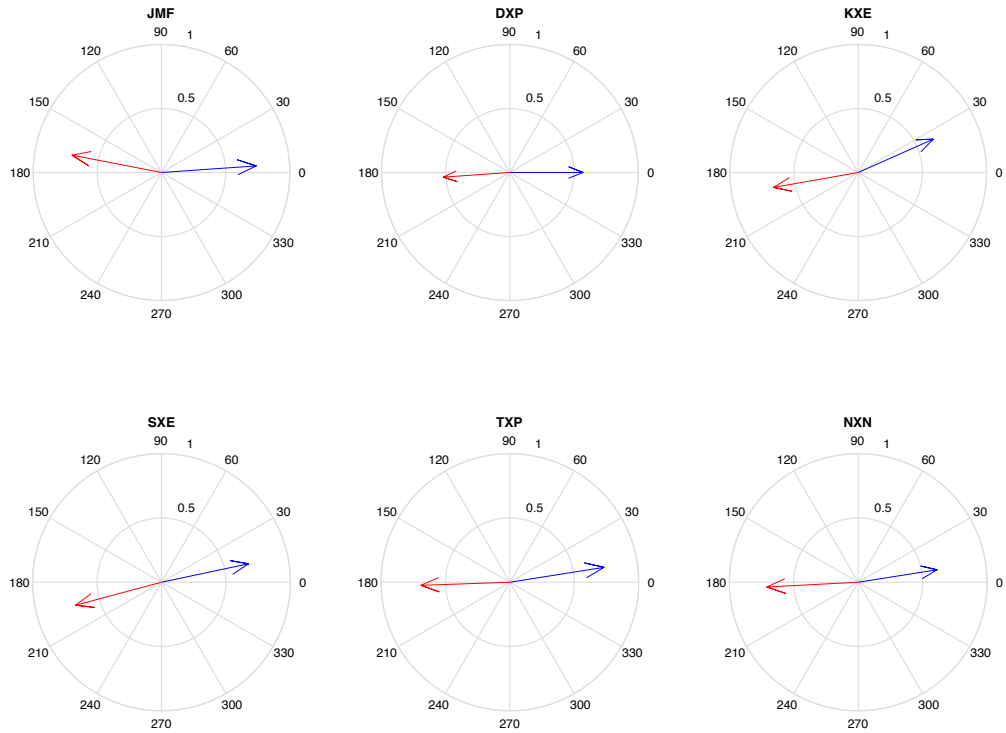
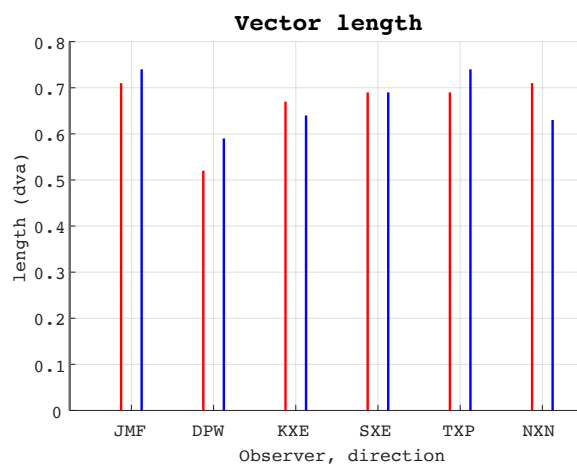


Figure 8.5: Resulting vectors of circular data analysis indicating direction and angle of saccade landing positions. Numbers around the circle indicate deg, starting with 0 at 3 o'clock and increasing in mathematical positive direction. Directions of vectors indicate the mean direction (φ) of saccadic landing positions for each observer and each direction of motion. The red and blue vectors represent mean directions of saccades elicited by leftward and rightward drifts, respectively. The length of each vector represents the mean Euclidian distance (r) to the horizontal/vertical centre of the Gabor. For more details read main text.

Figure 8.6: Length of vectors. The lengths of vectors within figure 8.5 are presented to simplify comparison. The x-axis indicates observers, and the y-axis the length (mean Euclidian distance) (r) of the vectors in dva. Blue and red coloured bars represent resulting vector length when Gabors drifted to the right and the left, respectively. For more details read main text.



The x-axis indicates observers and motion direction of the Gabor, and the y-axis indicates the length of the vectors (degree of visual angle). Blue and red coloured bars represent resulting vector length when Gabors drifted to the right and the left, respectively. The Euclidian distance was larger in rightwards than in leftwards drifting Gabors in three out of six observers (JMF, DPW and TXP) and smaller in rightward than in leftward drifting Gabors in two out of six observers (KXE and NXN). One observer (SXE) showed the same size of errors in right leftward drifts. In summary, there was no consistent pattern of saccadic errors between right and leftward drifts across observers.

In summary, the polar coordinates indicating the mean direction of motion were consistent with horizontal shifts determined in chapter 6 (figure 6.2).

The same procedure as described above was applied to compare saccadic landing positions to right and leftward drifting Gabors, when saccades were binned in two latencies. I binned data in latency intervals as described in chapter 6. Again, because saccadic latencies varied between observers, the intervals were different between observers. Around 50% of trials were binned in the low-latency saccades, and 50% of trials were binned in high-latency saccades. For four out of six observers (JMF, DPW, SXE, TXP) I binned data into saccades that started between 100-170 ms, and into saccades that started between 171-380 ms after fixation offset. Two observers made saccades comparatively late. The data of KXE were binned into saccades with latencies of 100-220 ms, and saccades with latencies of 221-380 ms. Saccades of observer NXN were separated into latency bins of 100-190 ms, and 191-380 ms. In both latency bins, the number of valid saccades ranged between 54 and 113 for rightward drifts, and between 48 and 127 saccades for leftward drifts. Figure 8.7 shows resulting mean directions (φ) and mean Euclidian distances (r) for rightward and leftward drifts; each drift direction separated high-latency saccades (red and blue) and low-latency saccades (black and cyan).

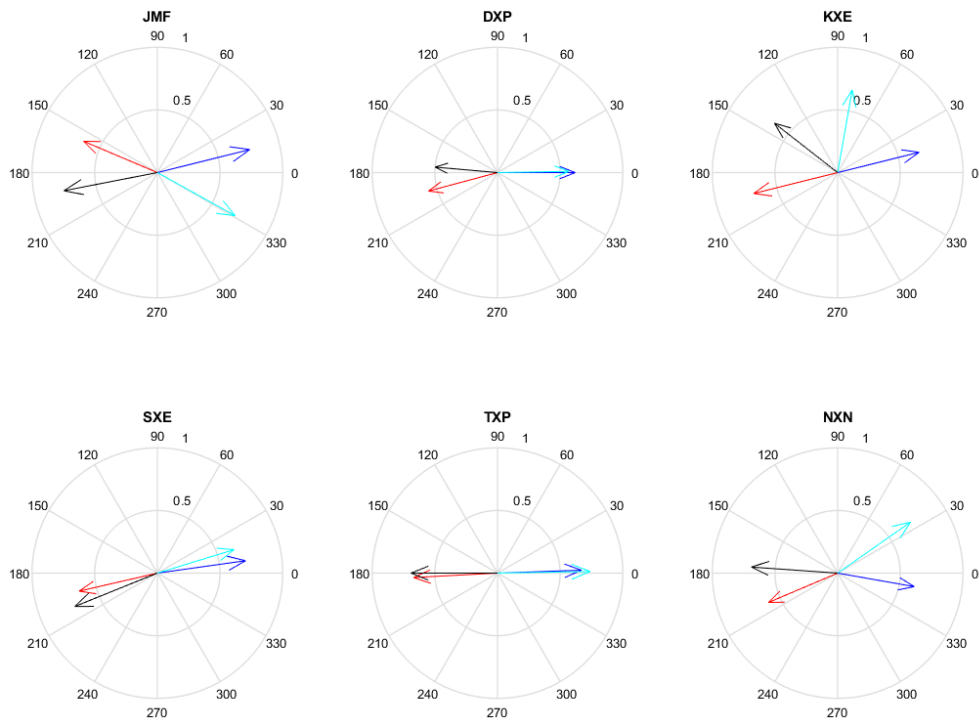


Figure 8.7: Results of circular data analysis – different latency bins. Numbers around the circle indicate deg, starting with 0 at 3 o'clock and increasing in mathematical positive direction. Directions of vectors indicate the mean direction (φ) of saccadic landing positions for each observer and each direction of motion. The red and blue vectors represent mean directions of high-latency saccades elicited by leftward and rightward drifts, respectively. The black and cyan vectors represent the mean direction of low-latency saccades elicited by leftward and rightward drifts, respectively. The length of each vector represents the mean Euclidian distance (r) to the horizontal/vertical centre of the Gabor. For more details read main text.

Figure 8.7 summarises saccadic landing positions to right- and leftward drifting Gabors that were binned in ‘early’ and ‘late’ saccades. Polar coordinates indicate that the saccadic landing positions of all observers were shifted in the direction of motion for all observers and both latency intervals. Confirming analysis of horizontal saccadic shifts (chapter 6), the smallest effect was found in late saccades of observer KXE. However, mean direction still pointed in the direction of motion, while no horizontal shift was found in motion directions to the right or to the left (see figure 6.4).

Figure 8.8 shows the mean Euclidian distance of each condition, high-latency saccades (red bar: leftward drifts; blue bar: rightward drifts) and low-latency saccades (black colour: leftward drifts; cyan colour: rightward drifts).

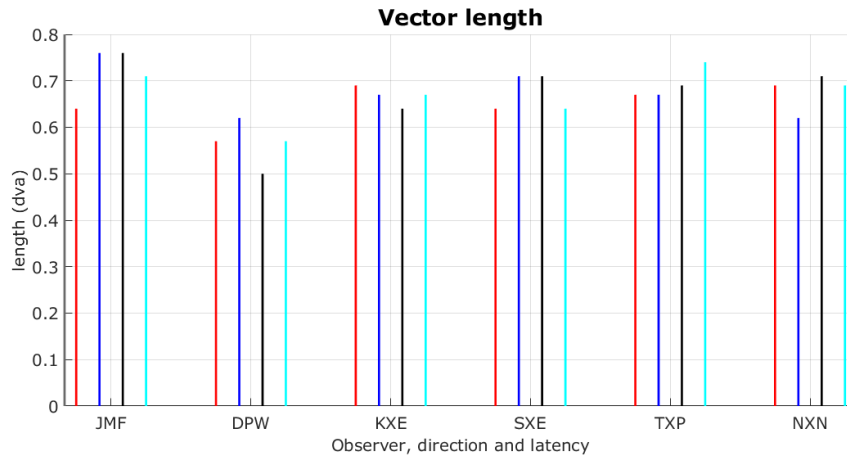


Figure 8.8: Length of vectors – different latency bins. The lengths of vectors within figure 8.2 are presented to simplify comparison of their lengths (r). The x-axis indicates observers, and the y-axis the length (mean Euclidian distance) of the vectors in dva. Blue and red coloured bars indicate ‘early’ conditions; they represent resulting vector length when Gabors drifted to the right (blue) and the left (red). Green and magenta coloured bars indicate ‘late’ conditions; they represent resulting vector length when Gabors drifted to the right (cyan) and the left (black). For more details read main text.

One out of six observers (DPW) made saccades with the mean Euclidian distances relative to the centre of the Gabor being slightly smaller in low-latency saccades than in high-latency saccades in both conditions (right and leftward drifting Gabors). In contrast, one observer (NXN) made saccades with the mean Euclidian distance being slightly larger in low-latency saccades than in high-latency saccades in both conditions. Four out of six observers showed no consistent pattern in saccades starting early or late. Also the comparison of absolute shifts (sum of Euclidian distances in right and leftward drifts) did not result in a consistent pattern between high- and low-latency saccades.

Finally, a non-parametric test for equal medians in circular data (Fisher, N. I., 1995, p. 114) was employed to test whether landing positions towards rightward drifting Gabors in high-latency saccades were significantly different from landing positions towards rightward drifting Gabors in low-latency saccades. The same tests were applied to saccades guided to leftward drifting Gabors. All tests indicated a non-significant difference between high- and low-latency saccades for 5 out of 6 observers (all p-values between 0.07 and 0.96). Only for one observer (NXN) there was a

significant difference between high- and low-latency saccades when the Gabors drifted to the right side ($p < 0.001$). Interestingly, employing the test to evaluate whether landing positions towards rightward drifting Gabors are significantly different to landing positions towards leftward drifting Gabors in high-latency saccades resulted in significant test results across all observers (all p values < 0.007), while tests indicated a significant difference between saccades towards rightward and leftward moving Gabors in low-latency saccades in only two out of six observer (observer DXP and observer NXN, p values < 0.001).

The non-significant test results might be due to comparatively large variance in landing positions of low-latency saccades. Therefore, I computed the sample circular standard deviations (STD; Fisher, N.I., 1995, p. 32) for each observer, as well as the drift direction and the latency interval as shown in table 8.1. As expected, the STD was larger in low-latency saccades than in high-latency saccades across all observers and drift directions, except in one dataset (observer SXE, rightward drifting Gabor).

Observer	Gabor: Left drift Latency: high STD	Gabor: Left drift Latency: low STD	Gabor: Right drift Latency: high STD	Gabor: Right drift Latency: low STD
JMF	1.67	2.17	1.57	2.34
DPW	1.24	1.27	1.17	1.55
KXE	1.53	2.71	1.77	2.58
SXE	1.07	1.56	1.27	1.07
TXP	1.27	1.63	1.23	1.45
NXN	1.12	1.28	1.10	1.14

Table 8.1: Circular standard deviation. Sample circular standard deviations for each observer, drift direction and latency interval. For more details read main-text.

8.4 Summary

First, I found consistent results in horizontal errors and mean directions when saccades of observers were combined (figure 6.2 and figure 8.5), demonstrating that both methods indicated the same effect. Secondly, when saccades were binned in high-latency saccades and low-latency saccades for each observer, I found that the mean directions pointed in directions of motion in both latency bins and in all observers. The mean Euclidian distances in early and late saccades, however, did not show a consistent pattern across observers. Thirdly, statistical tests for equal medians in

circular data showed no significant difference between saccadic landing positions in low-latency saccades and high-latency saccades (neither when the Gabor drifted to the right, nor when it drifted to the left). A comparatively large variance was found in low-latency saccades (see table 8.1).

8.5 Discussion

The mean directions and mean Euclidian distances did not indicate a decrease of saccadic errors with increasing latency in four out of six observers (DPW, SXE, TXP, NXN): mean directions pointed in the direction of motion in both latency bins, and Euclidian distances did not decrease with increasing latency.

In chapter 6, analysis of horizontal errors did not indicate a significant difference in high-latency saccades for two observers, JMF and KXE (see figure 6.4).

Circular data analysis did not indicate a clear difference in high- and low-latency saccades of JMF. First, mean directions clearly pointed in the direction of motion in both latency bins; i.e. in high-latency saccades the mean direction pointed to 157 deg for leftward drifts and to 14 deg in rightwards drifts. Mean directions of low-latency saccades pointed to 191 deg and 331 deg in leftward and rightward moving Gabors, respectively. Secondly, the mean Euclidian distance increased with increasing latency for rightward drifting Gabors, and decreased with increased latency for leftward drifting Gabors. The sum of Euclidian errors elicited by right and leftward moving Gabors was larger in high-latency saccades than in low-latency saccades.

In the data of observer KXE, the mean direction of high-latency saccades pointed to 194 deg and to 14 deg in leftwards and rightwards drifts, respectively. The data indicated a smaller difference in angles between right and leftward drift in low-latency saccades. More precisely, rightward drifting Gabors elicited saccades with a mean direction of 142 deg and leftward drifting Gabors elicited saccadic landing positions with a mean direction of 80 deg. However, the Euclidian distance was slightly smaller in high-latency saccades than in low-latency saccades in leftward drifts; i.e. 0.69 dva for high-latency saccades and 0.64 dva in low latency saccades. The Euclidian distance was of the same size in high- and low-latency saccades in rightward drifts; i.e. 0.67 dva.

Statistical circular data tests were employed in order to examine if there was a significant difference in polar coordinates representing early and late saccades in right and leftward drifting Gabors. I found no significant difference between high-latency saccades and low-latency saccades towards leftward drifting Gabors, and no significant difference between high-latency saccades and low-latency saccades toward rightward drifting Gabors. However, tests indicate a highly significant difference between saccadic landing positions towards rightward drifting Gabors and saccadic landing positions towards leftward drifting Gabors when saccades were made early (high-latency saccades), but no significant difference when saccades were made late (low-latency saccades). The comparatively large variance in low-latency saccades (see table 8.1) might explain the non-significant test results. For dataset with large variances a larger sample size is necessary to test if one condition is different from another condition.

8.6 Conclusion

I hypothesised that the negative correlation in saccadic landing positions and saccade latencies might not be caused by a smaller error in saccades for high-latency saccades than in those for low-latency saccades. I introduced a different method to analyse saccadic landing positions in a two-dimensional plane, which was based on circular data analysis. According to current results, there is evidence that low-latency saccades are highly affected by motion for at least two out of six observers. I showed that the circular standard deviation of saccadic landing positions increases with increasing latencies. However, a larger sample size is necessary to reject the hypothesis that saccadic landing positions are significantly different from one-another.

9. GENERAL DISCUSSION

9.1 Summary

In chapter 3, I found a clear effect on the perceived position of the dot superimposed on a drifting Gabor. Target dots were perceived as shifted along the direction of motion: When the Gabors were drifting rightwards, target dots were perceived to be shifted to the left (up to 0.21 dva), and when the Gabors were drifting leftwards, target dots were perceived to be shifted to the right (up to 0.33 dva) relative to the true centre of the Gabor. Volitional saccadic eye movements were also distorted by the motion-induced position shift of a Gabor. The effect was consistent with the perceptual effect: After the normalisation process, saccadic landing positions were shifted to the left (up to 0.20 deg) in leftward drifting Gabors, and shifted to the right (up to 0.175 deg) in rightward drifting Gabors. I did not find that the magnitude of effects depended on motion direction toward the midline or away from the midline, either in the perceptual system, or in volitional saccades.

The experiment described in Chapter 5 excluded the possibility that the drift direction (right or left) of the Gabor was used as a cue to engage saccadic adaptation mechanisms in different directions, and the shift in saccadic landing position could be due to an error signal arising from the position of the target dot relative to the eye position after saccade landing.

Chapter 4 indicates that volitional saccades are more accurate than the perceptual system. Kerzel & Gegenfurtner (2005) compared perceptual effects to the average landing positions of volitional saccades relative to the horizontal centre of the Gabor, but pointed out that shifts in perception strongly depend on the measurement method. I was the first to measure saccadic landing positions and perceptual effect when 1) perception task and saccade task were both made on the centre of the Gabor and 2) both task were done within one trial. Therefore comparison of both measurements is more accurate than in the study by Kerzel & Gegenfurtner (2005). However, as admitted in chapter 4, my experiment to compare saccades and perception had some issues. Also discussed in chapter 4, the smaller bias in saccades than in perception might also be due to a decisional-bias in the perception task. In the perceptual task, the

key indicating ‘dot seen on the right’ was pressed with the right hand, while the key indicating ‘dot seen on the left’ was pressed with the left hand. Results may be manipulated by the observer’s decisional criterion, such as that the observer may have decided in favour of one alternative when unsure. To find out whether a decisional bias might affect perceptual shifts, one could design an experiment such that it was difficult for the observer to influence the effect of drifting direction with a decisional criterion.

Kosovicheva, Wolfe & Whitney (2014) studied the motion induced position shift in perception tasks and reflexive saccades. Group-level statistics of the horizontal error in saccadic landing positions relative to the horizontal centre of the Gabor indicated that saccadic errors were negatively correlated with saccadic latencies. In chapter 6, I critically examined whether this finding might be a statistical artefact of group-level statistics with slow observers made more accurate saccades than fast observers. Replication of the study by Kosovicheva, Wolfe & Whitney (2014) showed that also within-observer statistics resulted in a negative correlation between saccadic errors and saccadic latencies in six out of six observers.

In chapter 7 I posited that the finding by Kosovicheva, Wolfe & Whitney (2014) might be caused by a confusion of the visual system. More precisely, the visual system may confuse motion inside an object with motion of the object itself, especially when viewing time is short. I hypothesised that short-latency saccades were programmed to intercept a feature of the drifting carrier. To test this hypothesis I compared saccadic errors induced by a drifting Gabor with saccadic errors induced by a pseudo-plaid and found that horizontal saccadic errors are negatively correlated with saccadic latencies.

In my last experimental chapter I reanalysed the data of chapter 6 a second time, but considered the Euclidian distance relative to the horizontal and vertical centre of the Gabor. So far, applying a method called statistical data analysis (Fisher, 1995), indicates no decreasing error in saccadic landing positions with increasing saccadic latencies. Therefore, I claim that there may not be dissociation between reflexive and volitional saccades towards drifting Gabors. The negative correlation between errors and latencies may rather be due to a varying two-dimensional distribution of landing positions over latencies.

9.2 Reflection on previous studies

9.2.1 Saccadic eye movements

I found that volitional saccades in humans are affected by the motion-induced position shift (experiment described in chapter 3). Rightward drifting Gabors induce saccades with landing positions shifted to the right relative to landing positions of saccades towards leftward drifting Gabors.

A study by De'Sperati and Baud-Bovy (2008) (described in detail below) suggested that the different systems might depend on independent thresholds to pick-up the visual positional signal at different moments of its temporal evolution. As mentioned in the introduction, volitional saccades are longer in their latencies than reflexive saccades (e.g. Mort et al., 2003). Therefore, Kosovicheva, Wolfe & Whitney (2014) suggested that the effect of an illusion might be larger with volitional saccades than with reflexive saccades. Inspired by this theory, Kosovicheva, Wolfe & Whitney (2014) studied reflexive saccades towards single Gabors, confirming that they are affected in the same manner as volitional saccades; i.e. saccadic landing positions were shifted in the direction of motion (see also Kerzel & Gegenfurtner, 2005; Schafer and Moore, 2007). Interestingly though, Kosovicheva, Wolfe & Whitney (2014) claimed that the magnitude of this bias was negatively correlated with saccadic latencies, with high-latency saccades not affected by the illusory position shift at all. As discussed in this thesis, the negative correlation between errors in reflexive saccades and saccadic latencies is controversial. The negative correlation may be due to 1) dissociation between volitional saccades/perception and reflexive saccades, suggesting a dual-visual-processing system. Or 2) similar to an idea of De'Sperati and Baud-Bovy (2008); both reflexive saccades and perception/volitional saccades depend on independent thresholds, which would then depend on the visual signal at different moments of its temporal evolution. Or 3) the negative correlation between errors in reflexive saccades and saccadic latencies towards single Gabors may be due to a change in the two-dimensional distribution of saccadic landing positions, instead of a decreasing horizontal error with increasing latencies (described in chapter 8).

The first hypothesis seems to be more likely than the second hypothesis: Arnold, Thompson & Johnston (2007) measured the build-up of perceptual shifts, and found that the perceptual illusory position shifts are positively correlated with presentation

duration of a Gabor, and saturates after ~150 ms. Also Kosovicheva, Wolfe & Whitney (2014) measured perceptual motion-induced position shifts and confirmed a positive correlation between shifts and stimulus duration (duration 20 – 100 ms).

In principle, the first and third hypothesis are plausible. Supported by results of circular data analysis, the negative correlation between saccadic errors and saccadic latencies in a Gabor may be due to the third hypothesis. Some of the evidence to support this approach has come from previous studies demonstrating that errors in reflexive saccades are not negatively correlated with saccadic latencies.

As discussed before in this thesis Zimmerman, Morrone & Burr (2012) induced the flash-lag effect (Whitney & Cavanagh, 2000) to investigate whether there was dissociation in action and perception tasks. A sinusoidal windmill rotated continuously clockwise and anticlockwise in the centre of the screen. The windmill caused a position shift in the direction of motion, in both saccadic landing positions and perceived position of the flashed bar. In contrast to Kosovicheva, Wolfe & Whitney (2014), Zimmerman, Morrone & Burr (2012) state that saccades showed increasing shifts with increasing latencies. The saturation was reached with a latency of 157 ms (upward shift) and with a latency of 171 ms (downward shift) indicating a non-monotone relationship between saccadic errors and saccadic latencies. However, like Kosovicheva, Wolfe & Whitney (2014), Zimmerman, Morrone & Burr (2012) analysed saccades in each dimension separately (vertical and horizontal), which I already criticised above. Furthermore, the numbers of saccades were not mentioned in their paper. Hence, in some latency bins the number of trials may be too small to make a significant conclusion.

The study by De'Sperati and Baud-Bovy (2008) also supports the idea that high-latency reflexive saccades do not escape illusory position shifts. The authors used a very similar paradigm to Zimmermann, Morrone & Burr (2012). Like Zimmermann, Morrone & Burr (2012), but in contrast to Kosovicheva, Wolfe & Whitney (2014) they found that saccadic errors were positively correlated with saccadic latencies. More precisely, saccades with latencies of ~100-250 ms were found to land accurately at the target, whereas at higher latencies of ~250-450 ms, saccades

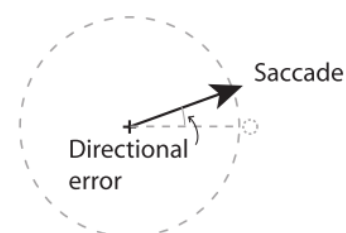


Figure 9.1: Analysis of saccadic landing positions by De'Sperati and Baud-Bovy (2008). The angle between response direction (thick line or arrow) and flash direction (dashed line). From De'Sperati and Baud-Bovy, 2008.

were increasingly biased by visual motion until they reflected the perceptual illusion. De'Sperati and Baud-Bovy (2008) described how saccades would not wait for the completion of the perceptual analysis; therefore concluding that seeing and looking would be based on asynchronous processes. Importantly, they did not analyse saccadic landing positions in vertical or horizontal directions but determined by the angle between response direction of the eye movement (thick line or arrow in figure 9.1) and the direction of the flashed stimulus (dashed line in figure 9.1).

Evidence for dissociation between reflexive saccades and volitional saccades/perception is given by a study of Wong and Mack (1981). They investigated volitional saccades (memory-guided saccades) and reflexive saccades (saccades towards a suddenly presented target) to perception tasks by presenting a target inside a frame inducing an illusory position shift. Shifting the frame or both the frame and the target in the same or opposite directions induces an illusory displacement of the target in the opposite direction of frame motion. In experiment 1 a trial started with fixating the target centred within the frame. Next, the screen went blank for 500 ms. Afterwards a displaced frame and target reappeared for 100 ms, which triggered observers to saccade towards the new target location. The frame remained visible for 700 ms. Next observers were asked to judge the direction of the perceived target displacement and adjust the separation between the target point after moving, so that it matched the magnitude of the perceived displacement. Interestingly, the reflexive saccades towards the briefly presented new target location were not affected by the illusion; i.e. saccades were directed to targets' retinal position. In a second experiment, observers were asked to make a reflexive saccade towards a target (as in experiment 1), followed by a volitional saccade back to the previous target location (memory-guided saccade). The first saccade was guided toward the retinal position (duplicating the results obtained in experiment 1). The second saccade (look back saccade) was guided by perceived displacement of the target. In summary, the first saccade was guided by the physical position of the target, the second saccade was guided by the perceived displacement of the target. Wong and Mack (1981) posited that the same stimulus elicited two different oculomotor responses, indicating dissociation between memory-guided volitional saccades and reflexive saccades.

9.2.2 Perception tasks

I found consistent perceptual shifts for Gabors that appeared on the right side of the visual field with randomised Gabor positions. Perceived target positions were shifted leftwards with Gabors drifting to the left, and shifted rightwards with Gabors drifting to the right. These results are comparable to previous results (e.g. Yamagishi, Anderson & Ashida, 2001; De Valois & De Valois, 1991; Kosovicheva, Wolfe & Whitney, 2014).

As discussed in this thesis, the magnitude of perceptual shift measured in hitherto existing studies might be influenced by a decisional-bias. To find out whether a decisional bias might affect perceptual shifts, one could design an experiment such that it was difficult for the observer to influence the effect of drifting direction with a decisional criterion. Morgan, Melmoth, & Solomon (2013) suggested using a 2-Alternative Forced Choice (2AFC) method instead of the Method of Single Stimuli.

9.3 Conclusion

As introduced in section 1.3, we intuitively assume that it is absolutely crucial to accurately compute our actions towards or away from moving objects in order to manage our every-day life. However, my experiments indicate that both, our perception and visually guided actions are misguided by visual illusions; i.e. my experiments showed that volitional saccades are largely affected by the motion-induced position shift.

Volitional saccades are not as quickly initiated as reflexive saccades, are triggered internally and rely on high cortical areas such as the dorsolateral prefrontal cortex, while reflexive saccades are triggered externally and rely heavily on lower cortical and subcortical areas (e.g. Mc Dowell et al., 2008). Interestingly, Kosovicheva, Wolfe & Whitney (2014) found that short-latency reflexive saccades were effected and long-latency saccades were not affected by the motion-induced position shift. However, the effect size in the perceptual system increases with time until it reaches an asymptotic value (e.g. Arnold, Thompson, Johnston, 2007). Applying circular data analysis, I found that landing positions of both, short-latency reflexive saccades and long-latency reflexive saccades, are shifted in direction of motion and that the circular standard deviation of saccadic landing positions increases with increasing latencies. As

mentioned in chapter 8, for dataset with large variances a larger sample size is necessary to test if one condition is different from another condition. As a consequence, there is no relevant evidence that long-latency reflexive saccades are not affected by the motion-induced position shift.

APPENDICES

Appendix A: Cluster Algorithm

When an expert encodes regions-of-interest by hand, he groups nearby fixations together. That is an easy task for humans but a difficult task for computers. An example of that is shown in figure A1. For humans it is obvious that the regions of interest (i.e. the places where most fixations lie) are the eyes, nose and mouth of the woman in the photograph. To find the region-of-interest, researchers used an analysis that is based on an existing algorithm that can be used for robust clustering of eye-movements (Santella & Doug

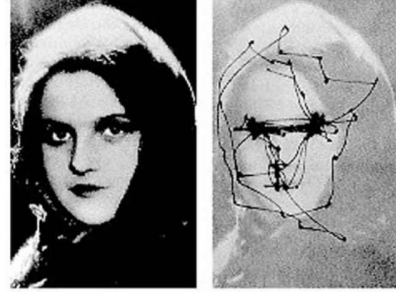


Figure A1: Experiment of Alfred Yarbus (1967). Observers had to look at the woman for one minute. The resulting eye movements are shown as dark lines between different target-locations.

DeCarlo, 2004). It is based on the mean-shift-procedure (Fukunaga & Hostetler, 1975), which makes the entire process of finding a location-of-interest robust. The algorithm arranges modes of data deterministically and is entirely data-driven.

The process starts by the mean-shift procedure with shifting the set of points $(x, y)_i$, $i = 1, \dots, n$ into a denser configuration. It iteratively moves a point $(x, y)_i$ to a location $s((x, y)_i)$ until the distance between $(x, y)_i$ to $s((x, y)_i)$ will converge. So it iteratively moves all points towards a location of higher density, also called the modes.

For all iterations we have to find the distance from $(x, y)_i$ to $(x, y)_j$. The weights of points $(x, y)_j$ are based on a kernel function

$$k = e^{\left(-\frac{(x_i - x_j)^2 + (y_i - y_j)^2}{\sigma^2}\right)} \quad (\text{A.1})$$

σ describes the spatial extent and provides robustness against extreme outliers. It is like a free parameter to control the algorithm. Decreasing σ will result in several, small clusters and increasing σ will result in fewer, large clusters.

After finding all distances and determining the weight for each point $(x, y)_j$, we are able to determine

$$s(x_i) = \frac{\sum_{j=1}^n k \cdot x_j}{\sum_{j=1}^n k} \quad (\text{A.2})$$

and

$$s(y_i) = \frac{\sum_{j=1}^n k \cdot y_j}{\sum_{j=1}^n k} \quad (\text{A.3})$$

The second step of the process would be to define different clusters. Hence all points are collected to their modes; a good method of doing this is a cluster-method, which uses a distance threshold.

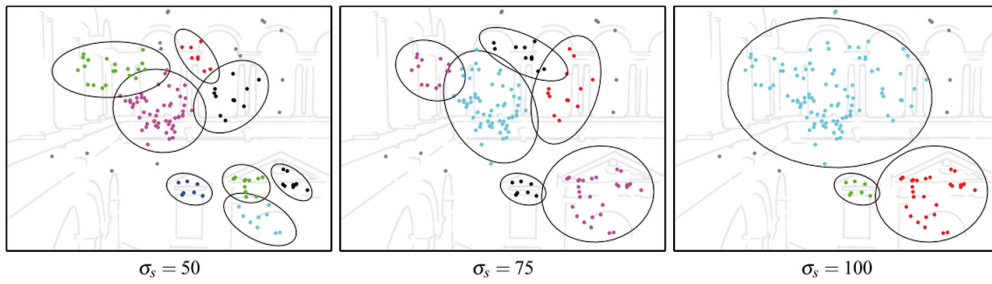


Figure A2: Example given by Santella & DeCarlo (2004): clustering of the region of interest of one observer. Different figures show resulting regions of interest depending on varying spatial scales σ . From Santella & DeCarlo (2004).

Appendix B: Psychometric Function

I will take the psychophysical data by sampling an observer's performance on a task with different stimulus levels. Observers had to judge if the point superimposed on the Gabor appeared on the right or left relative to the perceived centre of the Gabor. It is called a 'Method of Single Stimuli' (MSS). As mentioned above, in my experiment the stimulus levels were determined by an APE-Procedure depending on the observers' previous perceptual responses. If the observer gave false responses, the position of the point was shifted away from the centre of the patch so that judging would be easier. If the observer gave several correct responses, the position of the point was shifted toward the centre of the patch and judging would be more difficult again. I measured responses

$$p(\text{stimulus was seen on the right} | x = x_i) = y_i \quad (\text{B.1})$$

where x_i , $i = 1, \dots, k$ indicates the different stimuli levels. n is the total number of trials for all stimulus-levels $i = 1, \dots, k$, n_i the total number of trials for each stimulus-level i . The relative frequency for each stimulus-level

$$r(x_i) = p(\text{stimulus was seen on the right} | x = x_i) = \frac{y_i}{n_i} \quad (\text{B.2})$$

will be greater for stimuli which are positioned on the right side than for stimuli which are positioned on the middle of the patch. For our measurements $r(x_i)$ we have to find a function $\phi(x)$, which specifies the relationship between underlying probabilities $r(x_i)$ and the stimulus-levels x_i . That function is called a 'psychometric function' that is, in my case, based on a Gaussian c.d.f.. Its shape is determined by the parameters μ, σ . μ determines its displacement along the abscissa and σ will determine its slope. To model the underlying data we assume the number of responses 'right' in a given level of stimulus to be the sum of a Bernoulli-Process with $p := \phi(x_i)$. Hence, all measurements of the stimuli levels are binomially distributed with $x_i \sim B(n_i, p_i)$. The probability of deciding y_i times for the answer 'right' within n_i trials on stimulus-level x_i is given by

$$P(y_i) = \binom{n_i}{y_i} \phi(x_i)^{y_i} (1 - \phi(x_i))^{n_i - y_i}, i = 1, \dots, k \quad (\text{B.3})$$

Let $L(\mu, \sigma|y)$ be the maximum likelihood function and $l(\mu, \sigma|y)$ its log likelihood function respectively based on observers' data $y = (y_1, \dots, y_k)$.

The maximum likelihood function of the probability function stated above is given by

$$L(\mu, \sigma|y) = \prod_{i=1}^k \binom{n_i}{y_i} \phi(x_i)^{y_i} (1 - \phi(x_i))^{n_i - y_i} \quad (\text{B. 4})$$

and its log maximum likelihood function is given by

$$l(\mu, \sigma|y) = \sum_{i=1}^k y_i \log \left(\binom{n_i}{y_i} \right) + \sum_{i=1}^k y_i \log (\phi(x_i)) + (y_i - n_i) \log (1 - \phi(x_i)) \quad (\text{B. 5})$$

(Mallot, 2011)

The maximum likelihood estimator is that set of parameters μ, σ for which the likelihood value is largest. In our application the maximum-likelihood maximization uses the Nelder-Mead simplex search algorithm.

The Nelder-Mead Algorithm will find the minimum of the log-likelihood function $l(\mu, \sigma|y)$.

Because of $\max_{x \in D} f(a) = \min_{x \in D} -f(a)$ the algorithm will find a minimum for $-l(\mu, \sigma|y)$. For that procedure we use the function `fminsearch`, which is already defined in Matlab. Note that the sums of the binomial coefficient have no influence on maximum-likelihood maximisation. Therefore, we were allowed to ignore them.

REFERENCES

- Adelson, E.H. & Movshon, J. A. (1982). Phenomenal coherence of moving visual patterns. *Nature*, 300(5892): pp. 523–525
- Albright, T. D. (1989). Centrifugal directional bias in the middle temporal visual area (MT) of the macaque. *Visual Neuroscience*, 2: pp. 177-188
- Algina, J., Olejnik, S. & Ocanto, R. (1989). Type I error rates and power estimates for selected two-sample tests of scale. *Journal of Educational Statistics* 14: pp. 373–383
- Amano, K., Edwards, M., Badcock, D. R. & Nishida, S. Y. (2009). Adaptive pooling of visual motion signals by the human visual system revealed with a novel multi-element stimulus. *Journal of Vision*, 9(3):4: pp. 1–25
- Anderson, S.J. & Burr, D.C. (1985). Spatial and temporal selectivity of the human motion detection system. *Vision Research*, 25(8): pp. 1147–1154
- Arnold, D. H., Marinovic, W. & Whitney, D. (2014). Visual motion modulates pattern sensitivity ahead, behind, and beside motion. *Vision Research* (98): pp. 99–106
- Arnold, D. H., Thompson, M. & Johnston, A. (2007). Motion and position coding. *Vision Research*, 47(18): pp. 2403–2410
- Barlow, B.H.B. (1958). Temporal and spatial summation in human vision at different background intensities, *Journal of Neurophysiology* (141): pp. 337–350
- Becker, W., Fuchs, A. F., (1969). Further properties of the human saccadic system: eye movements and correction saccades with and without visual fixation points. *Vision Research* 9(10): pp.1247-1258
- Bender, D.B. (1982). Receptive-field properties of neurons in the macaque inferior pulvinar. *Journal of neurophysiology*, 48(1): pp. 1–17
- Berry, M., Brivanlou, I., Jordan, T. & Meister, M. (1999). Anticipation of drifting stimuli by the retina. *Nature* (398): pp. 335-338

- Blackmore, C., Nachmias, J. & Sutton, P. (1970). The perceived spatial frequency shift: evidence for frequency-selective neurons in the human brain. *J. Physiol.* 210: pp. 727-750
- Blakemore, C. & Campbell, F. W. (1969). On the existence of neurons in the human visual system selectively sensitive to the orientation of size of the retinal images. *J. Physiol.* 201: pp. 237-260
- Bowns, L. (1996). Evidence for a feature tracking explanation of why Type II plaids move in the vector sum direction at short durations. *Vision Research*, 36(22): pp. 3685–3694
- Bradley, D. C. & Andersen, R. A. (1998). Center-surround antagonism based on disparity in primate area MT. *Journal of Neuroscience*, 18, pp. 7552–7565
- Bredfeldt, C. E. & Cumming, B. G., A. (2006). simple account of cyclopean edge responses in macaque V2. *Journal of Neuroscience*, 26: pp. 7581–7596
- Bremmer, F., Kubischik, M., Hoffmann, K.-P., Krekelberg, B. (2009). Neural Dynamics of Saccadic Suppression. *Journal of Neuroscience*, 29 (40): pp. 12374-12383
- Bressler, D.W. & Whitney, D. (2006). Second-order motion shifts perceived position. *Vision Research*, 46(6-7): pp. 1120–1128
- Bridgeman, B., Hendry, D., Stark, L. (1975). Failure to detect displacement of the visual world during saccadic eye movements. *Vision Research* 15(6): pp. 719-722
- Burbeck, C. A. (1988). Large-scale relative localization across spatial frequency channels. *Vision Research*, 28: pp. 857-859
- Burke, D., Alais, D. & Wenderoth, P. (1994). A role for a low level mechanism in determining plaid coherence. *Vision Research*, 34: pp. 3189-3196
- Burr, D. C. (1980). Motion smear. *Nature* (285): pp. 164-165
- Burr, D. C. & Morgan, M. J. (1997). Motion deblurring in human vision. *Proceedings of the Royal Society B: Biological Sciences*, 264 (1380): pp. 431–436

- Burr, D.C., Ross, J. & Morrone, M.C. (1986). Seeing Objects in Motion. *Proceedings of the Royal Society B: Biological Sciences*, 227(1247): pp. 249–265.
- Campbell, F. W. , Cooper, G. F. & Enroth-Cugell C. (1969). The spatial selectivity of the visual cells of the cat. *J. Physiol.* 203: pp. 223-235
- Caniard, F., Bühlhoff, H. H., Mamassian, P., Lee, S. W. & Thornton, I. M. (2011). Active control does not eliminate motion-induced illusory displacement. *Proceedings of the ACM SIGGRAPH Symposium on Applied Perception in Graphics and Visualization 8*: pp. 101–108
- Caniard, F., Bühlhoff, H. H. & Thornton, I. M. (2014). Action can amplify motion-induced illusory displacement. *Frontiers in Human Neuroscience*, 8:1058
- Cavanagh, P. (1992). Attention-based motion perception. *Science*, 257(5076): pp. 1563–1565
- Cavanagh, P., Anstis, S. (2013). The flash grab effect. *Journal of Vision*, 12(9): pp. 778
- Chahine, G., Krekelberg, B. (2009). Cortical Contributions to Saccadic Suppression. *PLoS ONE*, 4(9) e6900
- Chung, S.T.L., Patel S. S., Bedell H. E., Yilmaz O. (2007). Spatial and temporal properties of the illusory motion-induced position shift for drifting stimuli. *Vision Research*, 47(2): pp. 231–243
- Corey, D.P. & Hudspeth, A.J. (1979). Response latency of vertebrate hair cells. *Biophys. J.* 26: pp. 499-506
- Daniel, B. Y. P. M., Whitteridge, D., Hospital, M. & London, S. E. (1961). The Representation Of The Visual Field On The Cerebral Cortex In Monkeys. *Journal of Neurophysiology* (159): pp. 203 – 221
- DeAngelis, G. C., Cumming, B. G. & Newsome, W. T. (1998). Cortical area MT and the perception of stereoscopic depth. *Nature*, 394: pp. 677–680

- Derrington, A. M. & Lennie, P. (1984). Spatial and temporal contrast sensitivities of neurones in lateral geniculate nucleus of macaque. *The Journal of Physiology*, 357: pp. 219–240
- De'Sperati, C. & Baud-Bovy, G. (2008). Blind saccades: an asynchrony between seeing and looking. *The Journal of neuroscience : the official journal of the Society for Neuroscience*, 28(17): pp. 4317–4321
- De Valois, R.L. & De Valois, K.K. (1991). Vernier acuity with stationary moving Gabors. *Vision research*, 31(9): pp. 1619–1926
- Derrington, A. M. & Badcock, D. R. (1985). Seperate detectors for simple and complex grating patterns? *Vision Reserach*, 25 (12): pp. 1869-1878
- Dillenburger, B. (2005). Perception and Processing of Illusory Contours der Fakultät für Biologie der Eberhard Karls Universität Tübingen zur Erlangung des Grades eines Doktors der Naturwissenschaften
- Dodge, R. (1900). Visual perception during eye movement. *Psychological Review*, Vol 7(5): pp. 454-465
- Durant, S. & Zanker, J.M. (2009). The movement of motion-defined contours can bias perceived position. *Biology letters*, 5(2): pp. 270–273
- Eagleman, D.M., Sejnowski, T. J. (2006). Motion Integration and Postdiction in Visual Awareness. *Science Magazine* (287): pp. 2036-2038
- Efron, B. & Tibshirani, R. (1993). *An introduction to the bootstrap*. London: Chapman & Hall
- Favreau, O. E. (1976). Motion aftereffects: evidence for parallel processing in motion perception. *Vision Research* 16: pp. 181-186
- Findlay, J. M. & Harris, L. R. (1984). Small saccades to double-stepped targets moving in two dimensions. *Advances in Psychology*, 22: pp. 71–78

- Fisher, N. I. (1993). *Statistical Analysis Of Circular Data*. Cambridge, UK, Cambridge University Press
- Fröhlich, F. (1923). Über die Messung der Empfindungszeit. *Pflüger's Archiv für die gesamte Physiologie des Menschen und der Tiere*, 202(1): pp. 566–572
- Fu, Y.-X., Shen, Y., Gao, H. & Dan, Y. (2004). Asymmetry in visual cortical circuits underlying motion-induced perceptual mislocalization. *The Journal of Neuroscience : The Official Journal of the Society for Neuroscience*, 24(9): pp. 2165 -2171
- Fukunaga, K. & Hostetler, L. (1975). The estimation of the gradient of a density function, with applications in pattern recognition. *IEEE Transactions on Information Theory*, 21(1): pp. 32–40
- Gardner, E.P., Srinivasa, B. K., Reitzen S. D., Ghosh, S., Brown, S. A., Chen, J., Hall, A. L., Herzlinger, M. D., Kohlenstein, J.B., Ro, J. Y. (2007). Neurophysiology of Prehension. I. Posterior Parietal Cortex and Object-Oriented Hand Behaviors, *Journal of Neurophysiology*, 97 (1): pp. 387-406
- Gegenfurtner K.R., Kiper D.C., Levitt J.B. (1997). Functional properties of neurons in macaque area V3. *J Neurophysiol* 77: pp. 1906–1923
- Geisler W. S., Albrecht D.G., Crane A.M. & Stern L. (2001). Motion direction signals in the primary visual cortex of cat and monkey. *Visual Neuroscience* (18): pp. 501–516
- Girard, P., Salin, P.A. & Bullier, J. (1992). Response selectivity of neurons in area MT of the macaque monkey during reversible inactivation of area V1. *Journal of neurophysiology*, 67(6): pp.1437–1446
- Goodale, M. A., Milner D. A. (1992) Separate visual pathways for perception and action. *Trends of Neuroscience* 15(1): pp. 20-25
- Harp, T.D., Bressler, D.W. & Whitney, D. (2007). Position shifts following crowded second-order motion adaptation reveal processing of local and global motion without awareness. *Journal of Vision*, 7(2):15: pp. 1–13

- Hisakata, R. & Murakami, I. (2009). Illusory position shift induced by plaid motion. *Vision Research*, 49: pp. 2902–2910
- Hisakata, R., Terao M. & Murakami I. (2013). Illusory position shift induced by motion within a moving envelope during smooth-pursuit eye movements. *Journal of Vision* 13(12):21: pp.1–12
- How, M.J., & Zanker, J.M. (2014). Motion camouflage induced by zebra stripes. *Zoology*, 117(3): pp.163–170
- Hughes, A.E., Troscianko, J., & Stevens, M. (2014). Motion dazzle and the effects of target patterning on capture success. *BMC Evolutionary Biology*, 14(201)
- Hubel, D.H. (1959). Single unit activity in striate cortex of unrestrained cats. *The Journal of physiology*, 147(2): pp. 226–238
- Hubel, D.H. & Wiesel, T.N. (1962). Receptive fields, binocular interaction and functional architecture in the cat's visual cortex. *The Journal of Physiology*, 160(1): pp. 106–154
- Kalman, R.E. (1960). A New Approach to Linear Filtering. *Transactions of the ASME–Journal of Basic Engineering*, 82 (Series D): pp. 35–45
- Kandel, E.R., Schwartz, J.H., Jessell, T.M. Spiegelbaum, S. A., Hudspeth, A.J. (2000). *Principles of Neural Science*, 4th ed. McGraw- Hill, New York.
- Kerzel, D. & Gegenfurtner, K. R. (2005). Motion-induced illusory displacement reexamined: differences between perception and action? *Exp. Brain Res.* 162: pp. 191–201
- Knudsen, I. (1982). Auditory and visual maps of space in the optic tectum of the owl. *J. Neurosci.* 2: pp. 1177–1194.
- Kohler, P.J., Cavanagh, P. & Tse, P.U. (2015). Motion-induced position shifts are influenced by global motion, but dominated by component motion. *Vision Research*, 110: pp. 93–99

- Kooi, F. L., De Valois, R. L. & Switkes, E. (1987). Vernier acuity with Gabor patches. *Investigative Ophthalmology and Visual Science*, 28: pp. 360
- Kosovicheva, A. A., Wolfe, B. A., & Whitney, D. (2014). Visual motion shifts saccade targets. *Attention, perception & psychophysics*, 76(6): pp.1778–1788
- Kwon, O.-S., Tadin, D. & Knill, D.C. (2015). Unifying account of visual motion and position perception. *Proceedings of the National Academy of Sciences of the United States of America*, 112(26): pp. 8142–8147
- Kuffler, S.W. (1953). Discharge Patterns and Functional Organization of Mammalian Retina. *Journal of Neurophysiology*, 16(1): pp. 37–68
- Ledgeway, T., Smith, A. T. (1994). Evidence for separate motion-detection mechanism for first- and second-order motion in human vision. *Vision Research*, 34: pp. 2727-2740
- Leigh, R. & Zee, D., *The neurology of eye movements* (4th ed.) (2006). New York: Oxford University Press
- Lorenceau, J., Shiffar, M. (1992). The influence of terminators on motion integration across space. *Vision Research*, 32(2): pp. 263-273
- Arnold, D. & Marinovic, W. (2013). An illusory distortion of moving form driven by motion deblurring. *Vision Research*, 88: pp. 47-54
- Majaj, N. J., Carandini, M., & Movshon, J. A. (2007). Motion integration by neurons in macaque MT is local, not global. *Journal of Neuroscience*, 27: pp. 366–370
- Mallot, H. A. (2011). *Datenanalyse mit Matlab. Mathematische Grundlagen. Skript zur Vorlesung*, Eberhard Karls Universität Tübingen
- Mather, G. & Pavan, A. (2009). Motion-induced position shifts occur after motion integration. *Vision Research*, 49(23): pp. 2741–2746

- Mathiesen, C., Caesar, K. & Lauritzen, M. (2000). Temporal coupling between neuronal activity and blood flow in rat cerebellar cortex as indicated by field potential analysis. *The Journal of Physiology* (523): pp. 235–246.
- Maunsell, J. & Gibson, J. (1992). Visual response latencies in striate cortex of the macaque monkey. *Journal of Neurophysiology* (68): pp. 1332 -1344
- McDowell, J. E., Dyckman, K. A., Austin, B. & Clementz, B. A. (2008). Neurophysiology and neuroanatomy of reflexive and volitional saccades: evidence from studies of humans. *Brain Cogn.* 68(3): pp. 255-270
- McGraw. P. V., Walsh, V. (2004). Barrett, B.T., Motion-Sensitive Neurons in V5/MT Modulate Perceived Spatial Position. *Current Biology* 14(12): pp. 1090-1093
- McGraw, P. V., Whitaker D., Skillen J., Chung S. (2002). Motion adaptation distorts perceived visual position. *Current Biology*, 12(23): pp. 2042–2047
- McLaughlin, S.C. (1967). Parametric adjustment in saccadic eye movements. *Attention, Perception & Psychophysics*, 2(8): pp. 359–362.
- Merabet L, Desautels A, Minville K, Casanova C. (1998). Motion integration in a thalamic visual nucleus. *Nature* 396: pp. 265–268
- Merigan, W.H., Katz, L.M., Maunsell, J.H. (1991). The effects of parvocellular lateral geniculate lesions in the acuity and contrast sensitivity of macaque monkeys. *J Neurosci.* 1991 Apr;11(4): pp. 994-1001
- Milner, A. D. (1999). Neuropsychological studies of perception and visuomotor control. In *Attention, space and action* (ed. G. W. Humphreys, J. Duncan & A. Treisman), pp. 217-231. Oxford University Press
- Milner, A.D., Goodale, M.A. (2008). Two visual systems re-viewed. *Neuropsychologia*. 46 (3): pp. 774-785
- Morgan, M. J., Melmoth, D. & Solomon, J. A. (2013). Linking hypotheses underlying Class A and Class B methods. *Visual Neuroscience*, 30(5-6): pp. 197–206.

- Morgan, M. J., Watamaniuk, S. N. J. & McKee, S. P. (2000). The use of an implicit standard for measuring discrimination thresholds. *Vision Research*, 40 (17): pp. 109– 117.
- Mort, D.J., Perry, R. J., Mannan, S.K., Hodgson, T.L., Anderson, E., Quest, R., McRobbie, D., McBride, A., Husain, M., Kennard, C. (2003). Differential cortical activation during voluntary and reflexive saccades in man. *NeuroImage*, 18(2): pp. 231–246.
- Movshon, J. A., Adelson, E. H. , Gizzi M. S. , and Newsome, W. T., The analysis of moving visual patterns. In *Pattern Recognition Mechanisms* (1985). ed. Chagas, C., Gattass R., Gross C. (Pontificiae Academiae Scientiarum Scripta Varia 54, 117-151). Rome: Vatican Press. (Reprinted in *Experimental Brain Research*, Supplementum 11: pp. 117-151, 1986).
- Movshon, J.A. & Newsome, W.T. (1996). Visual response properties of striate cortical neurons projecting to area MT in macaque monkeys. *Journal of Neuroscience*, 16(23): pp.7733–7741
- Movshon, J.A. & Newsome, W.T. (1984). Functional characteristics of striate cortical neurons projecting to MT in macaque. *Soc Neurosci Abstr* 10:993
- Murakami, I. & Kashiwabara, Y. (2009). Illusory position shift induced by cyclopean motion. *Vision research*, 49(15): pp. 2037–2043
- Mussap, A.J. & Prins, N. (2002). On the perceived location of global motion. *Vision Research*, 42(6): pp. 761–769
- Nakayama, K. & Silverman, G.H. (1988). The aperture problem-I. Perception of nonrigidity and motion direction in translating sinusoidal lines. *Vision Research*, 28(6): pp.739–746
- Niehorster, D.C. & Cheng, J.C.K. (2010). Optimal combination of form and motion cues in human heading perception. *Journal of Vision* 10(11):20: pp. 1–15
- Nishida, S. & Johnston, A. (1999). Influence of motion signals on the perceived position of spatial pattern. *Nature*, 397(6720): pp. 610–612

- Nishida, S., Sato, T. (1995). Motion aftereffect with flickering test patterns reveals higher stages of motion processing. *Vision Research*, 35(4): pp. 477-490
- Pöppel, E., Held, R. & Frost, D. (1973). Residual Visual Function after Brain Wounds involving the Central Visual Pathways in Man. *Nature*, 243: pp. 295–296
- Purves D.; Augustine G.J.; Fitzpatrick D.; Katz L. C.; LaMantia A.-S.; McNamara J. O. & Williams S.M. (2001). *Neuroscience*, 2nd ed. Sunderland (MA), Sinauer Associates.
- Ramachandran, V. S. & Anstis, S. M. (1990). Illusory displacement of equiluminous kinetic edges. *Perception*, 19(5): pp. 611–616
- Raymond, J.E. (1994). Directional anisotropy of motion sensitivity across the visual field. *Vision Research*, 34(8): pp. 1029–1937
- Rider, A.T., McOwan, P.W. & Johnston, A. (2009). Motion-induced position shifts in global dynamic Gabor arrays. *Journal of Vision* 9 (13):8: pp. 1–8
- Roach, N. W., McGraw, P. V & Johnston, A. (2011). Visual motion induces a forward prediction of spatial pattern. *Current Biology* 21(9): pp. 740–745
- Rodman, H. R. & Albright, T. D. (1989). Single-unit analysis of pattern-motion selective properties in the middle temporal visual area (MT). *Exp Brain Res* 75: pp. 53-64
- Rodman, H. R., Gross, C. G., & Albright T. D. (1989). Afferent basis of visual response properties in area MT of the macaque. I. Effects of striate cortex removal. *Journal of Neuroscience* ,9(6): pp. 2033-2050
- Santella, A. & DeCarlo, D. (2004). Robust clustering of eye movement recordings for quantification of visual interest. *Proceedings of the Eye Tracking Research & Applications Symposium on Eye Tracking Research & Applications*: pp. 27–34
- Schafer, R. J. & Moore, T. (2007). Attention Governs Action in the Primate Frontal Eye Field. *Neuron* 56 (3): pp. 541–551

- Schmid, M.C., Mrowka, S.W., Turchi, J., Saunders, R. C., Wilke, M., Peters, A. J., Ye, F. Q., Leopold, D. A. (2010). Blindsight depends on the lateral geniculate nucleus. *Nature*, 466(7304): pp. 373–377
- Schreiber, K., Dillenburger, B. & Morgan, J. M. (2014). Effects of pupil size on measurements of eye position using video oculography, Talk at ‘Applied Vision Association’
- Semmlow, J. L., Gauthier, G., Vercher, J. (1989). Mechanisms of short-term saccadic adaptation. *Journal of experimental psychology* 15(2): pp. 249-258
- Sereno, M. I., Dale, a M., Reppas, J. B., Kwong, K. K., Belliveau, J. W., Brady, T. J., ... Tootell, R. B. (1995). Borders of multiple visual areas in humans revealed by functional magnetic resonance imaging. *Science (New York, N.Y.)*, 268(5212): pp. 889-893
- Shapiro, A., Lu, Z. L., Huang, C. B., Knight, E., Ennis, R. (2010). Transitions between central and peripheral vision create spatial/temporal distortions: A hypothesis concerning the perceived break of the curveball. *PLoS One* 5(10): e13296
- Sparks, L. (1986). Translation of sensory signals into commands for control of saccadic eye movements: role of primate superior colliculus. *Physiol. Rev.* 66: pp. 118–171
- Stocker, A. A. & Simoncelli, E.P. (2006). Noise characteristics and prior expectations in human visual speed perception. *Nature neuroscience*, 9(4): pp. 578–585
- Thiele, A., Kubischick, M., Hoffmann, K.P. (2002). Neural Mechanisms of Saccadic Suppression. *Science* 295; pp. 2460 – 2462
- Thilo, K. V., Santoro, L., Walsh, V., Blakemore, C. (2004). The site of saccadic suppression. *Nature Neuroscience* 7(1): pp. 13-14
- Thompson, B., Aaen-Stockdale, C., Koski, L., Hess, R. F. (2009). A double dissociation between striate and extrastriate visual cortex for pattern motion perception revealed using rTMS. *Human brain mapping*, 30: pp. 3115–3126

- Thorson, J., Lange, G. D. & Biederman-Thorson, M. (1969). Objective measure of the dynamics of a visual movement illusion. *Science*, 164: pp. 1087-1088
- Toet, A. & Koenderink, J. J. (1988). Differential spatial displacement thresholds for Gabor patches. *Vision Research*, 28: pp. 133-143
- Tsui, S.Y., Khuu, S.K. & Hayes, A. (2006). The perceived position shift of a pattern that contains internal motion is accompanied by a change in the pattern's apparent size and shape. *Vision Research*, 47(3): pp. 402–410
- Tsui, S.Y., Khuu, S.K. & Hayes, A. (2007). Apparent position in depth of stationary moving three-dimensional objects. *Vision Research*, 47: pp. 8–15
- Tynan, P.D. & Sekuler, R. (1982). Motion processing in peripheral vision: Reaction time and perceived velocity. *Vision Research*, 22(1): pp. 61–68
- Villeneuve M.Y., Kupers R., Gjedde A., Ptito M. (2005). Casanova C., Pattern-motion selectivity in the human pulvinar. *Neuroimage* 28: pp. 474–480.
- Watt, R.J. & Andrews, D.P. (1981). APE : Adaptive Probit Estimation of Psychometric Functions. *Current Psychological Reviews* 1(2): pp. 205-213
- Sanders, M. D., Warrington, E., Marshall, J., & Weiskrantz, L. (1974). Blindsight': vision in a field defect. *Lancet*, 1(7860):pp. 707-708
- Westheimer, G. (1975). Visual Acuity and Hyperacuity. *Investigative Ophthalmology*, 64(8): pp. 570–572
- Whitney, D. (2005). Motion distorts perceived position without awareness of motion. *Current Biology*, 15, R324 - R326
- Whitney, D. (2006). Contributions of bottom-up and top-down motion processes to perceive position. *Journal of experimental Psychology: Human Perception and Performance*, 32: pp. 1380 -1397
- Whitney, D., Goltz, H. C., Thomas, C. G., Gati, J. S., Menon, R. S. & Goodale, M. A. (2003). Flexible retinotopy: motion-dependent position coding in the visual cortex. *Science (New York, N.Y.)*, 302(5646): pp. 878–881

- Whitney, D., & Cavanagh, P. (2000). Motion distorts visual space: Shifting the perceived position of remote stationary objects. *Nature Neuroscience*, 3: pp. 954–959
- Whitney, D., Cavanagh, P. (2003). Motion adaptation shifts apparent position without the motion after-effect. *Perception & Psychophysics*, 65: pp. 1011-1018
- Wilson, H.R., Ferrera, V.P. & Yo, C. (1992). A psychophysically motivated model for two-dimensional motion perception. *Vis. Neurosci.*, 9 (1): pp. 79-97
- Wong, E., & Mack, A. (1981). Saccadic programming and perceived location. *Acta Psychologica*, 48: pp. 123–131
- Yamagishi, N., Anderson, S.J. & Ashida, H. (2001). Evidence for dissociation between the perceptual and visuomotor systems in humans. *Proceedings. Biological Sciences/The Royal Society*, 268(1470): pp. 973 – 977
- Yarbus, A. (1967). *Eye Movements and Vision*. Plenum Press, New York
- Zhao B, Chen H, Li B. (2005). Pattern motion and component motion sensitivity in cat superior colliculus. *Neuroreport* 16: pp. 721–726
- Zimmermann, E., Morrone, M.C., Burr, D. (2012). Visual motion distorts visual and motor space. *Journal of Vision* 12(2):10: pp. 1-8